Silver nanoparticles of *Albizia adianthifolia*: The induction of apoptosis in a human lung carcinoma cell line.

By

RISHALAN GOVENDER

B. Sc. B. Med. Sc. (Hons) (UKZN)

Submitted in fulfilment of the requirements for the degree of M. Med. Sci

in the

Discipline of Medical Biochemistry and Chemical Pathology

School of Laboratory Medicine and Medical Sciences

College of Health Sciences

University of KwaZulu-Natal

Durban

2012

ABSTRACT

Silver nanoparticles (AgNP), the most popular nano-compounds, possess unique chemical, physical and biological properties. *Albizia adianthifolia* (AA) – rich in saponins – is a plant of the Fabaceae family, found abundantly on the East coast of Africa. This plant is well known for its medicinal properties, and although the exact phytochemistry of AA is unknown, recent research suggests that AA can be used for the treatment of certain pathologies. The biological properties of a novel silver nanoparticle (AA_{AgNP}) synthesised from an aqueous leaf extract of AA, were investigated on A549 lung carcinoma cells. Cell viability was determined by the 3-(4,5-Dimethyl-2-thiazolyl)-2,5-diphenyl-2H-tetrazolium bromide assay. Cellular oxidative status (lipid peroxidation and glutathione (GSH) levels) were determined by the TBARS and GSH-Glo™ Glutatione assays respectively. ATP concentration was measured using the CellTitre-Glo™ assay. Caspase-3/-7, -8 and -9 activities were determined by Caspase-Glo® assays. Flow cytometry was used to measure apoptosis, mitochondrial (mt) membrane depolarisation, expression of CD95 receptors and intracellular smac/DIABLO levels. DNA fragmentation was assessed with the comet assay. The expression of p53, bax, PARP-1 and smac/DIABLO was evaluated by western blotting. Quantitative polymerase chain reaction was used to determine mRNA levels of bax and p53. AA_{AgNP} caused a dose-dependent decrease in cell viability with a significant increase in lipid peroxidation (5-fold vs. control; p=0.0098) and decreased intracellular GSH (p=0.1184). A significant 2.5-fold decrease in cellular ATP was observed upon AA_{AgNP} exposure (p=0.0040) with a highly significant elevation in mt membrane depolarisation (3.3-fold vs. control; p<0.0001). Apoptosis was also significantly higher (1.5-fold) in AA_{AgNP} treated cells (p<0.0001) with a significant decline in expression of CD95 receptors (p=0.0416). AA_{AgNP} caused a significant 2.5-fold reduction in caspase-8 activity (p=0.0024) with contrasting increases in caspase-3/-7 (1.7-fold vs. control; p=0.0180) and -9 activity (1.4-fold vs. control; p=0.0117). Western blots showed increased expression of smac/DIABLO (4.1-fold) in treated cells (p=0.0033). Furthermore, AA_{AgNP} significantly increased the expression of p53, bax cleaved PARP-1 (1.2-fold; p=0.0498, 1.6-fold;

p=0.0083 and 1.1-fold; *p*=0.0359 respectively). The expression of mRNA for both p53 and bax was also elevated post AA_{AgNP} treatment, with 6-fold (*p*=0.0036) and 5-fold (*p*=0.0080) changes respectively compared to untreated cells. Data suggests that AA_{AgNP} induces cell death in the A549 lung cells via the mt-mediated intrinsic apoptotic program. Further investigations are required to assess the potential use of AA_{AgNP} in cancer treatment.

DECLARATION

This dissertation contains the original work by the author and has not been submitted in any form to another university. The use of work by others has been duly acknowledged in the text.

The research described in this study was carried out in the Division of Medical Biochemistry and Chemical Pathology, School of Laboratory Medicine and Medical Science, Faculty of Health Sciences, University of KwaZulu-Natal, Durban, under the supervision of Prof. A.A. Chuturgoon and Miss A. Phulukdaree.

.....

Mr. R. Govender

ACKNOWLEDGEMENTS

My parents

You are my Gods, my pillars of strength, the reason for my existence. I owe credit for all my achievements to you both. Thank you for your unwavering support and encouragement throughout my studies and for always having faith in me. I hope I have done you proud, in every way possible.

Professor A.A Chuturgoon

Words can never express my gratitude to you. More than a mentor, and wizard of Medical Biochemistry, you have adopted the role of a father to me. I thank you for giving me the greatest opportunity of being a part of your department and experiencing Medical Biochemistry through your visions. You are a blessing to us all and I only pray that your every ambition in life is fulfilled.

Miss. A. Phulukdaree

You have been a true inspiration to me. I can't imagine what I would have done without your expertise, advice and knowledge of Medical science. For all your assistance, supervision and guidance, I place you on a pedestal. God bless you, and I know you will grow to great heights both as a person, and a scientist.

Dr. R.M. Gengan and Mr. K. Anand

My sincere appreciation for the contribution you have made in this study. It is your innovation, without which this would not have been possible. I thank you for your support.

The master students of 2012 in the discipline of Medical Biochemistry

I could have never asked for another group of colleagues to have gone through my post-graduate studies with. Mr. I.S. Govender, Miss P. Ramkaran, Miss S. Nagiah and Miss C. Tiloke, it has been a riveting experience with you guys. Thank you for all the discussions, assistance in the laboratory, support and most of all for your unconditional friendship. I will treasure you all.

The PhD students and staff in the discipline of Medical Biochemistry

Miss S. Gounden and Mr. K. Anwar, I am grateful for all that you have done to assist me throughout the year. Thank you for being not only mentors, but good friends. I wish you well for your studies. To the rest of the staff, master and PhD students, thank you for your assistance.

Friends and loved ones

To my brother, and to the rest of my friends and family, thank you for the support and encouragement. A special thanks to the KMK eisteddfod group, my second family. You guys are very dear and special to me, and for all your support in my endeavours, I thank you.

PUBLICATIONS

The following manuscript has been submitted to and accepted by the Journal of Nanobiotechnology (MS 1840103851838905):

R. Govender, A. Phulukdaree, R.M. Gengan, K. Anand and A.A. Chuturgoon. The induction of apoptosis, by silver nanoparticles of *Albizia adianthifolia,* in a human lung carcinoma cell line. DOI: 10.1186/1477-3155-11-5

PRESENTATIONS

Induction of apoptosis, by silver nanoparticles of *Albizia adianthifolia,* in human lung carcinoma A549 cells.

R. Govender, A. Phulukdaree, R.M. Gengan, K. Anand and A.A. Chuturgoon.

UKZN College of Health Science research symposium (September 2012), Durban, South Africa.

LIST OF ABBREVIATIONS

$\Delta\Psi$	mt membrane potential
AA	*Albizia adianthifolia*
Ag	Silver
$AgNO_3$	Silver nitrate
AgNP	Silver nanoparticles
AA_{AgNP}	Silver nanoparticles of *Albizia adianthifolia*
AIDS	Acquired immunodeficiency syndrome
AIF	Apoptosis inducing factor
Apaf-1	Apoptotic protease activating factor-1
APC	Allophycocyanin
ARV	Anti-retro viral
AVPI	Ala-Val-Pro-Ile
BCA	Bicinchononic acid
BIR	Baculoviral IAP repeat
BHT	Butylated hydroxytoluene
c	Complementary
cFLIP	Cellular flice inhibitory protein
CAD	Caspase activated DNase

CCM	Complete culture medium
Ct	Cycle time
Cu^{+}	Cuprous ion
Cu^{2+}	Cupric ion
DD	Death domain
DED	Death effector domain
DISC	Death inducing signalling complex
DMSO	Dimethyl sulphoxide
dNTP	Deoxynucleotide triphosphate
ds	Double stranded
DUT	Durban University of Technology
EtBr	Ethidium bromide
ETC	Electron transport chain
FADD	Fas associated protein with death domain
$FADH_2$	Flavin adenine dinucleotide
Fas-L	Fas ligand
Fas-R	Fas receptor
FITC	Fluorescein isothiocyanate
FITR	Fourier transform infrared

g	Gravitational force
GAPDH	Glyceraldehyde-3-phosphate dehydrogenase
GPx	Glutathione peroxidase
GSSG	Glutathione disulphide
GST	Glutathione-S-transferase
h	Hours
H	Hydrogen
H_2O_2	Hydrogen peroxide
HIV	Human immunodeficiency virus
HRP	Horseradish peroxidase
IAP	Inhibitor of apoptosis protein
IC_{50}	Half maximal inhibitory concentration
ICAD	Inhibitor of caspase activated DNase
Ig	Immunoglobulin
IMB	IAP-binding motifs
JC-1	J-aggregate-forming cationic dye
LMPA	Low melting point agarose
MDA	Malondialdehyde
mRNA	Messenger ribonucleic acid

mt	Mitochondria/mitochondrial
MTT	3-(4,5-Dimethyl-2-thiazolyl)-2,5-diphenyl-2H-tetrazolium bromide
NADH	Nicotinamide adenine dinucleotide
NAIP	Neuronal apoptosis inhibitory protein
Np	Nanoparticle
PARP-1	Poly (ADP-ribose) polymerase-1
PBS	Phosphate buffer saline
PI	Propidium iodide
PIG	p53-induced gene
PS	Phosphatidyl serine
PT	Permeability transition
PUFA	Polyunsaturated fatty acid
Q-PCR	Quantitative polymerase chain reaction
RBI	Relative band intensity
RING	Really interesting new gene
RLU	Relative light unit
ROS	Reactive oxygen species
RT	Room temperature
SCGE	Single cell gel electrophoresis

SDS-PAGE	Sodium dodecyl sulphate - polyacrylamide gel electrophoresis
SEM	Standard error of the mean
SH	Thiol
Smac/DIABLO	Second mitochondria-derived activator of caspases/DIABLO
ss	Single stranded
TBA	Thiobarbituric acid
TBARS	Thiobarbituric acid reactive substances
TBST	Tris buffer saline tween 20
TCA cycle	Tricarboxylic acid cycle
TEM	Transmission electron microscopy
TNF-RI	Tumour necrosis factor -α receptor 1
TNF-α	Tumour necrosis factor-α
TRADD	Tumour necrosis factor –receptor 1 associated protein with death domain
TRAIL-R1/R2	Tumour necrosis factor -related apoptosis-inducing ligand-receptor 1/2
USA	United States of America
VEGF	Vascular endothelial growth factor
XIAP	X-linked mammalian inhibitor of apoptosis protein

LIST OF FIGURES

Chapter one

Chapter two

Chapter three

Chapter four

LIST OF TABLES

TABLE OF CONTENTS

INTRODUCTION

Nanotechnology is a rapidly expanding branch of modern technology. Nanoparticles (NPs) are commonly defined as small sized (1-100nm) compounds that are able to function as whole units. These compounds are becoming widespread for their use in consumer products and medical applications; with prospective for utilization as therapeutic compounds, transfection vectors, anti-microbial agents and fluorescent labels (Su et al., 2008). Silver nanoparticles (AgNP) are the most commercialised and prominent group of nano-compounds, attributed to their diverse applications in the health sector.

Cancer is one of the leading causes of global morbidity and mortality. It is estimated that the world cancer burden will increase by 50% in the next 20 years (Bello et al., 2011). The South African Medical Research Council ranked cancer as the fourth leading cause of death in South Africa (SA) in 2003; in 2006 alone, there were 4525 deaths due to lung cancer in SA (Bello et al., 2011). As much as 80-90% of lung cancer cases are attributed to smoking, with the smaller proportion (10-20%) as a result of occupational exposure to heavy metals and other toxic compounds (Siemiatycki et al., 2004; Driscoll et al., 2005). Recently, an association has been found between the acquired immunodeficiency syndrome (AIDS) and the development of lung cancer (Long et al., 2008). This is of great concern in view of the AIDS crisis in SA. The financial strain of anti-retroviral (ARV) treatment and cancer therapy on the health system in SA necessitates the need for alternate means of medication that is cost effective, easily accessible and safe.

Silver (Ag) is known to possess unique and unusual chemical, physical as well as biological properties (Moaddab et al., 2011). Since the introduction of Ag as a colloidal form in the 1990s, immense progress has been made regarding the usage of Ag for treatment of bacterial infections in open wounds, with Ag based ointments, bandages and wound dressings being readily available in the present age (Arora et al., 2008). Also, nanosilver has been used as a contraceptive and a water disinfectant (Hansen et al., 2008; Madhumathi et al., 2010).

The use of AgNPs as anti-cancer agents has proved promising in research, creating new avenues for therapeutic intervention in the field of oncology (Moaddab et al., 2011). Various attempts to incorporate AgNPs into cancer treatments have been made, with positive outcomes (Vaidyanathan et al., 2009). Although the induction of oxidative stress by AgNP induced mitochondrial (mt) damage has been observed as the general mode of AgNP toxicity, mechanistic pathways remain unclear (Foldbjerg et al., 2011).

Albizia adianthifolia (AA), also known as 'Flatcrown' or 'Rough-barked flat-top', is a plant member of the Fabaceae family found abundantly on the east coast of SA. This plant contains saponins such as prosapogenins and triterpene saponins (Lacaille-Dubois, 2000; Haddad et al., 2004). Saponins are plant glycosides that possess significant anti-cancer properties (Man et al., 2010). The isolated biological properties of Ag and AA were considered for the synthesis of a novel NP (AA_{AgNP}). This study sought to determine the anti-cancer properties of AA_{AgNP} conjugated to leaf extracts of the plant.

Originating from human lung carcinoma, A549 cells belong to the most well-characterised and extensively used *in vitro* model. The A549 cell line has been used frequently to study nanotoxocity and nanoparticle interactions (Sahu and Casciano, 2009). It was hypothesised that AA_{AgNP} induced apoptotic death in the cancerous lung cells by AA_{AgNP} mediated increased generation of reactive oxygen species (ROS).

CHAPTER ONE

1 LITERATURE REVIEW

1.1 Nanosilver: emerging benefits in the medical sector

The vast extension of nanoscience has resulted in a large scale escalation in consumer products that contain nano-compounds. Nanotechnology is a burgeoning field, offering benefits in healthcare with endless interventions. Silver nanoparticles are the most commercialised group of nano-compounds in the current generation. Skin creams, wound dressings, catheter tubes and bone cements are but a few of a long list of medical necessities being manufactured containing AgNPs. Diagnostics have subjugated nanoparticles as imaging contrast agents. Furthermore, the performance of surgical tools and the biocompatibility of tissue and organ implants have been enhanced by nanostructured surface modifications (Sahu and Casciano, 2009).

The revolutionary notion that AgNPs can be used to improve the way diseases are treated is now being exploited, affording potential in the treatment of ailments such as retinal neurovascularisation (Bhattacharya and Mukherjee, 2008; Kalishwaralal et al., 2010) and AIDS as a result of human immunodeficiency virus (HIV) infection (Sun et al., 2005; Lara et al., 2010). Silver nanoparticles are well known for their anti-microbial properties and are used as antiviral agents against hepatitis B, herpes simplex virus type 1, monkey pox virus and respiratory syncytial virus (Lu et al., 2008; Rogers, 2008; Sun, 2008; Baram-Pinto et al., 2009).

Silver nanoparticles have also proved promising in cancer therapy. Silver oxide NPs were shown to possess anti-tumour properties in transplanted Pliss lymphosarcoma tumour models upon intravenous administration (Rutberg et al., 2008). In a study using bovine retinal endothelial cells, AgNPs were found to inhibit vascular endothelial growth factor (VEGF) induced

angiogenesis (Kalishwaralal et al., 2009). Silver nanoparticles induced tumour inhibitory effects on Dalton's lymphoma ascites (DLA) cells as well as on Swiss albino mice, without toxicity to normal cells (Sriram et al., 2010). Sriram et al. (2010) further elucidated that the mechanism by which AgNPs exerted cytotoxic effects on the DLA tumour cell line was by the induction of apoptosis as a result of caspase-3 activation (Sriram et al., 2010). Silver nanoparticles have been synthesised with a wide range of compounds that have valuable medicinal properties.

1.2 *Albizia adianthifolia*: potential in cancer therapy

The *Albizia* genus is comprised of about 150 species that are largely distributed in the tropics. The greatest diversity of these plants is in Africa and Central/South America (Abdel-Kader et al., 2001). *Albizia adianthifolia* (Figure 1) is one species that is easily cultivated and found in excess in SA. This species is used in parts of Africa for the treatment of bronchitis, headaches, skin diseases, tapeworm, sinusitis, typhoid fever, inflamed eyes and urinary and respiratory infections (Tamokou Jde et al., 2012). These plants are well known for their constituent alkaloids, steroids, triterpenoid saponins and flavonols all of which possess medicinal value (Haddad et al., 2003). Saponins from AA, in particular, have received much attention for the wide range of properties they offer.

Figure 1: Illustration of the tree, leaves and flowers of *Albizia adianthifolia.*

Saponins, produced primarily by plants, are bioactive glycosides that have various biological and pharmacological properties (Figure 2). Saponins are grouped chemically into steroid or polycyclic triterpene saponins (Kensil, 1996). Some of the well characterised and significant biological actions of saponins include; cell membrane permeabilisation (Hostettmann and Martson, 1995), sequestering of serum cholesterol (Francis et al., 2002), stimulation of luteinising hormone release (Francis et al., 2002), toxicity enhancement of immunotoxins (Bachran et al., 2008b), immuno-modulation via cytokine interplay (Sun et al., 2009) and cytostatic and - toxic effects on malignant tumours (Bachran et al., 2008a).

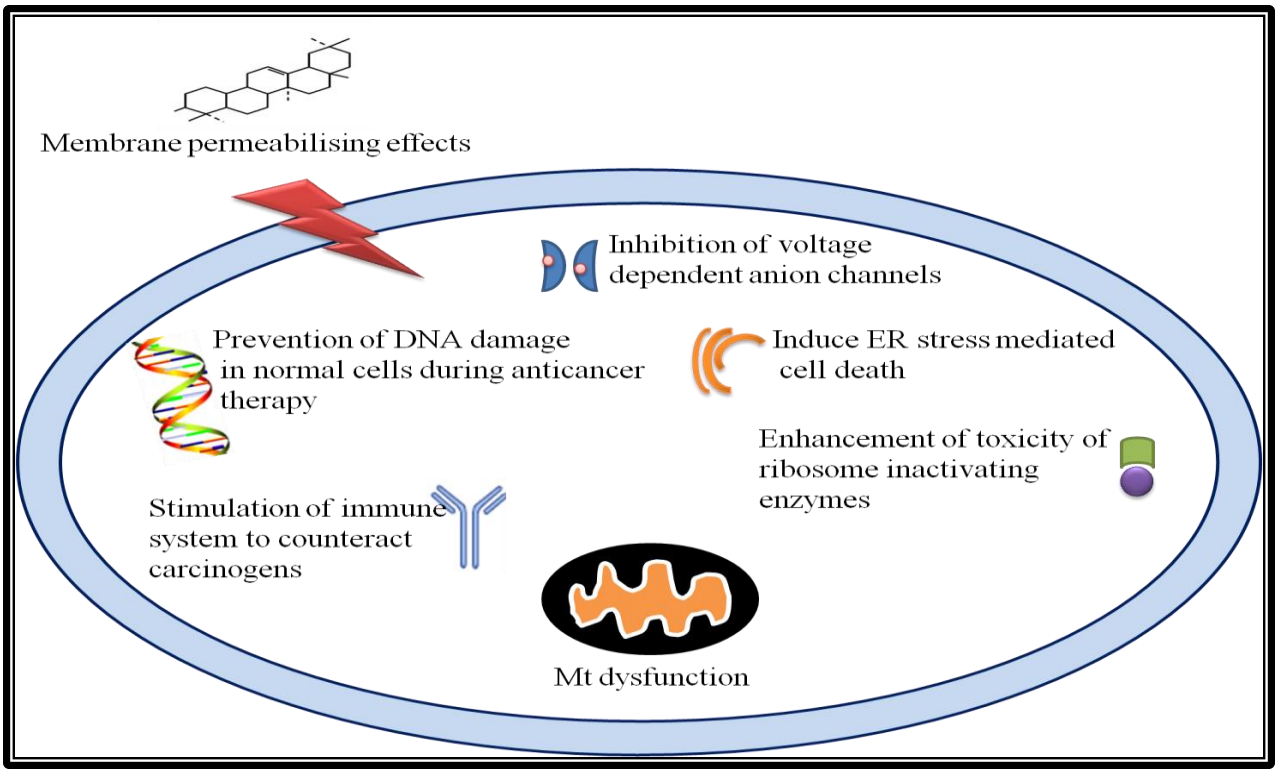

Figure 2: The biological functions of saponins.

In 1960, the very first investigation on the use of saponins for the treatment of tumours was documented (Friess et al., 1960). To date, over 1200 studies (Pubmed search: "cancer", "saponins") on the ability of saponins to inhibit tumour growth or induce apoptosis have been reported. Saponins are used successfully in combination with chemotherapeutic agents for the enhancement of drugs in tumour treatment as well as to enhance membrane transportation (Mayank et al., 2011). The delivery of drugs to target cells in cancer therapy is a vital consideration. Extensive studies were conducted to determine if saponins could selectively aid drug delivery to cancer cells. Cisplatin, for example, used in combination with saponins isolated from AA possesses potent anti-tumour properties (Haddad et al., 2003; Haddad et al., 2004). In an investigation in 2001, triterpene saponins exhibited selective inhibition of tumourigenesis by inducing cell cycle arrest in a human breast cancer cell line and initiation of apoptosis in a

leukemia cell line (Mujoo et al., 2001). Haddad et al. (2004) investigated the biological properties of triterpene saponins (Figure 3) extracted from the root of AA on leukemic cells *in vitro* (Jurkats cells). They reported that the saponins exhibited a cytotoxic effect and induced apoptosis (Haddad et al., 2004). These properties make AA an ideal plant for the isolation of active compounds against cancer. Although, the exact phytochemistry of the plant still needs to be elucidated.

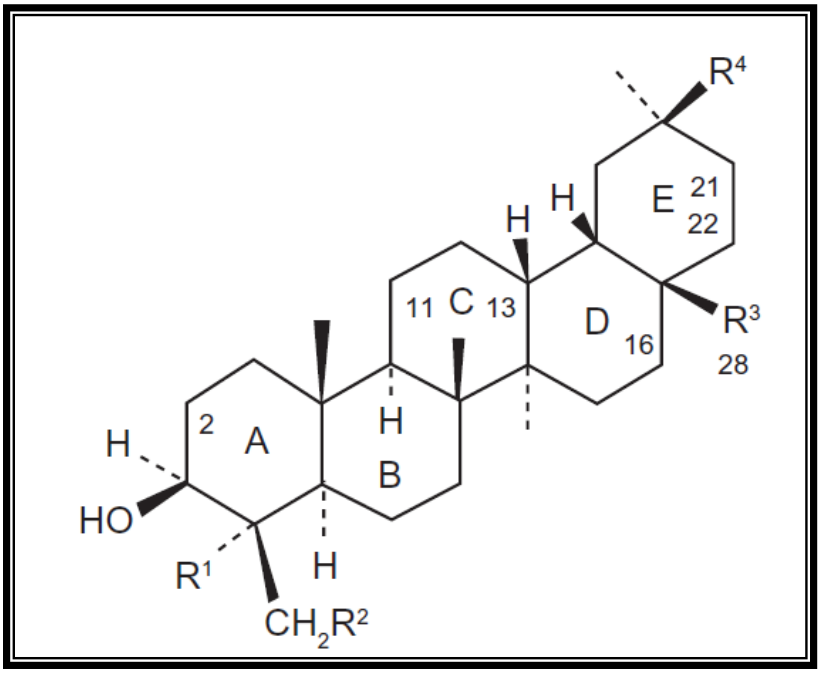

Figure 3: Biochemical structure of a triterprene saponin isolated from *Albizia adianthifolia* (Mayank et al., 2011). Copyright permission for reproduction was granted from the author.

1.3 Apoptosis: a programmed cell death

Regulation in the number of cells in multicellular organisms is an important process. Each day, billions of cells are subjected to an altruistic death in order to maintain functionality of the organism as a whole (Fischer and Schulze-Osthoff, 2005). Characterised by distinct morphological changes, apoptosis involves a series of precisely regulated events that lead to cell

destruction and disintegration. A group of aspartate-specific cysteinyl proteases referred to as caspases are the executioners of- and form the engine of apoptosis. Categorised into two distinct groups, initiator or activator caspases are responsible for proteolytic cleavage and subsequent activation of the second group of caspases, the executioners or effectors (Fischer and Schulze-Osthoff, 2005). All caspase enzymes contain an active-site cysteine and are known to cleave substrates that possess aspartate residues. Over twelve caspases have been discovered in humans thus far, of which two thirds have been implicated in apoptotic cell death (Thornberry and Lazebnik, 1998; Earnshaw et al., 1999). Caspases are synthesised as inactive zymogens that are made up of three domains: a prodomain at the N-terminus, a p20 and a p10 domain both found in a mature caspase. For activation of caspases, the zymogen must usually undergo cleavage between p20 and p10 domains or between the prodomain and the p20 domain. Executioner caspase are functional in inflicting morphological changes of apoptosis-undergoing cells; cell shrinkage, hypercondensation of chromatin, chromosomal cleavage into nucleosomal fragments, blebbing of plasma membrane and packaging of cellular contents into apoptotic bodies – membrane enclosed vesicles (Hengartner, 2000). Two major apoptotic pathways exist in mammalian cells: the extrinsic death receptor-mediated and intrinsic mt-mediated pathways (Figure 3). Both pathways are tightly regulated and controlled by a host of regulatory molecules, some of which are highlighted further on.

1.3.1 The extrinsic apoptotic program: death receptor pathway

The extrinsic pathway of apoptosis involves transmembrane death receptor-mediated reactions. The best documented and characterised mechanism for caspase activation via the extrinsic pathway involves the tumour necrosis factor (TNF)-α family of death receptors. These include TNF-α receptor 1 (TNF-R1), TNF-related apoptosis-inducing ligand (TRAIL)-R1/R2, Fas

(CD95)-R, DR3 and CAR-1 all known to transduce apoptotic signals (Reed, 1999). Receptors of the TNF-α family share a common cysteine rich extracellular domain, with a cytoplasmic domain known as the death domain (DD) (Ashkenazi and Dixit, 1998). The role of these DDs is significant in the transmission of death signals from the outer cell surface to intracellular signalling pathways. Downstream events that define the extrinsic program of apoptosis following ligand-receptor binding have been most extensively characterised with TNF/TNF-R and Fas-ligand (Fas-L)/Fas-receptor (Fas-R) models (Chicheportiche et al., 1997; Ashkenazi and Dixit, 1998; Peter and Krammer, 1998; Suliman et al., 2001; Rubio-Moscardo et al., 2005). A clustering of death receptors is seen on the membrane with subsequent binding and attachment of homologous trimeric ligands. Cytoplasmic adaptor proteins that present with corresponding DDs for binding to death receptors are then recruited. Fas-L/Fas-R recruits Fas associated protein with DD (FADD) whereas TNF/TNF-R recruits TNF-R1 associated protein with DD (TRADD) with FADD and RIP (Hsu et al., 1995; Wajant, 2002). FADD contains an additional domain known as the death effector domain (DED). Via dimerisation of the DED, FADD associates with procaspase-8 and which contains a homologous DED. A death inducing signalling complex (DISC) is then formed, resulting in the auto-catalytic cleavage and activation of caspase-8 (Kischkel et al., 1995). The execution phase of apoptosis is administered upon caspase-8 activation, with the cleavage of procaspase-3 and -7. Research has revealed that a protein called cellular flice inhibitory protein (c-FLIP) inhibits death receptor-mediated apoptosis by binding to caspase-8 and FADD, rendering them ineffective (Scaffidi et al., 1999) (Figure 4).

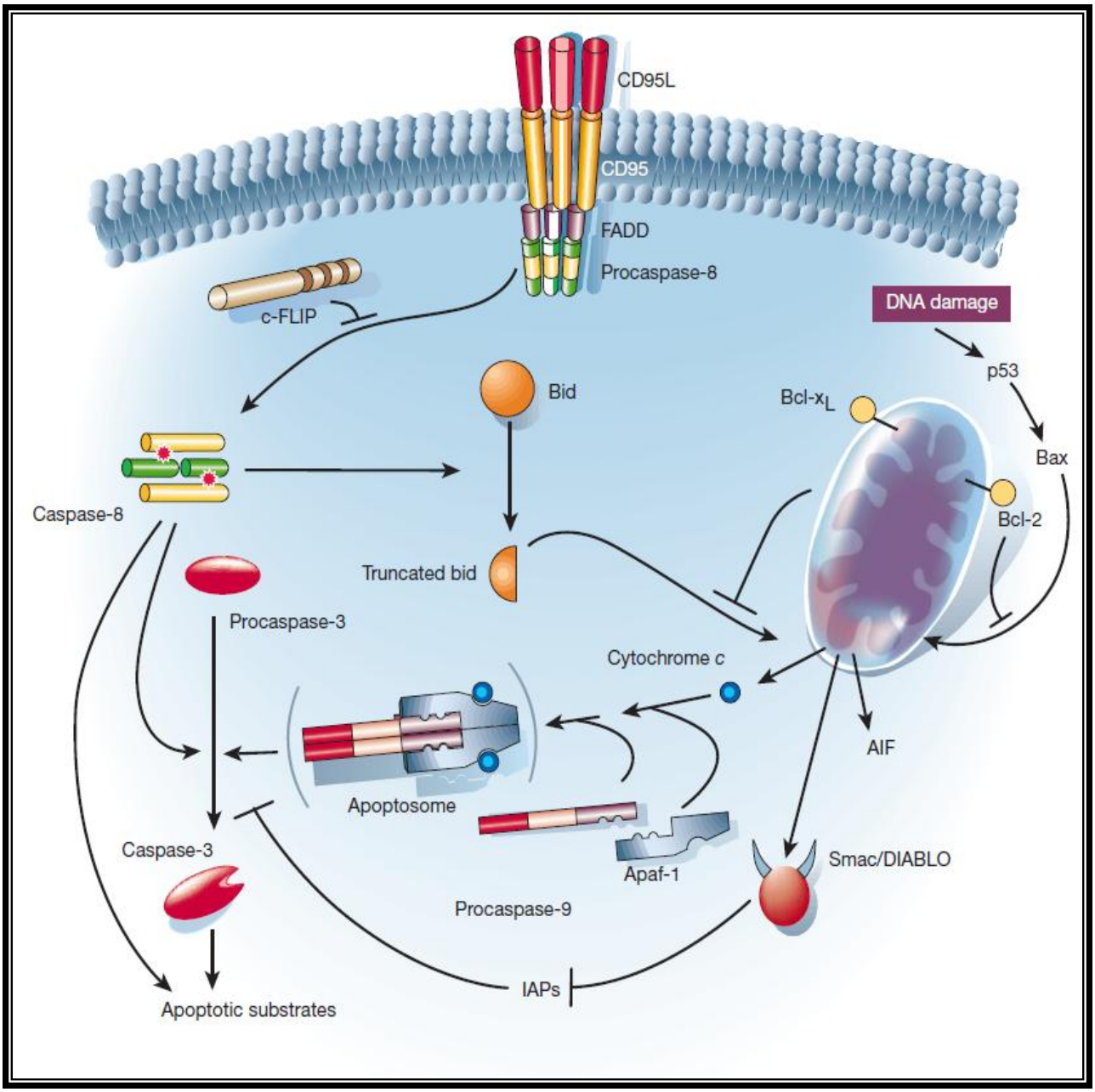

Figure 4: Overview of the extrinsic and intrinsic apoptotic pathways (Hengartner, 2000). Copyright permission for reproduction was granted from the author.

1.3.2 The intrinsic apoptotic program: mitochondrial-mediated pathway

Independent of receptor-mediated stimuli, the intrinsic pathway of apoptosis is controlled by stimuli that produce intracellular signals to directly target molecules within the cell, and is

mediated by the mt. Such stimuli induce changes to the inner mt membrane. A crucial step for the release of mt apoptotic proteins is the permeabilisation of the mt membrane. The Bcl-2 family of proteins is involved in the control of mt permeabilisation during apoptosis (Lalier et al., 2007). Bax is one proapoptotic protein of the Bcl-2 family. Two conformational states of bax are present in cells: 1) cytosolic native bax and 2) activated bax associated with mt membrane permeabilisation. The switch from native to activated bax occurs during apoptosis. Oligomerised bax forms mt membrane permeability transition (PT) pores, loss of mt membrane potential with subsequent intermembrane release of two main groups of apoptogenic molecules into the cytosol (Wang, 2001; Saelens et al., 2004). Cytochrome c, second mitochondria-derived activator of caspases (smac)/DIABLO, and the serine protease HtrA2/Omi belong to the first group. This group of proteins brings about the activation of the caspase-dependent mt pathway (Elmore, 2007). An apoptosome is formed with cytochrome c, apoptotic protease activating factor (Apaf)-1 and procaspase-9. The oligomerisation of procaspase-9 in apoptosome formation results in the activation of caspase-9 which in turn activates the executioner caspases. Smac/DIABLO and HtrA2/Omi promote apoptosis by impeding the activity of inhibitor of apoptosis proteins (IAP) (van Loo et al., 2002; Schimmer, 2004). The second group of pro-apoptotic proteins includes caspase activated DNase (CAD), apoptosis inducing factor (AIF) and endonuclease G. The release of these proteins from the mt is a late event and occurs after the onset of apoptosis. Apoptosis inducing factor induces DNA fragmentation and condensation of peripheral nuclear chromatin after being translocated to the nucleus (Joza et al., 2001). Endonuclease G produces oligonucleosomal DNA fragments as a result of cleavage of nuclear chromatin (Li et al., 2001). Caspase activated DNase, whose cleavage and activity is dependent on caspase-3, also results in

oligonucleosomal DNA fragmentation but with more pronounced and advanced condensation of chromatin (Enari et al., 1998).

1.3.3 Executioner caspases and the inhibition of poly (ADP-ribose) polymerase-1 activity

The intrinsic and extrinsic pathways both converge at the activation of executioner caspases. Caspases-3 and -7 are responsible for the activation of cytoplasmic endonucleases (which degrade nuclear material) and proteases (which degrade cytoskeletal and nuclear proteins). Of the executioner caspases, caspase-3 is considered the most important (Elmore, 2007). Caspase activated DNase is an endonuclease that is specifically activated by caspase-3. Caspase activated DNase is complexed with an inhibitor ICAD in normal proliferating cells, but, caspase-3 cleaves ICAD to release CAD in apoptotic cells (Sakahira et al., 1998). Additionally, caspase-3 is instrumental in the disintegration of cells into apoptotic bodies by cytoskeletal reorganisation.

Another significant function of caspase-3 is the cleavage of poly (ADP-ribose) polymerase (PARP)-1. In response to DNA damage, the process of poly-ADP-ribosylation is vital for genomic maintenance (D'Amours et al., 2001). Poly (ADP-ribose) polymerase -1 is responsible for this process, and is known to be a key regulator of the DNA base excision repair system (de Murcia et al., 1997; Trucco et al., 1998; d'Adda di Fagagna et al., 1999; Vodenicharov et al., 2000). The activation of PARP-1 is also implicated in the regulation of transcription, DNA replication, protein degradation and cytoskeletal organisation (Hong et al., 2004). In apoptosis however, PARP-1 is cleaved by caspase-3, rendering it inactive (D'Amours et al., 2001) (Figure 5).

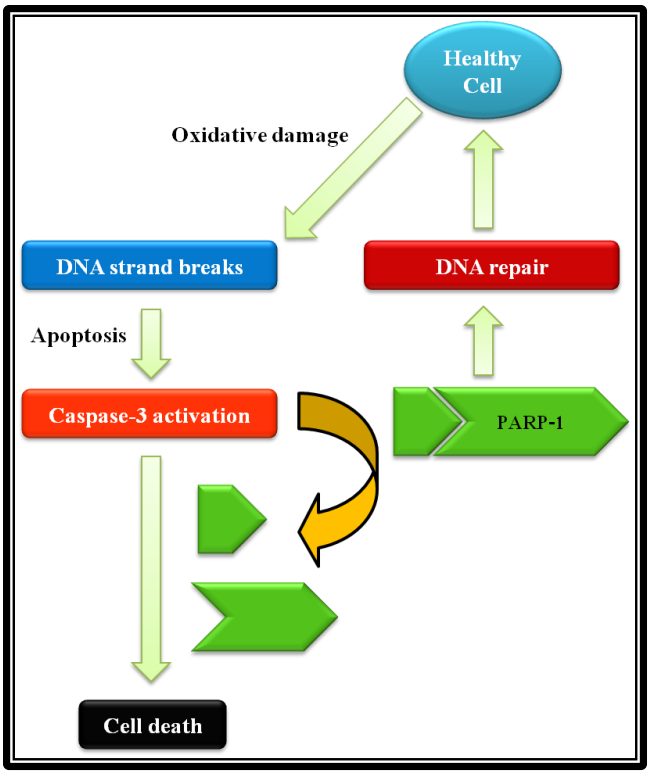

Figure 5: Fate of PARP-1 during apoptosis.

1.3.4 Inhibitor of apoptosis proteins

Amongst various molecules that are involved in the regulation of apoptosis, inhibitor of apoptosis proteins (IAPs) represent a group of proteins that serve as major control factors in the execution of cell death. Inhibitor of apoptosis proteins are characterised by a shared conserved sequence, the baculoviral IAP repeat (BIR) at the N-terminus and a conservative C-terminal really interesting new gene (RING) domain (Salvesen and Duckett, 2002). Baculoviral IAP repeat domains are 70 amino acid zinc-finger like structures that are essential for the anti-apoptotic functions of IAPs. These zinc fingers are able to bind to the surface of caspases such that amino acid linker sequences between BIR regions block the catalytic sites of caspases (Fan et al., 2005). One or more (up to three) BIR domains may be contained within IAPs (Chai et al., 2000). In humans, the following are some of IAP members that have been identified: cIAP1,

cIAP2, X-linked mammalian (X)-IAP, neuronal apoptosis inhibitory protein (NAIP), survivin and livin (Fan et al., 2005).

Inhibitor of apoptosis protein molecules function as endogenous inhibitors of caspase activity, the main executioners of programmed cell death (Fan et al., 2005). The mt- and death receptor-mediated programs of apoptosis both converge on the activation of executioner caspases. Studies have revealed more than one mechanism by which IAPs inhibit caspase activity; 1) the association of the IAP-BIR domain with the active sites of caspases, rendering them inactive, 2) IAP mediated degradation of active caspases and 3) the sequestering of caspases, by IAPs, away from their substrates (Wei et al., 2008). Different IAPs, in mammals, regulate caspase activity in various ways. Additionally, different BIR domains even within the same IAP molecule execute different caspase-inhibitory functions. For instance, in the death receptor-mediated apoptotic pathway, IAPs are not bound to caspase-8; rather, they inhibit its substrate – caspase-3. On the other hand, there are three ways by which IAPs execute their caspase suppression roles in the mt-mediated apoptotic pathway; 1) by competitively binding procaspase-9 and thus interfering with apoptosome formation between procaspase-9 and Apaf-1, 2) directly binding to caspase-9 and -3) directly binding to caspase-3 (Cheung et al., 2006).

X-linked mammalian IAP is recognized as the most well characterised IAP molecule and potent endogenous caspase inhibitor. This IAP contains three BIR regions namely BIR1, BIR2, and BIR3, each with high affinity for caspases but with varying functions. The BIR2 region and the linker area between BIR1 and BIR2 domains are known to specifically bind to and inhibit caspases-3 and -7. Specifically, the BIR2 region associates across the catalytic site of caspase-3, blocking the substrate binding pocket and thus inhibiting the activity of caspase-3. The BIR3 and RING domains are required for the inhibition of caspase-9. Inhibition of caspase-9, unlike that of

caspase-3, doesn't involve the binding of BIR domains to the active site. Rather, the BIR3 domain associates with monomeric procaspase-9 forming a heterodimer, preventing the dimerisation of procaspase-9 and activation of caspase-9 thereafter.

1.3.5 Smac/DIABLO

Smac/DIABLO is a proapoptotic protein that is released from the mt, during apoptosis, into the cytosol. The function of smac/DIABLO, as discussed earlier, is to promote the activation of caspases by competitively binding to IAP molecules, thus relieving caspases from the inhibitory effects of IAPs (Figure 6). Smac/DIABLO is synthesised with a 55 amino acid mt targeting sequence at the N-terminus. In a mature smac/DIABLO, the first four amino acids are crucial for their interaction with IAPs. The amino acids Ala-Val-Pro-Ile (AVPI) bind with BIR domains of IAPs (Chai et al., 2000). Alanine only becomes exposed once the signal sequence has been removed following mt entry. As a result, mt targeting becomes a vital step in the functioning of smac/DIABLO. Furthermore, this strategy makes certain that smac/DIABLO does not execute premature apoptosis before its entry into the mt (Wu et al., 2000).

The AVPI sequence of smac/DIABLO that binds to BIR3 domains of XIAP is much like the sequence of active caspase-9 to which XIAP binds (Ala-Thr-Pro-Phe). The IAP-binding region of caspase-9 is exposed only once procaspase-9 has been processed to its active form. Caspase-9 activity is thus inhibited upon XIAP binding, but is neutralised when smac/DIABLO competes off caspase-9 (Srinivasula et al., 2001).

It was also discovered that apart from the BIR3 domain of, smac/DIABLO can also form stable complexes with the BIR2 domain of XIAP (Chai et al., 2000). As mentioned earlier, the BIR2 domain and the linker area between BIR1 and BIR2 domains bind to and inhibit caspases-3 and -

7. Smac/DIABLO interacts with the BIR2 domain, hindering the XIAP inhibition of active caspases-3 and -7 sterically (Chai et al., 2000).

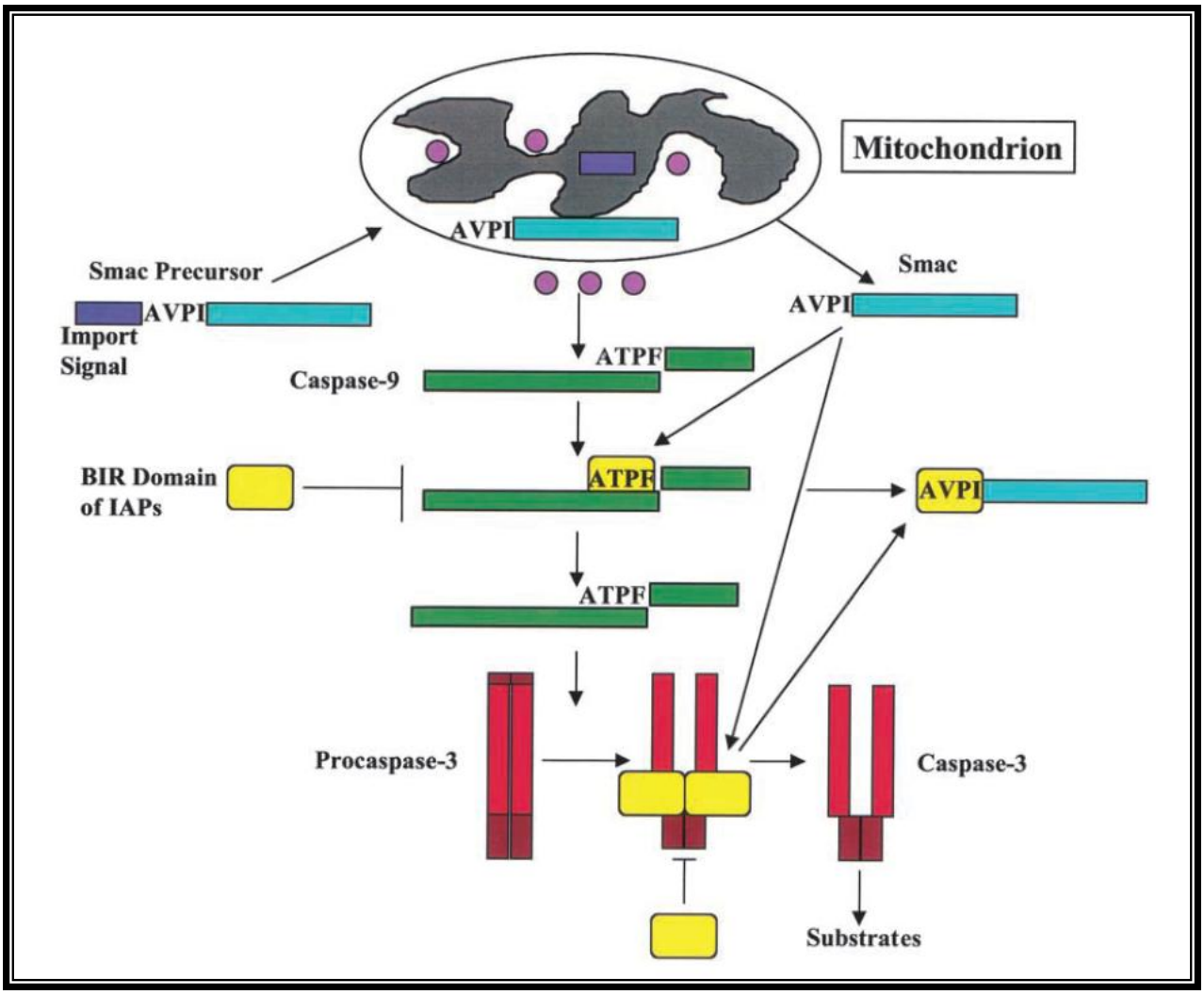

Figure 6: Regulatory function of smac/DIABLO in apoptosis (Wang, 2001). Copyright permission for reproduction was granted from the author.

The regulation between smac/DIABLO activation and IAP inhibition of caspases is an interesting one, suggesting a tightly controlled feedback system in cells. The release of cytochrome c from the mt results in apoptosome formation, upon associating with Apaf-1, with subsequent activation of caspase-9. However, this pathway is aborted when levels of IAP are

elevated. Inhibition of caspases by IAPs could be permanent as many IAPs contain a RING domain, which induces the proteosomal degradation of caspases (Yang et al., 2000; Suzuki et al., 2001). This feedback mechanism ensures that in the event of incidental mt leakage of cytochrome c, IAPs are readily available to sequester apoptosome formation and prevent uncontrolled and inappropriate cell death. However, if damage to the mt is extensive such as in a pathological state, more smac/DAIBLO will be released from the mt to counteract the effects of IAPs (Wang, 2001).

1.3.6 p53 and apoptosis

The p53 (tumour suppressor/transcription factor) protein is an extensively studied protein. p53 is implicated in a variety of cellular processes, however, its function in cell cycle arrest and apoptosis has been well documented. A range of stimuli can activate p53: hypoxia, DNA damage, cellular senescence and apoptosis (Fridman and Lowe, 2003). The disruption of p53 activity has been associated with genomic instability and the survival and proliferation of damaged cells. As such, it is not surprising that in human cancers, p53 is found most commonly dysregulated.

A well known trait of p53 is its ability to regulate transcriptional activity of genes in apoptosis. p53 has been reported to directly activate genes that promote apoptosis (el-Deiry, 1998; Yu et al., 1999; Sax and El-Deiry, 2003). The bax gene, for instance, harbours p53-binding spots in the promoter region and is thus upregulated in response to DNA damage and p53 (Miyashita and Reed, 1995). Members of a class of genes known as p53-induced genes (PIG) are involved in the induction of oxidative stress. p53-induced gene-3 was found to contain consensus p53 responsive elements for the binding of p53 in the promoter segment (Polyak et al., 1997).

1.4 Cancer cells evade apoptosis: promotion of tumourigenesis

Apoptosis plays an integral role in homeostatic control of cell proliferation and death. On one hand, the regulation of development and generation of the immune system is dependent on apoptosis. On the other hand, dysregulation of apoptotic pathways could lead to severe pathological conditions.

Cancer is a fatal outcome of disturbances in the apoptotic cascade. Particularly, incongruously low rates of apoptosis drive the proliferation of abnormal cells to form tumour masses. In this light, apoptosis is perceived as a 'barrier' to cancer (Hanahan and Weinberg, 2000). The ability of cancerous cells to evade apoptosis was first discovered during studies of follicular lymphoma, a cancer similar to Burkitt's lymphoma. This disease is characterised by the chromosomal translocation of the immunoglobulin (Ig) heavy chain locus to chromosome 18 known as bcl-2. The over expression of this gene in B cells permitted their survival, even under conditions that would sequester normal cell proliferation and promote apoptosis (Vaux et al., 1988).

Of the major external signals that trigger apoptosis, is Fas-L. Upon binding to its cognate receptor, Fas-receptor (CD95), the extrinsic apoptotic program is activated with the cleavage of procaspase-8 and activation of executioner caspases. The interaction between Fas-r/Fas-L and the respective signalling are thought to play a role in the pathology of carcinogenesis, the growth of tumours as well as metastasis (Owen-Schaub et al., 2000). Other members of membrane-associated death receptors include TNF-α- and TRAIL-receptors, whose function is similar to that elicited by CD95 upon ligand binding. It was discovered, in the 1990s, that cancerous cells have developed a mechanism to evade apoptosis mediated by Fas and TRAIL. This involved the

synthesis, by cancer cells, of decoy receptors that upon ligand binding would not induce apoptosis (Pitti et al., 1998; Ashkenazi and Dixit, 1999; Marsters et al., 1999).

Another strategy by which cancer cells acquire resistance to cell death is by a loss of function of the p53 tumour suppressor gene through a mutation (Hanahan and Weinberg, 2000). Functional inactivation of the p53 protein is seen in an excess of 50% of human cancers, resulting in the removal of one of the key components of the DNA damage sensory system that can initiate apoptosis (Harris, 1996).

Inhibitor of apoptosis proteins are found to be over expressed in various cancers. Survivin is one IAP that is expressed at high levels in cancer cells compared to normal cells (Ambrosini et al., 1997). Survivin is thought to play a role in cell division (Reed and Bischoff, 2000; Uren et al., 2000), which could explain why their expression is high in actively dividing cancer cells as opposed to normal differentiated cells.

1.5 Drug intervention: induction of apoptosis in cancer

A number of efforts have been made on the drug development frontier for the induction of apoptosis in tumour cells, some of which have proved beneficial. An in depth understanding of the apoptotic cascade under physiological as well as pathological conditions is essential for the development of apoptotic inducing/inhibiting drugs.

In cancer, various approaches have been postulated with many drugs currently in preclinical trials. The activation of caspases, the chief executioners of apoptosis, in tumour cells is one such approach. Inducible caspases have been engineered by fusing them with chimeric dimerisation domains. Following delivery of these chimeric domains to tumour cells via adenoviral gene transfer, caspases may be triggered on demand to induce apoptosis (MacCorkle et al., 1998; Shariat et al., 2001). A report on the success of inducible caspase-9 in targeted prostate cancer cells *in vitro* was published (Xie et al., 2001). Prostrate tumour growth was suppressed just by simple intraperitoneal injection of the inducible caspase into mice, increasing survival.

Inhibitor of apoptosis proteins are another target for apoptosis induction, considering their stringent regulatory attributes. Antisense strategies that target XIAP and survivin are presently in preclinical testing (Fischer and Schulze-Osthoff, 2005). Various antisense oligomeric nucleotides are constructed with short sequences that are complementary to the messenger ribonucleic acid (mRNA) of target IAP molecules. The hybridisation of antisense oligonucleotide constructs with target mRNA prevents the translation of mRNA. Additionally, it has been shown that enzymes such as RNase H target the mRNA/antisense oligonucleotide complex, degrading the mRNA freeing the antisense construct to target and bind to another mRNA strand (Fischer and Schulze-

Osthoff, 2005). This strategy has been shown to sensitise a range of tumour cell lines to chemo- or radiotherapy (Holcik et al., 2000; Sasaki et al., 2000).

As described previously, smac/DIABLO functions in antagonising the caspase-inhibitory effects of IAPs, making smac/DIABLO another target candidate for the promotion of apoptosis in cancer therapy. Smac peptides or smac mimetic drugs have been manufactured by companies for restoration of caspase activity; however, these approaches have not been successful when used as single agents (Fischer and Schulze-Osthoff, 2005). Nonetheless, smac peptides were found to sensitise cancerous cell lines as well as murine models of human glioma and lung cancer to chemotherapy (Arnt et al., 2002; Fulda et al., 2002; Guo et al., 2002; Tamm et al., 2003; Yang et al., 2003). Smac mimetic drugs synthesised from oxazoline were able to target XIAP, cIAP1 and cIAP2, with synergised effects upon TNF and TRAIL administration in cancer cell cultures (Li et al., 2004). Sun et al., in 2004, reported on a synthesised smac mimetic drug that bound XIAP and enhanced apoptosis induced by cisplatin in human prostate cancer cells with no effect when exposed to these cells alone (Sun et al., 2004).

Various problems have been encountered with the use of smac mimetic drugs and peptides. For example, small smac peptides bind with less efficiency to XIAP compared to the wild type protein due to a difference in the length. The extent to which smac peptides interact with XIAP is not sufficient to relieve caspase-9. Some tumours express high levels of various isoforms of IAPs thus the inhibition of a single IAP isoform by drugs might be inadequate (Krajewska et al., 2003).

Although these few mentioned therapies may be of use in the near future, the cost factor may be prohibitive. Attention should be given to the development of safer and cheaper therapeutics that

are easily accessible. This study is a preliminary one that highlights the potential use of AA_{AgNP} as an alternative for cancer therapy.

1.6 Aims and objectives

This study was conducted to determine the following:

- The effect of AA_{AgNP} on human lung carcinoma A549 cell viability.
- The oxidative status of A549 cells exposed to AA_{AgNP}.
- The expression of selected apoptotic markers induced by AA_{AgNP} in A549 cells.
- The apoptotic pathway activated in A549 cells when treated with AA_{AgNP}.

CHAPTER TWO

2 MATERIALS AND METHODS

2.1 Materials

The A549 cells were purchased from Highveld Biologicals (Johannesburg, SA). Cell culture reagents were purchased from Whitehead Scientific (Johannesburg, SA). LumiGLO® chemiluminescent substrate kit was purchased from Gaithersburg (United States of America (USA)) and western blot reagents were purchased from Bio-Rad (USA). All other reagents were purchased from Merck (South Africa). AA_{AgNP} was obtained from Dr. Robert M. Gengan (Steve Biko campus), Durban University of Technology (DUT), Durban, SA.

2.2 Synthesis and characterisation of AA_{AgNP}

The preparation and characterisation of AA_{AgNP} was conducted by Dr. R.M Gengan, DUT. A one-pot green synthesis technique was used. Briefly, fresh leaves of AA were extracted, washed with deionised water and 20g of finely cut leaves were added to 200ml of deionised water. Leaves were boiled (15min) and the crude extract was filtered after cooling with Whatman no.1 filter paper. The supernatant (1ml) was then allowed to react with 0.001 M silver nitrate ($AgNO_3$) solution (49ml) at room temperature (RT). The AA_{AgNP} solution (pH 7) was then characterised using UV spectrometry. Particle size was determined by transmission electron microscopy (TEM). To assess the interaction between nanosilver and compounds of the aqueous extracts of AA leaves, Fourier transform infrared (FTIR) spectrophotometry was employed (Gengan et al., 2012). Data for these assays can be accessed from the appendix section (Appendix A1-3).

2.3 Cell culture and exposure protocol

The A549 cells were cultured in complete culture media (CCM) consisting of Eagle's minimum essential medium supplemented with 1% L-glutamine, 1% penstrepfungizone and 10% foetal bovine serum. Cultures were maintained at 37°C with 5% CO_2. For the 3-(4,5-Dimethyl-2-thiazolyl)-2,5-diphenyl-2H-tetrazolium bromide or methylthiazol tetrazolium (MTT) assay, cells were seeded into a 96-well microtitre plate, allowed to attach overnight and treated with AA_{AgNP} solution (0-75µg/ml) for 6h. For flow cytometry assays, caspase, ATP and lipid peroxidation assays, cells were cultured to 90% confluency in 25cm^2 tissue flasks and treated with AA_{AgNP}. For the GSH assay, cells were plated in 96-well microtitre plates and allowed to attach overnight, followed by treatment with AA_{AgNP}. For western blot analysis, quantitative polymerase chain reaction (Q-PCR) and the comet assay, cells were grown to 90% confluency in 6-well culture plates and treated with AA_{AgNP}.

2.4 Cell viability

2.4.1 MTT assay

2.4.1.1 Introduction

Cell viability was determined using the MTT assay. Methylthiazol tetrazolium is a yellow water soluble tetrazolium dye that when reduced by viable cells turns into a purple water insoluble formazan product. This reaction is dependent on the availability of cellular oxidoreductases, which are enzymes that catalyse the transfer of electrons from a reductant to an oxidant compound. Reducing equivalents nicotinamide adenine dinucleotide (NADH) and flavin adenine

dinucleotide ($FADH_2$) produced in the tricarboxylic acid (TCA) cycle are used as cofactors by oxidoreductases (Figure 7).

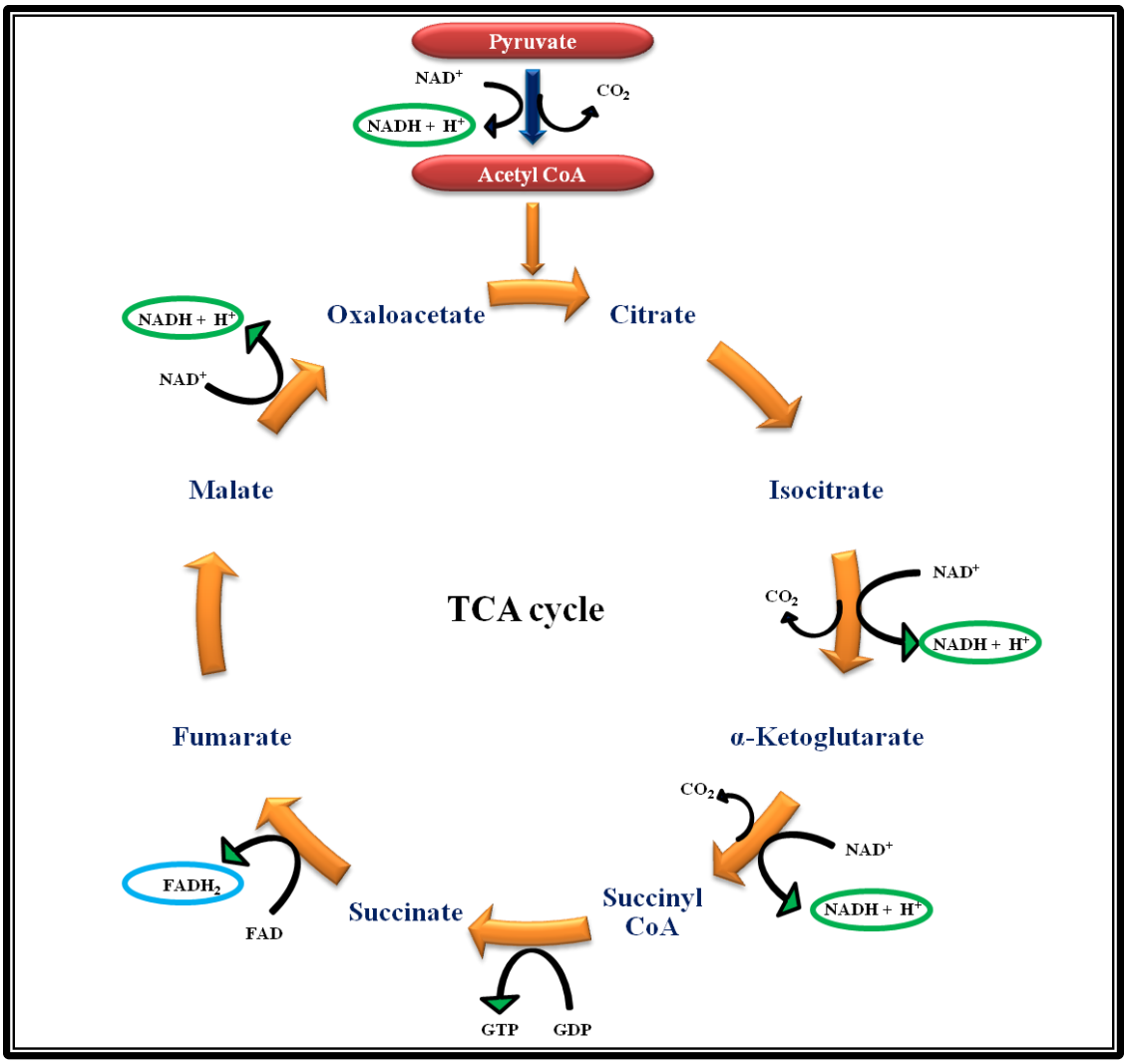

Figure 7: The production of NADH and $FADH_2$ in the TCA cycle for oxidative phosphorylation in the ETC for the generation of ATP.

The functioning of oxidoreductases is therefore indicative of the metabolic activity, thus viability, of the cell. The intensity of the formazan produced is proportional to the metabolic activity within the cell.

2.4.1.2 Protocol

For the MTT assay, approximately 20 000 cells (in six replicates) were used for exposure to AA_{AgNP} concentrations in the treatment range (0-75µg/ml). After incubation with AA_{AgNP} for 6h, cells were washed twice with 0.1M phosphate buffer saline (PBS) and incubated with MTT salt solution (5mg/ml in 0.1M PBS) and complete culture medium (37ºC, 4h). Thereafter, 100µl of dimethyl sulphoxide (DMSO) was added to each well and incubated (37ºC, 1h). The optical density of the formazan product was measured using a spectrophotometer (Bio-tek µQuant) at 570/690nm. The results were expressed as percentage cell viability vs. concentration of AA_{AgNP}, from which the half maximal inhibitory concentration (IC_{50}) was determined (Appendix B).

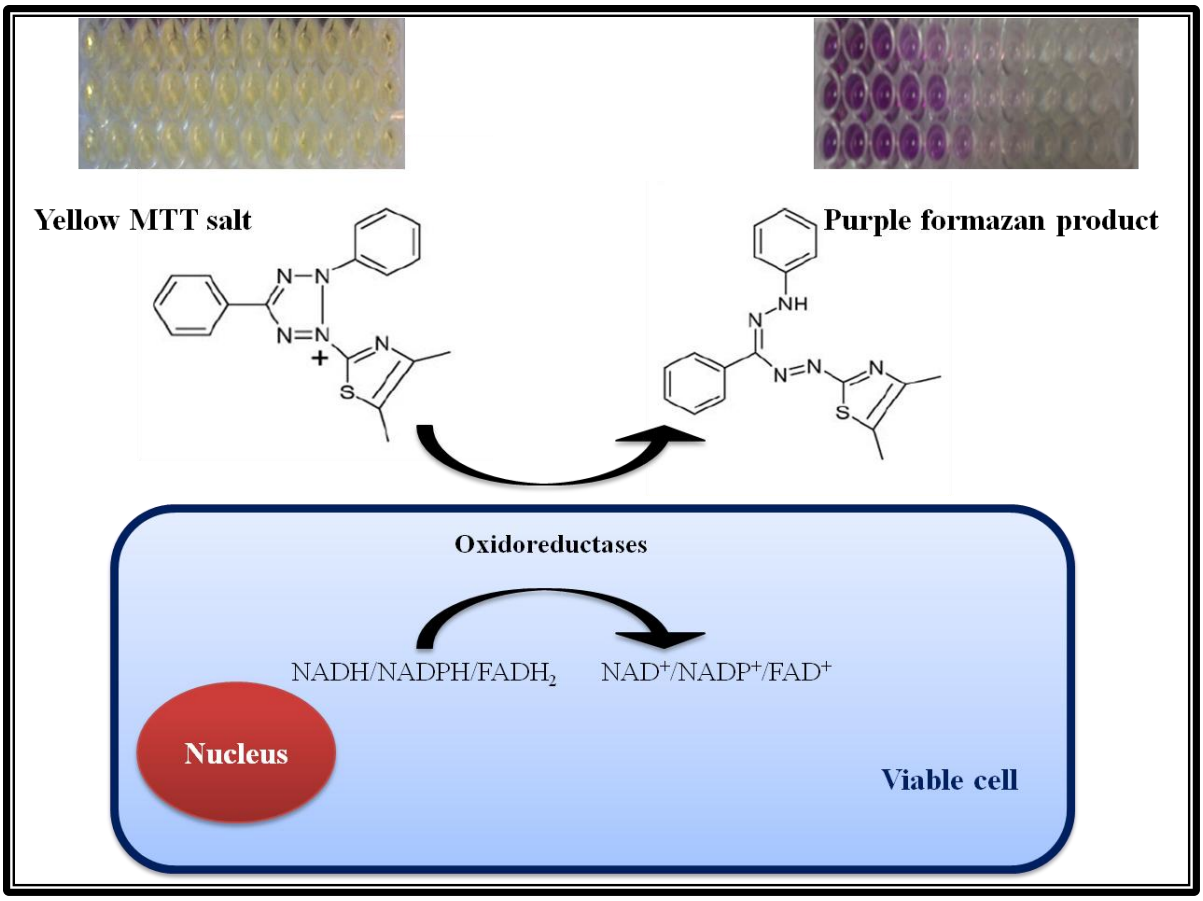

Figure 8: Schematic of the reduction of MTT salt to formazan by a viable cell.

2.4.2 ATP ASSAY

2.4.2.1 Introduction

Cellular ATP production is an essential process of living organisms. The mt respiratory chain or electron transport chain (ETC) is most responsible for ATP production. Located in the inner mt membrane, the respiratory chain entails two synchronised processes; 1) the passage of electrons through the complexes to generate an electrochemical proton gradient and 2) the phosphorylation of ADP via ATP synthase as protons is channelled through (Figure 9).

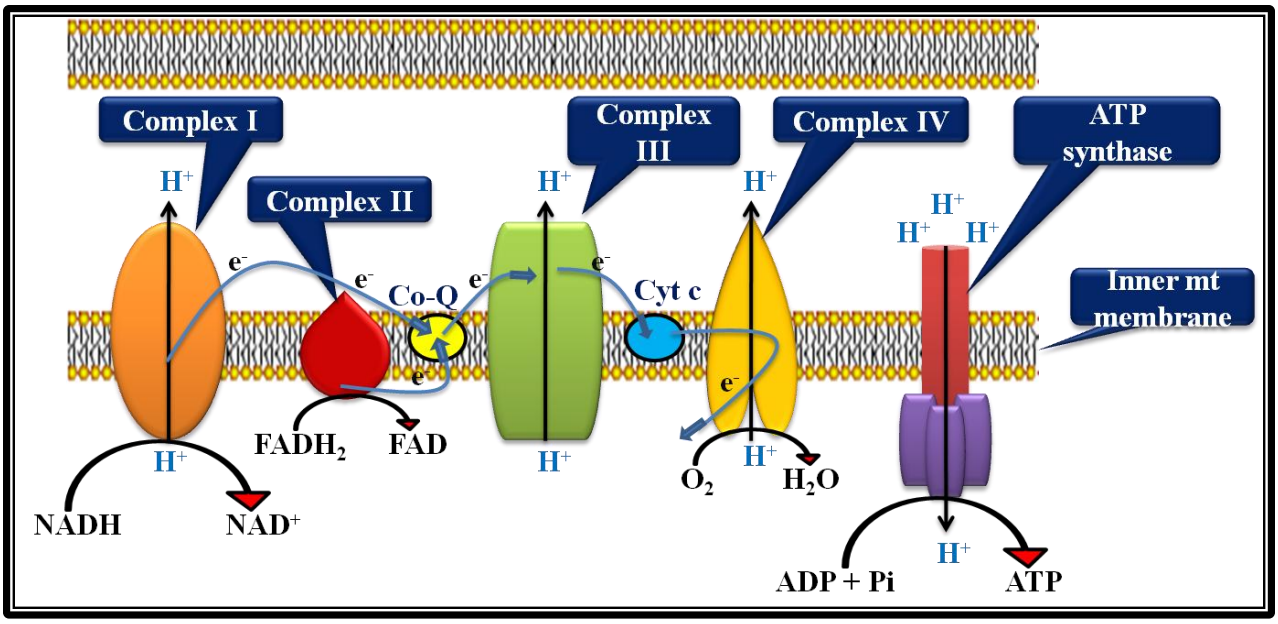

Figure 9: Illustration of the ETC located within the inner mitochondrial membrane.

Oxidative phosphorylation, in the ETC, coupled to substrate level phosphorylation, in glycolysis and the TCA cycle, ensures the optimum production of ATP required by the cell for its sustenance and viability. Essential cofactors NADH and $FADH_2$ are produced in the TCA cycle which feed into the ETC (Figure 7).

2.4.2.2 Protocol

To determine ATP concentration, the CellTire Glo™ (Promega) assay was used. Cells (20 000/well) were alliquoted in an opaque microtitre plate to which the ATP CellTitre Glo™ reagent (50µl) was added and allowed to react in the dark (30min, RT). Following incubation, the luminescent signal proportional to the cellular ATP content was detected with a Modulus™ microplate luminometer (Turner Biosystems, Sunnyvale, USA). Results are expressed as mean relative light units (RLU).

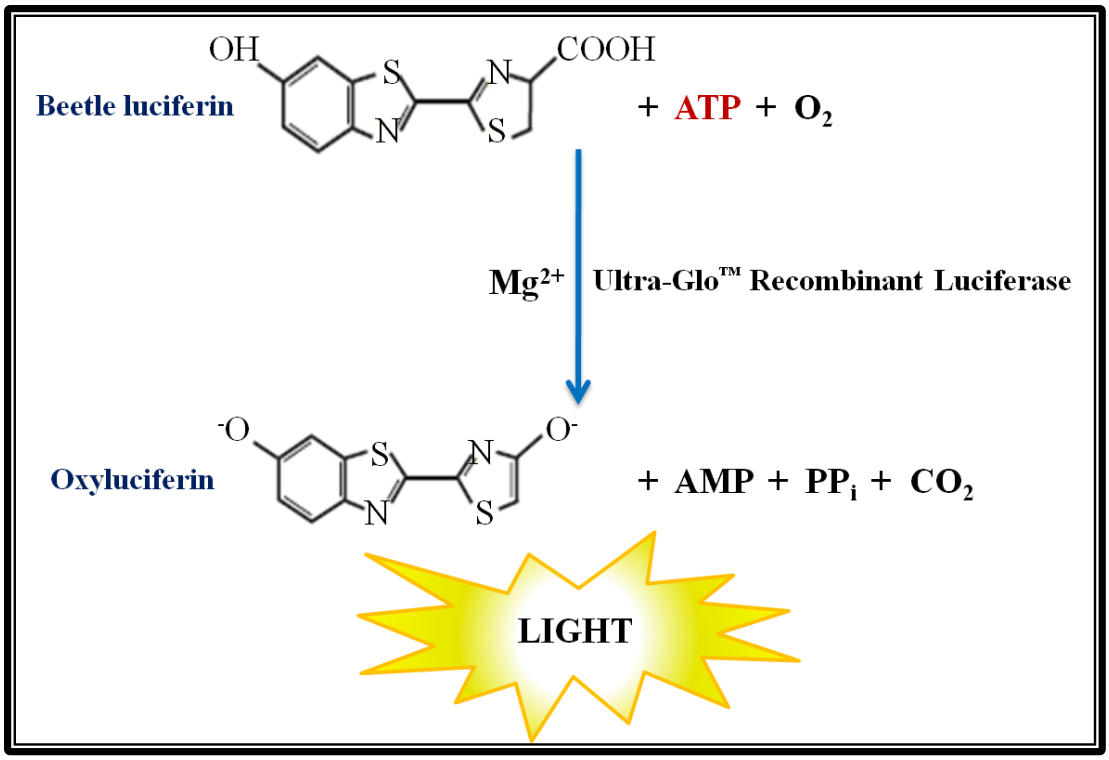

Figure 10: Principle of the CellTire Glo™ assay for the quantification of cellular ATP.

2.5 Oxidative stress

2.5.1 Glutathione assay

2.5.1.1 Introduction

An excessive formation of ROS is cytotoxic. Therefore, systems that metabolise and scavenge ROS are functionally critical and tightly regulated in the cell. Glutathione is a low molecular weight, water soluble thiol that is found most abundantly in the cytosol of cells. Composed of the amino acids glycine, cysteine and glutamine, this anti-oxidant tripeptide plays an important role

in the detoxification of peroxides and electrophilic species (Townsend et al., 2003). Glutathione is able to effectively scavenge ROS such as hydrogen peroxide (H_2O_2), peroxynitrite as well as hydroxyl- and lipid peroxyl radicals (Wu et al., 2004). The thiol exists in an oxidized (glutathione disulphide (GSSG)) and a reduced (GSH) form in cells. Glutathione-S-transferase (GST) and glutathione peroxidase (GPx) are enzymes that catalyse the GSH-mediated detoxification of electrophilic compounds. Glutathione serves as the electron donor in a reduction reaction catalysed by GPx to detoxify peroxides (Figure 11).

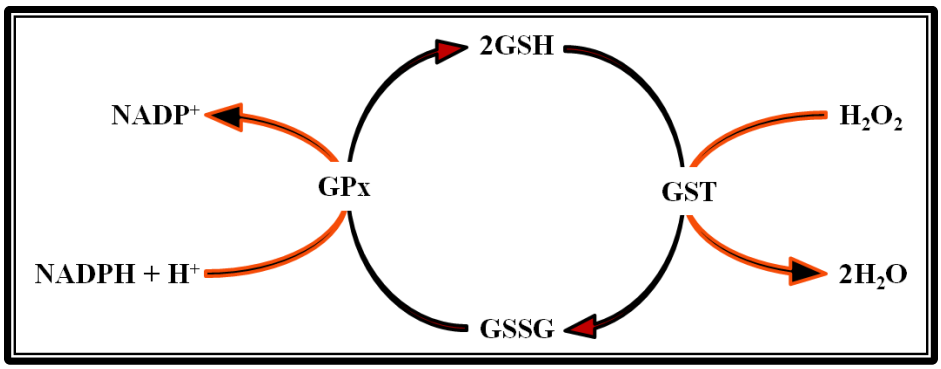

Figure 11: Detoxification of H_2O_2 by glutathione-S-transferase and the regeneration of glutathione from glutathione disulphide by peroxidase.

2.5.1.2 Protocol

The GSH-Glo™ Glutatione assay (Promega, Madison, USA) was utilized to quantify intracellular GSH levels. Subsequent to treatment of cells (10 000 cells/well in six replicates) in an opaque 96-well microtitre plate, culture medium was removed and 25µl of 1X GSH-Glo™ reagent (prepared according to manufacturer's guidelines) was added to each well. GSH standards (0-5µM) were serially diluted (two-fold) from a 5mM stock in deionised water. After

brief mixing on a shaker and 30min incubation at RT, 100µl of Luciferin detection reagent was added to the wells (15min, RT). Luminescence was detected on a Modulus™ microplate luminometer (Turner Biosystems, Sunnyvale, USA). A standard curve was constructed and sample GSH concentrations (µM) were calculated.

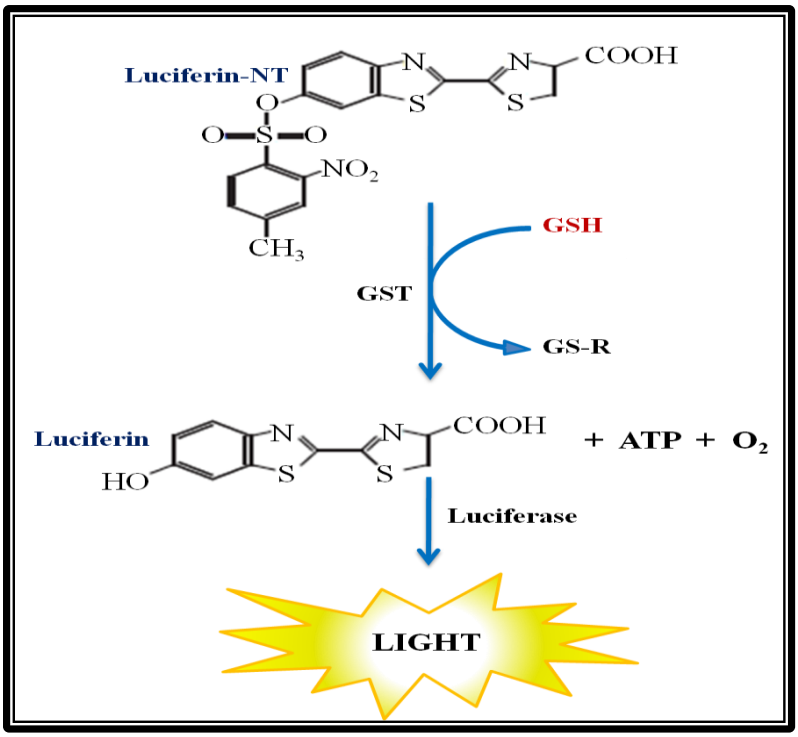

Figure 12: Schematic overview of the principle of the GSH-Glo™ Glutatione assay.

2.5.2 Lipid peroxidation

2.5.2.1 Introduction

Lipid peroxidation is a process whereby lipids become oxidised, forming lipid peroxides as a result of free radical attack during oxidative stress. Polyunsaturated fatty acids (PUFAs) are most

susceptible to lipid peroxidation due to the presence of double bonds between adjacent carbon atoms (Figure 13).

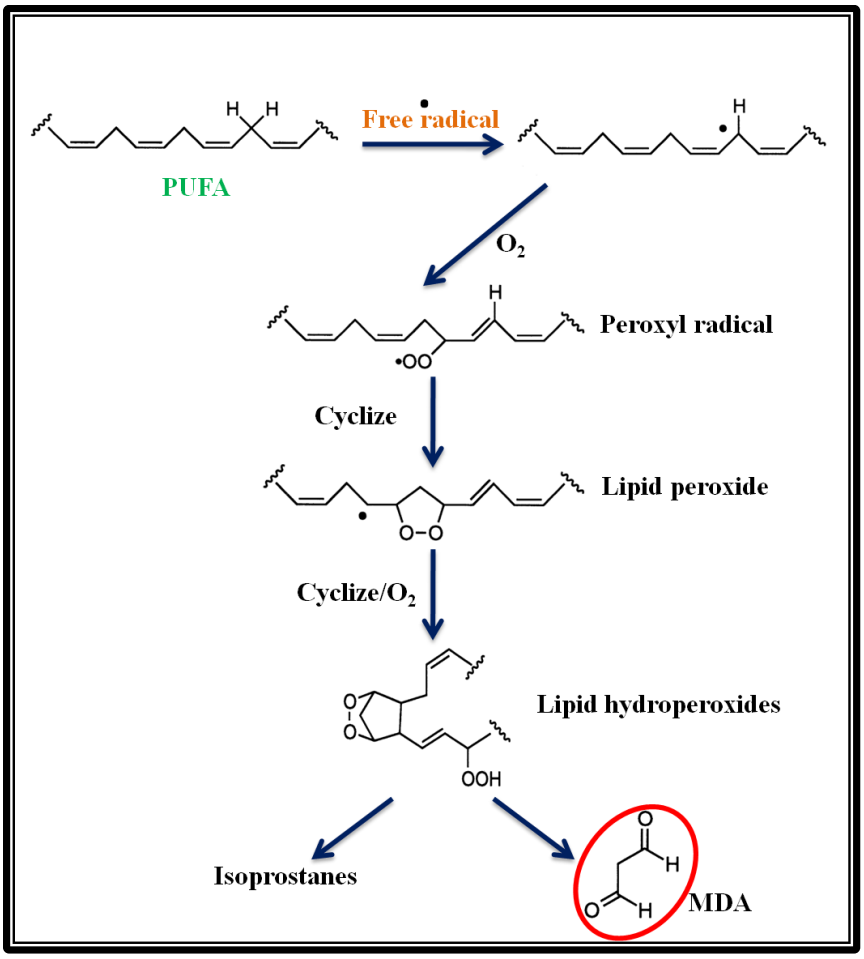

Figure 13: Chain reaction mechanism of lipid peroxidation.

The chain reaction mechanism of lipid peroxidation is initiated when oxidising agents, such as free radicals, react with and remove hydrogen (H) atoms from PUFAs. This results in the formation of carbon-centred radicals. In an oxidation reaction with oxygen (O_2) carbon-centred radicals form peroxyl radicals and hydroperoxides which are then reduced to form reactive isoprostanes and aldehyde by-products (Marnett, 1999) (Figure 13). Malondialdehyde (MDA) is

one such reactive by-product that is routinely used as a biomarker for lipid peroxidation (Janero, 1990).

2.5.2.2 Protocol

To investigate the AA_{AgNP}-mediated generation of ROS, MDA levels were measured using the thiobarbituric acid reactive substances (TBARS) assay.

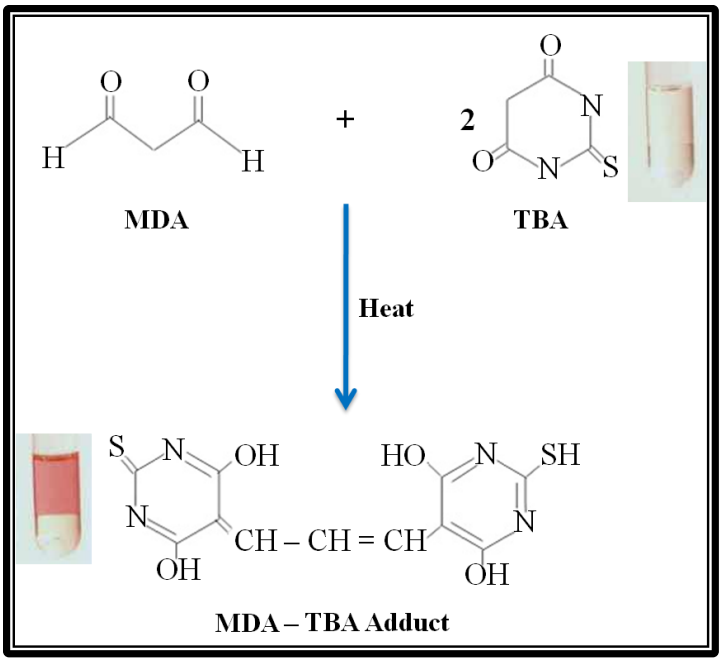

Figure 14: The reaction of malondialdehyde with thiobarbituric acid.

Briefly, the following was added to a set of test tubes: 200µl of 2% H_3PO_4, 400µl of 7% H_3PO_4, 400µl of thiobarbituric acid (TBA)/butylated hydroxytoluene (BHT) solution and 200µl of 1M HCL. Following treatment of cells (50 000 cells/well) in a 6-well plate, supernatants were recovered. For test samples, 100µl of cell supernatant (in triplicate) was then added to each test tube. A positive control was prepared by adding 1µl of MDA to a test tube. All tubes were incubated in a water bath (100°C, 15min) and after cooling; butanol (1.5ml) was added to each

tube, vortexed for 10 seconds and allowed to separate into two distinct phases. Approximately 800µl of the upper butanol phase was then transferred to 1.5ml tubes and centrifuged (840 x g, 24°C; 6min). To a 96-well micotitre plate, 100µl of supernatant was transferred in six replicates and the absorbance read using a spectrophotometer (Bio-tek µQuant) at 532/600nm. One molecule of MDA reacts with two molecules of TBA to form a coloured product (Figure 14). The mean absorbance was divided by the extinction co-efficient ($156mM^{-1}$) and results were expressed as µM concentrations.

2.6 Analysis of apoptotic parameters

2.6.1 Assessment of caspase activity

2.6.1.1 Introduction

As mentioned earlier, caspases form the engine of apoptosis. The cleavage of inactive caspases (zymogens) is necessary for their catalytic activity and subsequent execution of cell death. The caspase assay used in this study is a luminometric assay that determines the activity of caspases based on the cleavage of caspase-specific Luciferin substrates. The amount of light generated by Luciferase is therefore proportional to the activity of the caspase being analysed.

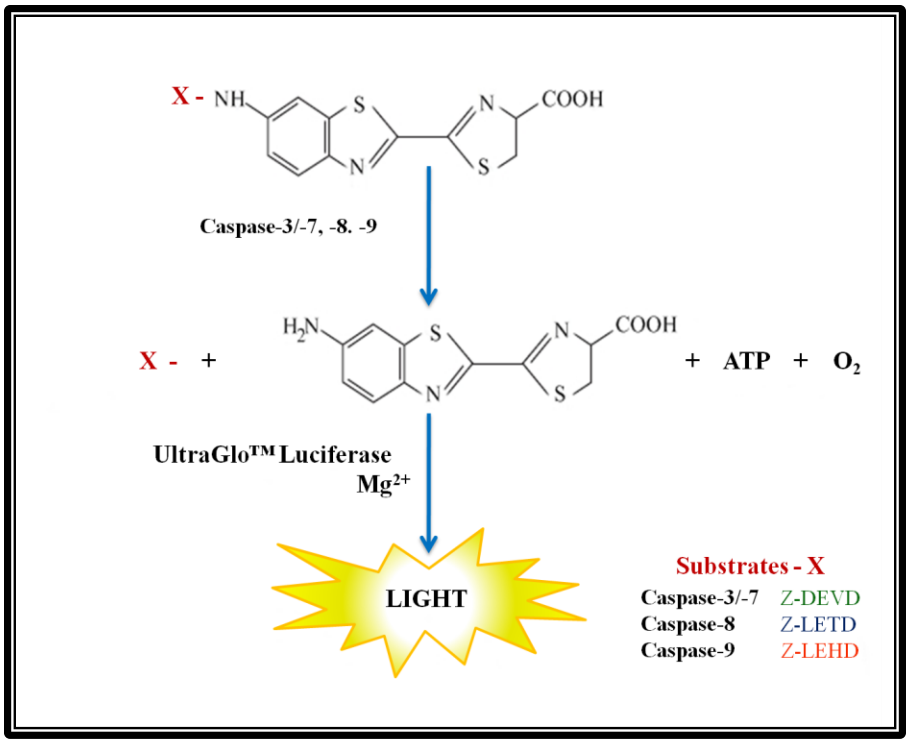

Figure 15: Principle for the detection of caspase activity.

2.6.1.2 Protocol

Caspase-3/-7, -8 and -9 activities were detected with Caspase-Glo® assays (Promega, Madison, USA). As per manufacturer's protocol, Caspase-Glo®-3/-7, -8 and -9 reagents were reconstituted and added to wells (in six replicates) of an opaque 96-well microtitre plate (40µl of reagent per 100µl of 10 000 cells/well). Samples were mixed and incubated in the dark (30min, RT). The luminescent signal was measured on a Modulus™ microplate luminometer (Turner Biosystems, Sunnyvale, USA). Caspase-3/-7, -8 and -9 activities were expressed as RLU.

2.6.2 Annexin-V Fluos assay

2.6.2.1 Introduction

To determine the mode of cell death, the annexin-V-Fluos kit (Roche) was used. This assay comprises of annexin-V and propidium iodide (PI) and relies on flow cytometry for analysis. An early stage characteristic of apoptotic cells is the externalisation of phosphatidyl serine (PS). Necrotic cells, however, are identified by the leakage of DNA. Therefore, the percentage of PS translocated cells and DNA leakage was measured to give an indication of the amount of cells undergoing apoptotic and necrotic cell death respectively. Annexin-V is a calcium dependent phospholipid binding protein with a high affinity for PS whereas PI stains DNA (Figure 16). Exploiting these two components allows for the differentiation of apoptotic and necrotic cells. Annexin-V is conjugated to the fluorochrome fluorescein isothiocyanate (FITC). When analysed flow cytometrically, cells with externalized PS fluoresce green (excitation-488nm; emission-518nm) and DNA stained with PI fluoresce red (excitation-488; emission-617nm).

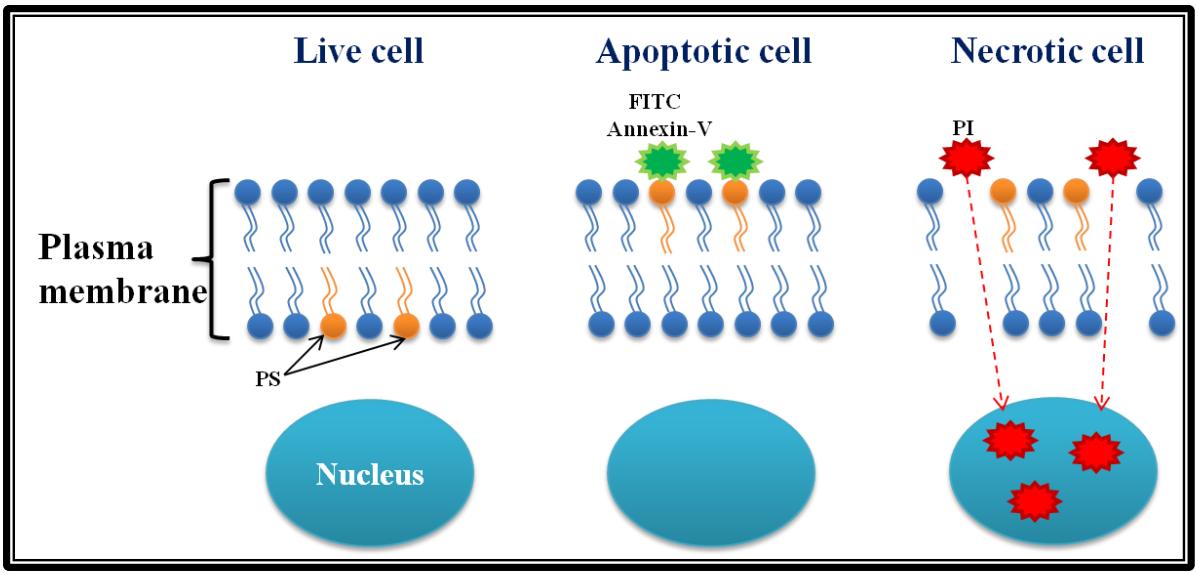

Figure 16: The use of annexin-V and propidium iodide for the analysis of apoptotic and necrotic cells**.**

2.6.2.2 Protocol

To each flow cytometry tube, 100µl of staining buffer, 100µl of annexin-V-Fluos labelling solution (annexin-V: PI: staining buffer (1:1:50 vol/vol/vol)) and 100µl of cell suspension was added, and incubated in the dark (15min, RT). Samples were analysed on a FACS Calibur (BD Biosciences) flow cytometer. Data were analysed using CellQuest PRO v4.02 software (BD Biosciences). Cells were gated to exclude cellular debris using FlowJo v7.1 software (Tree Star, Inc). Approximately 50 000 events were analysed for apoptotic (annexin-V +ve, PI -ve), necrotic (annexin-V +ve, PI +ve) and live cells (annexin-V -ve, PI -ve). The results were expressed as percentage of the total events.

2.6.3 JC-1 Mitoscreen assay

2.6.3.1 Introduction

Energy that is produced during oxidative phosphorylation is stored across the mt membrane as negative electrochemical potential. In this state the membrane is referred to as being polarised. Depolarisation of mt membrane occurs when there is a collapse in electrochemical potential. Mt depolarisation is observed as a crucial early event in apoptosis. The BD™ MitoScreen kit (BD Biosciences) was used to assess mt membrane potential ($\Delta\Psi$). J-aggregate-forming cationic dye (JC-1) is a lipophilic fluorochrome that is sensitive to $\Delta\Psi$. This dye exists in a monomeric (at low concentration) as well as an aggregated form (at high concentration), both of which emit fluorescence in the green spectral region. When incubated with live cells, the fluorochrome penetrates the cell membrane (in its monomeric form) and is taken up by the mt. This process is mediated by $\Delta\Psi$. The accumulation of JC-1 monomers inside the mt membrane leads to aggregation of the dye, which results in a spectral shift and the emission of red fluorescence (excitation-488nm; emissiom-590nm). When mt are depolarised, JC-1 remains in the cytoplasm as monomers and no spectral shift is seen (green fluorescent emission: excitation-488nm; emission-527nm) (Figure 17).

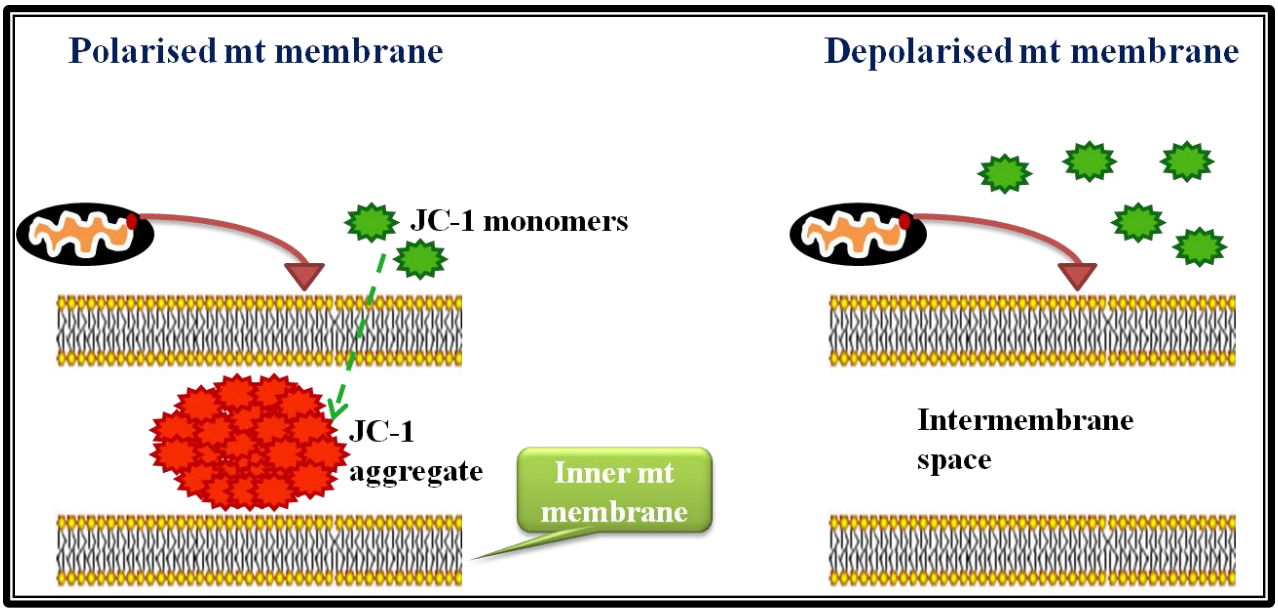

Figure 17: Distinction between mitochondrial membrane polarisation and depolarisation.

2.6.3.2 Protocol

J-aggregate-forming cationic dye working solution was prepared (JC-1; 1x JC-1 wash buffer (1:50 vol/vol)) and 100µl added to each flow cytometry tube, followed by 100µl of cell suspension. Tubes were incubated at 37°C with 5% CO_2 for 15min, after which 100µl of 1x JC-1 wash buffer was added. Approximately 50 000 events were analysed for mt depolarisation. A FACS Calibur (BD Biosciences) flow cytometer was used. Data were analysed using CellQuest PRO v4.02 software (BD Biosciences). Cells were gated to exclude cellular debris using FlowJo v7.1 software (Tree Star, Inc). The results were expressed as percentage of the total events.

2.6.4 Comet assay

2.6.4.1 Introduction

In mt-mediated apoptosis, a group of proteins are released from mt downstream of the apoptotic cascade that is responsible for the cleavage or fragmentation of DNA, an end stage feature of apoptosis. The comet assay or otherwise known as single cell gel electrophoresis (SCGE) is a simple procedure that detects DNA strand breaks and is used in genotoxicity testing. In this assay, cells are embedded on a microscopic slide with agarose and lysed with a high salt and detergent solution. The result is the formation of nucleoids that contain supercoiled DNA. When subjected to an electric field at high pH, loops of supercoiled DNA that contain breaks resemble comets following migration toward the anode (Collins, 2004). The application of the intercalating agent, ethidium bromide (EtBr), allows for the visualisation of comet tails using a fluorescent microscope. Comet tail lengths reflect the extent of DNA damage.

2.6.4.2 Protocol

The comet assay was used to determine DNA fragmentation in the AA_{AgNP} treated lung cells. Briefly, three slides per sample were prepared with a first layer containing 400µl of 1% low melting point agarose (LMPA, 37°C), a second layer of 25µl of cells from each sample with 175µl 0.5% LMPA (37°C) and a third layer containing 200µl of 1% LMPA (37°C). Cover slips were removed and slides were subjected to lysis (4°C, 1hr, protected from light) by being submerged in cells lysis buffer (2.5M NaCl, 100mM EDTA, 1% Triton X-100, 10mM Tris (pH 10) and 10% DMSO). The slides were equilibrated in electrophoresis buffer (300mM NaOH, 1mM Na_2EDTA, pH 13; 20min) then electrophoresced (300mA, 25V, 35min) after which slides were washed three times (0.4M Tris, pH 7.4; 5min) and finally stained with 40µl EtBr. Cover

slips were placed onto slides and maintained overnight at 4°C. Slides were viewed using a fluorescent microscope (Olympus IXSI inverted microscope/510-560nm excitation and 590nm emission wavelengths). Images were captured and comet tails of 50 cells were measured using Life Science-Soft Imaging System (analySIS® v5). The results were expressed as mean tail length in μm.

2.6.5 CD95 extracellular staining

2.6.5.1 Introduction

The extrinsic apoptotic pathway is mediated by cell surface death receptors. CD95 (Fas receptor) is one such receptor whose expression varies in different pathologies. Binding of Fas-L to CD95 initiates a cascade that leads to the activation of initiator caspase-8 (Figure 18). The expression of CD95 was determined by a cell surface staining assay. Treating cells with an antibody, against CD95, conjugated to FITC allows for the detection of cells expressing CD95 by virtue of fluorescent emission using a flow cytometer.

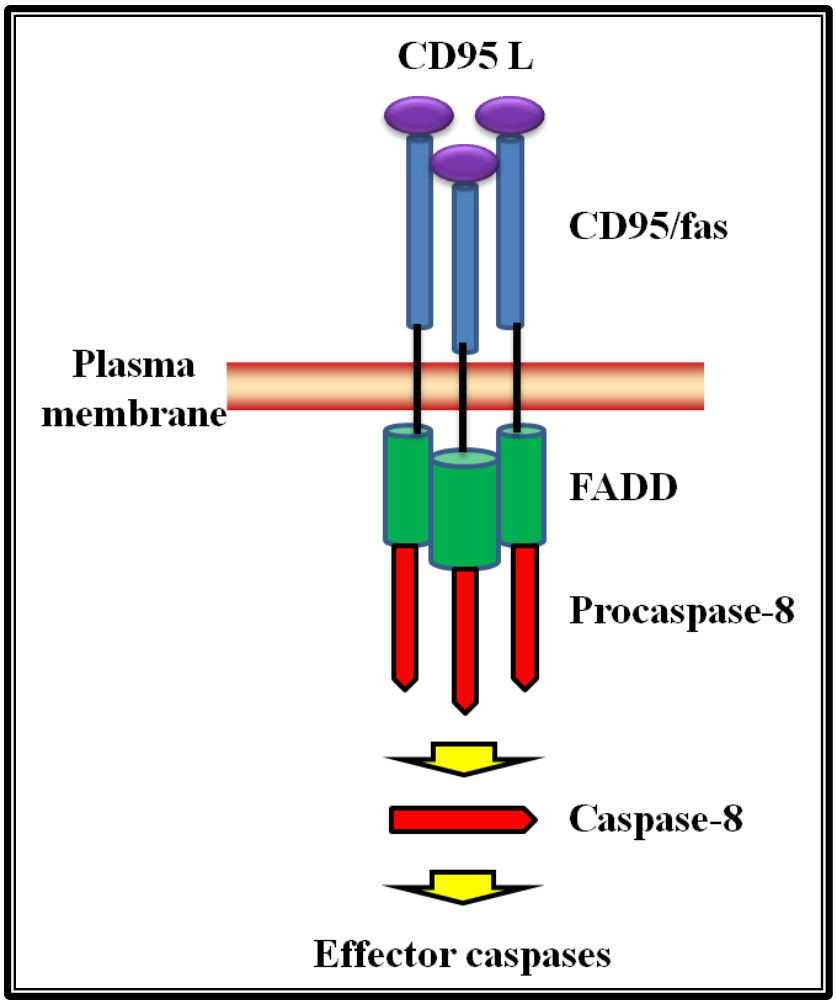

Figure 18: CD95 death receptor-ligand binding and the activation of caspase-8.

2.6.5.2 Protocol

Briefly, 100µl of 0.1M PBS and 1µl of FITC conjugated mouse anti-human CD95 antibody (BD Pharmingen, 555673) was added to 100µl of cell suspension. Reaction mixture was incubated in the dark for 15min at RT, thereafter run on a FACS Calibur. Data were analysed using CellQuest PRO v4.02 software. Cells were gated to exclude cellular debris using FlowJo v7.1 software. The results were expressed as a percentage. Histograms are presented in Appendix C1.

2.6.6 Smac/DIABLO intracellular staining

2.6.6.1 Introduction

Amongst various pro-apoptotic proteins that are released from the mt, is smac/DIABLO. This protein counteracts the caspase inhibitory effects of IAPs. Similar to CD95 analysis, intracellular levels of smac/DIABLO were assessed by intracellular staining using flow cytometry. Anti smac/DIABLO conjugated to a fluorochrome - allophycocyanin (APC: excitation-650nm; emission-660nm) is added to a suspension of cells after treatment with a permeabilising agent. When analysed on a flow cytometer, the amount of fluorescence emitted is proportional to the level of smac/DIABLO.

2.6.2.2. Protocol

Cells were rendered permeable by incubation in Fix and Perm medium A (Caltag) (15min in the dark), after which they were treated with Fix and Perm medium B (Caltag) containing monoclonal anti-smac/DIABLO primary antibody (smac/DIABLO, ab110291) (1:500; 30min, RT). After washing, cells were re-suspended in medium B containing APC conjugated anti-mouse secondary antibody (Thermo Scientific, 31430) (1:100; 15min, RT) protected from light. Cells were then washed, re-suspended in 0.1M PBS and run on a FACS Calibur. Data were analysed using CellQuest PRO v4.02 software. Cells were gated to exclude cellular debris using FlowJo v7.1 software. The results were expressed as percentage. Histograms are displayed in Appendix C2.

2.6.7 Western blotting

2.6.7.1 Introduction

2.6.7.1.1 Protein isolation

Following the isolation of protein from cells, crude extracts were quantified and standardised using the bicinchoninic acid (BCA) assay. Proteins and peptides do not absorb light in the visible region of the spectrum. However, when treated with an alkaline solution of Cu^{2+}/tartrate complex, a purple colour develops due to the complexing of the Cu^{2+} ions by peptide bonds. This colour reaction is characteristic of the biuret reaction in which a reduction of cupric (Cu^{2+}) ion to cuprous (Cu^{+}) ion by protein in an alkaline medium occurs. The Cu^{+} ion is then detected by a reaction with BCA to produce an intense purple colour that absorbs maximally at 562nm (Figure 20). The intensity of the colour produced is proportional to the number of peptides bonds participating in the reaction.

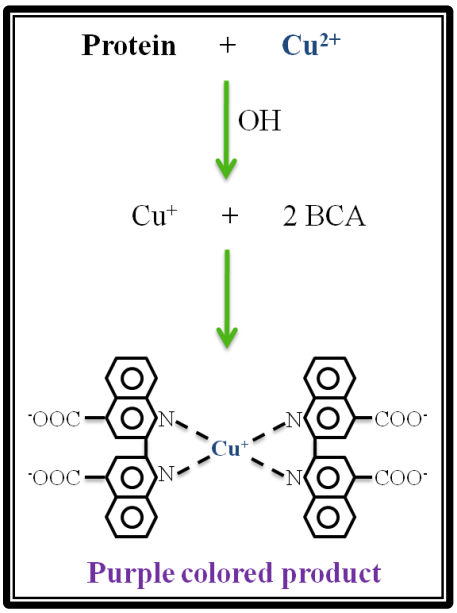

Figure 19: Mechanism of protein detection in the bicinchoninic acid assay.

2.6.7.1.2 Electrophoresis and transfer

Sodium dodecyl sulphate - polyacrylamide gel electrophoresis (SDS-PAGE) is a technique that is extensively employed to separate proteins. Polyacrylamide is a matrix that is formed by the copolymerisation of monomers of acrylamide and bis-acrylamide ("bis," N,N'-methylene-bisacrylamide). A strength of polyacrylamide is that it is inert, thus will not interact with proteins as they migrate through. Sodium dodecyl sulphate is an anionic detergent which denatures proteins by forming micelles around the polypeptide. Sodium dodecyl sulphate confers a uniform negative charge to the polypeptide. Since differences in charge and shape are eliminated as variables, separation in SDS-PAGE is based on the molecular weights of proteins. Following protein standardisation, samples are prepared with sample buffer (which contains SDS; a tracker dye – bromophenol blue; β-mercaptoethanol – to unfold tertiary protein structures by reducing disulfide bridges; and glycerol – adds density to the sample) before being electrophoresced on SDS-PAGE gels. These gels comprise of a stacking layer and a separating layer. Once electrophoresced, protein bands are transferred to nitrocellulose membranes via electroblotting (Figure 20). This involves the sandwiching of the gel and nitrocellulose membrane by fibre pads. Applying current at right angles to the gel achieves the transfer of proteins from the gel to the membrane.

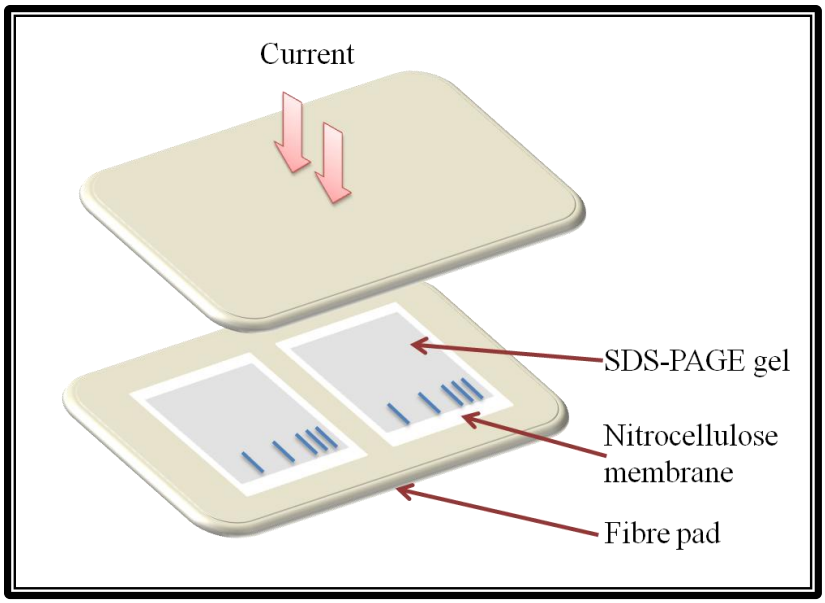

Figure 20: Set up of components for electroblotting.

2.6.7.1.3 Immuno-blotting

Proteins are analysed on the nitrocellulose membrane using antigen-specific antibodies. Subsequent to blocking of remaining hydrophobic binding sites on the membrane with a protein solution, membranes are incubated with primary antibody against the protein of interest. A second incubation with horseradish peroxidase (HRP)-conjugated secondary antibody, directed against the primary antibody, permits the visualisation of the interaction between primary antibody and the protein of interest. Horseradish peroxidase, in the presence of H_2O_2, oxidises luminol (chemiluminescent substrate) with concomitant generation of light. The use of a chemical enhancer results in a 1000-fold increase in the intensity of light, which is detected by a photographic film. The intensity of light produced is proportional to the expression of the protein of interest (Figure 21).

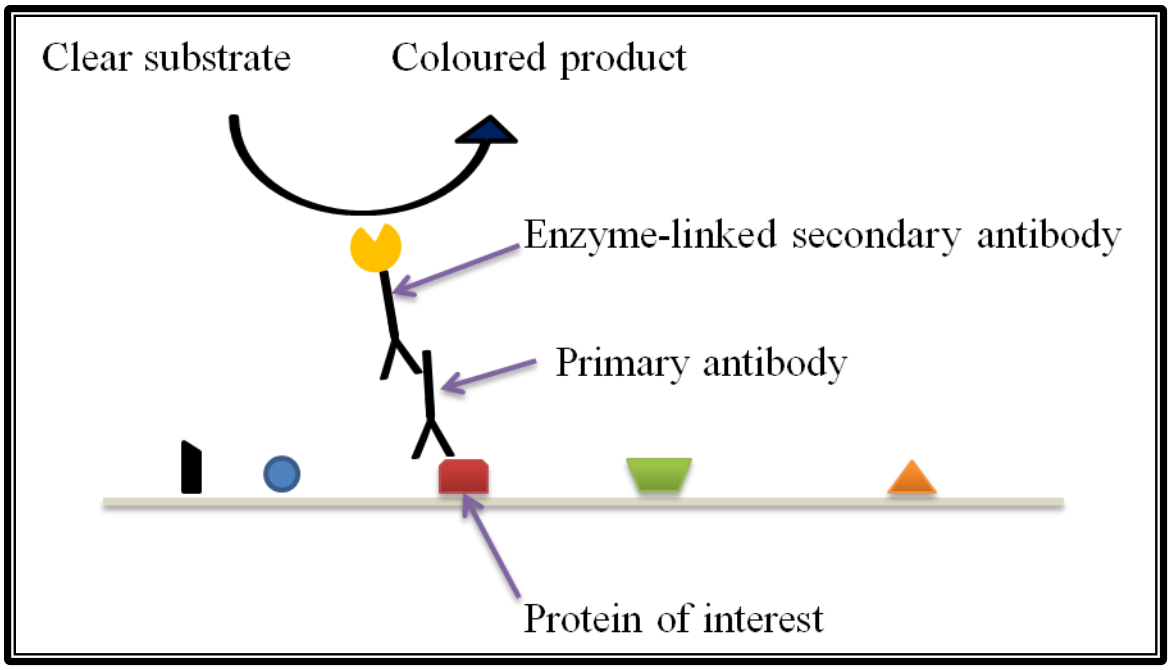

Figure 21: Antibody-antigen reaction for the detection of chemiluminescence.

2.6.7.2 Protocol

Cytobuster™ reagent (Novagen) supplemented with protease and phosphatase inhibitors (Roche, 05892791001 and 04906837001 respectively) was used for protein isolation. Cytobuster (200µl) was added to the cells (4°C, 10min) and centrifuged (180 x g; 4°C, 10min) to obtain a crude protein extract. Protein samples were quantified using the BCA assay and standardised to 1mg/ml. Samples (25µl) were electrophoresced on 7.5% SDS-PAGE gels and thereafter transferred to nitrocellulose membranes. Membranes were blocked with 3% bovine serum albumin (BSA) in Tris buffer saline (20mM Tris-HCl (pH 7.4), 500mM NaCl and 0,01% Tween 20 (TBST)) for 1h, and incubated with primary antibody (p53, ab26; bax, ab5714; PARP-1, ab110915; smac/DIABLO, ab110291 and β-actin, ab8226; 1:1,000) in 1% BSA in TBST at 4°C overnight. Membranes were then washed thrice (10ml TBST, 15min) and treated with HRP-conjugated secondary antibody (mouse, ab97046; 1:2,000) (1h, RT). Membranes were washed

again 3 times (TBST, 15min) and immunoreactivity was detected by the LumiGLO® chemiluminescent substrate system (KPL) with the Uvitech Image Documentation System (UViTech Alliance 2.7). Protein bands were analysed with the UViBand Advanced Image Analysis software (UViTech v12.14). The results were expressed as mean relative band intensity (RBI).

2.6.8 Quantitative-polymerase chain reaction

2.6.8.1 Introduction

PCR is a molecular technique, homologous to cellular DNA replication, which is used to amplify a precise region of DNA from a template starting material. Two oligonucleotide primers complementary to the sites flanking the target region are chemically synthesised. The primers attach to the 3' ends of each DNA template strand after which DNA polymerase incorporates deoxynucleotide triphosphates (dNTPs) in a stepwise manner to the 3' ends of the primers.

There are three defined steps in PCR: 1) denaturation, 2) annealing and 3) extension. Denaturation involves the separation, usually above 90°C, of double stranded (ds) DNA into two single stranded (ss) DNA template strands for accessibility of the target region. In the annealing step, the temperature is dropped to allow for the hybridisation of oligonucleotide primers to complementary sites flanking the target region. Finally, extension entails the synthesis of DNA (addition of dNTPs) at the free 3' hydroxyl end of the primers by thermostable *Taq* DNA polymerase. This cycle is repeated for 30-40 times, and the result is an exponential amplification of the target DNA (Figure 22).

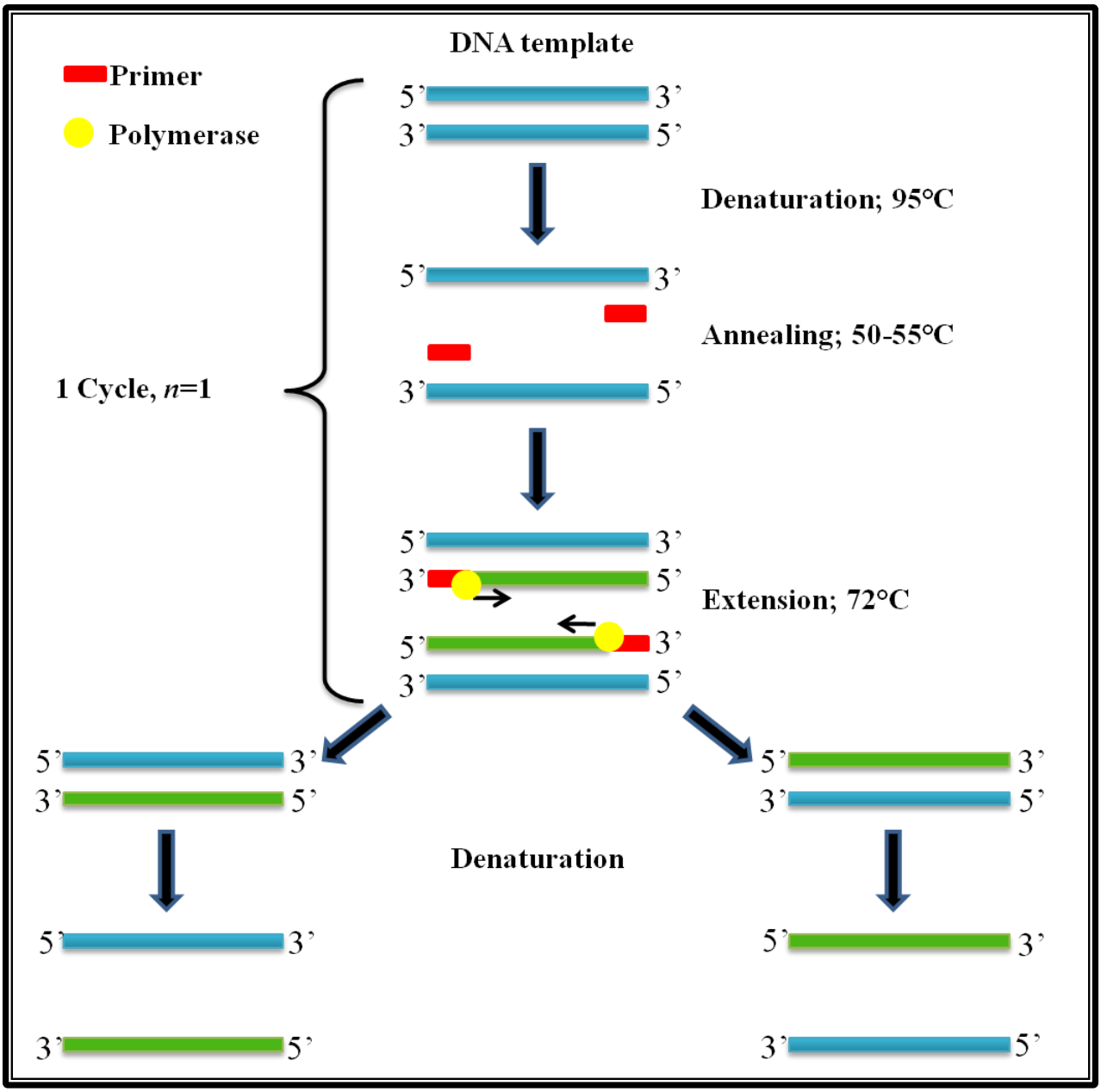

Figure 22: Exponential amplification of target DNA in polymerase chain reaction.

Although conventional PCR successfully achieves the amplification of DNA, it is not quantitative. Being able to quantify the DNA template or starting material is important in pathologies where a protein may be expressed abnormally. Quantitative-polymerase chain reaction is a technique that enables one to determine the amount of a target gene in a sample.

RNA is first isolated from cells and then reverse transcribed to ss complementary (c) DNA. cDNA is then used as the starting material for Q-PCR. The cycling steps of Q-PCR are similar to conventional PCR. Quantification of DNA is made possible by including a DNA-binding dye called SYBR Green in the reaction. SYBR Green binds to dsDNA amplicons proportionally and the fluorescence is detected after excitation. A curve is plotted with fluorescent emission over time from which the initial amount of DNA in each sample is obtained. A threshold is set at a constant point of exponential increase in the curves and the cycle time (Ct) value for each sample is determined. Along with the gene of interest, samples are analysed for expression of a house keeping gene, and the amount of target DNA is reported relative to the amount of the house keeping gene for each sample.

2.6.8.2 Protocol

2.6.8.2.1 RNA isolation

Total RNA was extracted using Trizol. Briefly, 500µl of Trizol was added to 500µl of cell suspension (50 000 in 0.1M PBS) in 1.5ml tubes. After 5min of incubation at RT, cells with Trizol were frozen (-80°C) for 1h. Subsequently, 100µl of chloroform was added to the thawed samples with vigorous mixing and thereafter incubation (3min, RT). Tubes were then subjected to centrifugation (12 000 x g, 15min, 4°C) following which the aqueous layer was transferred to a new 1.5ml tube on ice. To this, 250µl of isopropanol was added and incubated (-80°C, 1h). Tubes were centrifuged (12 400 x g, 20min, 4°C) and pellets containing total RNA were recovered. Cold ethanol (75%) was then used to wash pellets (7,400 x g, 15min, 4°C). Ethanol was discarded and RNA pellets left to air dry (10min) before being resuspended in 15µl of RNase-free water. After incubation (3min, RT) RNA samples were mixed well, quantified

spectrophotometrically and standardised to 100ng/µl with RNase-free water. Samples were stored at -80°C for further use.

2.6.8.2.2 cDNA synthesis

RNA was reverse transcribed to cDNA as per manufacturers' guidelines using the RT^2 First Strand Kit (SA Biosciences™). Firstly, genomic DNA elimination mixture (10µl) was prepared with 2µl (200ng) of total RNA, 2µl of 5X gDNA elimination buffer and 6µl of RNase-free water. Secondly, reverse transcriptase cocktail (10µl) was prepared with 4µl of reverse transcriptase buffer 3, 1µl of primer and external control mix, 2µl of reverse transcriptase enzyme mix and 3µl of RNase-free water. For the cDNA synthesis reaction, a 20µl reaction containing 10µl each of genomic DNA elimination buffer and reverse transcriptase cocktail for each sample was prepared and subjected to incubation at 42°C (15min) followed by heating at 95°C (5min) (GeneAmp® PCR System 9700, Applied Biosciences). Subsequently, 80µl of RNase-free water was added to each reaction mixture and stored at -70°C for further use.

2.6.8.2.3 Quantitative-polymerase chain reaction

The mRNA expression of p53 and bax were investigated using Q-PCR. Glyceraldehyde-3-phosphate dehydrogenase (GAPDH) was used as the house keeping gene. Primer sequences were obtained from Inqaba Biotechnologies: p53 (sense: 5'CCACCATCCACTACAACTACAT'3, antisense: 5'CAAACACGGACAGGACCC'3) bax (sense: 5'ATGCGTCCACCAAGAAGCTGAG'3, antisense: 5'GACTGCCGTTGAAGTTGACCCC'3) and GAPDH (sense: 5'TCCACCACCCTGTTGCTGTA'3, antisense: 5'ACCACAGTCCATGCCATCAC'3).

The iQ™ SYBR Green Supermix (cat. 170-8880, Biorad) was used for Q-PCR. Amplification proceeded in a 25µl reaction consisting of: 12.5µl of the iQ™ SYBR Green Supermix, 2µl of cDNA, 1µl of the primer set and 8.5µl of RNase-free water. Cycling conditions were: initial denaturation (95°C, 15min), 40 cycles of denaturation (95°C, 30s), annealing (55°C, 30s) and extension (72°C, 30s) followed by final extension (72°C for 7min) (Chromo4™ R-T PCR Detector, BIORAD).

For analysis of results, the method described by Livak and Schmittgen (2001) was used. Results are expressed as $2^{-\Delta\Delta Ct}$. In order to determine fold changes in the expression of genes between samples, the Ct values for the control samples was set at 1. Differences in Ct values between gene of interest and housekeeping gene for test samples and controls is represented by ΔΔCt, which is expressed as fold change ($2^{-\Delta\Delta Ct}$) (Livak and Schmittgen, 2001).

Quantitative-polymerase chain reaction products were verified using electrophoresis (120V, 30min) on a 2% agarose gel supplemented with 0.5mg/ml EtBr. Bands were visualised using the Uvitech Image Documentation System (UViTech Alliance 2.7).

2.7 Statistical analysis

Statistical analyses were performed using GraphPad Prism version 5.00 software package (GraphPad PRISM®) and Microsoft excel 2007. Data are expressed as mean ± standard error of the mean (sem). Comparisons were made using the unpaired Student t-tests. Statistical significance was set at 0.05.

CHAPTER THREE

3 RESULTS:

3.1 Cell viability

3.1.1 MTT assay

The toxicity of AA_{AgNP} to A549 cells was determined using the MTT assay. A dose-dependent decline in cell viability was observed using AA_{AgNP} concentrations in the range 0 to 75µg/ml for 6h (95% Cl=31.96 to 57.72) (Figure 23). An IC_{50} value of 43µg/ml was obtained and used in all subsequent assays.

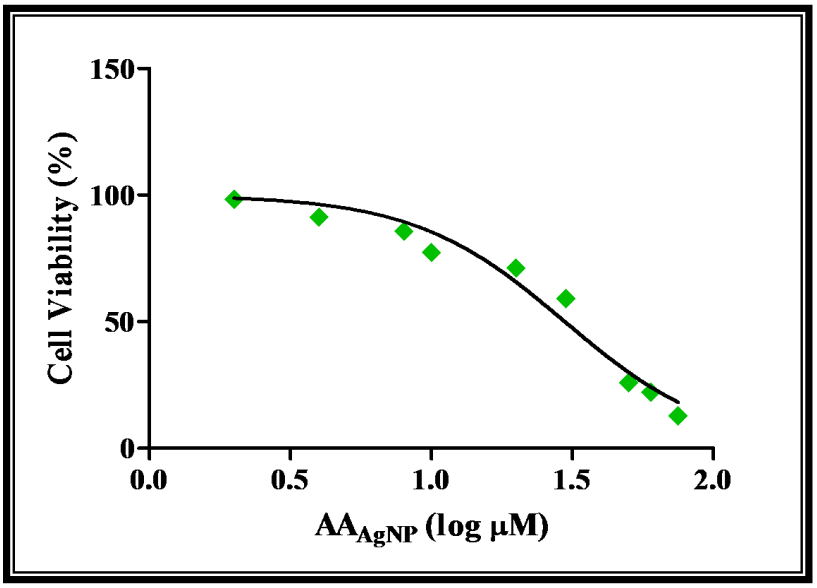

Figure 23: A dose-dependent decline in A549 cell viability after AA_{AgNP} treatment.

3.1.2 ATP assay

Cellular ATP levels were assessed using the CellTire Glo™ assay. AA_{AgNP} significantly reduced ATP levels with a 2.5-fold decrease (350 000±1500RLU; 95% CL=330 000 to 370 000)

compared to the control (990 000±40 000RLU; 95% Cl=480 000 to 1 500 000; p=0.0040) (Figure 24).

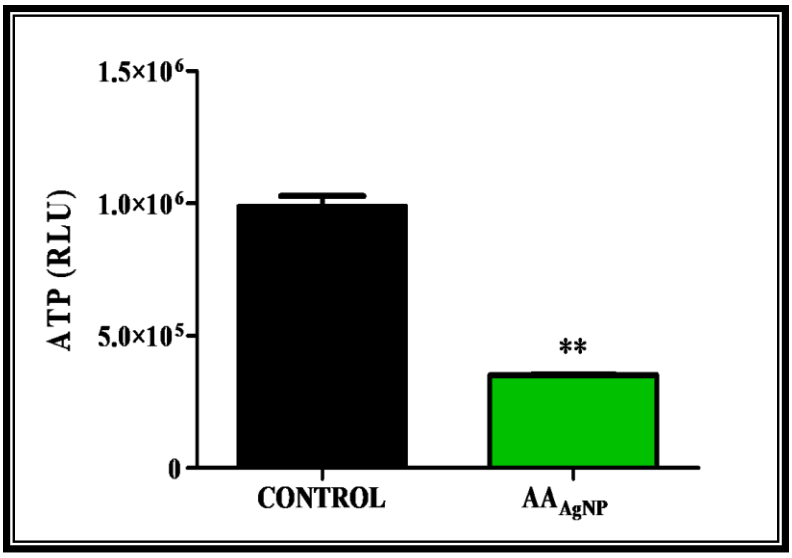

Figure 24: ATP levels in control and AA_{AgNP} treated A549 cells (p=0.0040). RLU: relative light units.

3.2 Oxidative stress

3.2.1 Glutathione assay

Glutathione concentrations were measured using the GSH-Glo™ Glutatione assay as a marker for intracellular anti-oxidant capacity. The concentration of GSH was higher in untreated cells (15±1.3µM) compared to AA_{AgNP} treated cells (12±0.24µM, 95% Cl=-1.0 to 6.2; p=0.1184) (Figure 25**)**.

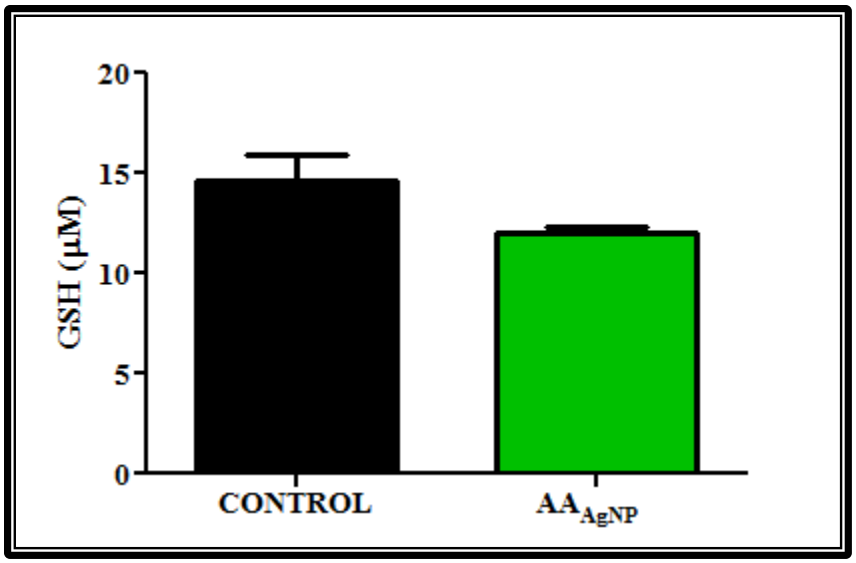

Figure 25: Glutathione levels in AA_{AgNP} treated cells (p=0.1184).

3.2.2 Lipid peroxidation

Additionally, lipid peroxidation (MDA-measured by the TBARS assay) was significantly 5-fold higher in cells exposed to AA_{AgNP} (0.16±0.023µM) compared to controls (0.032±0.016µM, 95% Cl=-0.21 to -0.049; p=0.0098) (Figure 26).

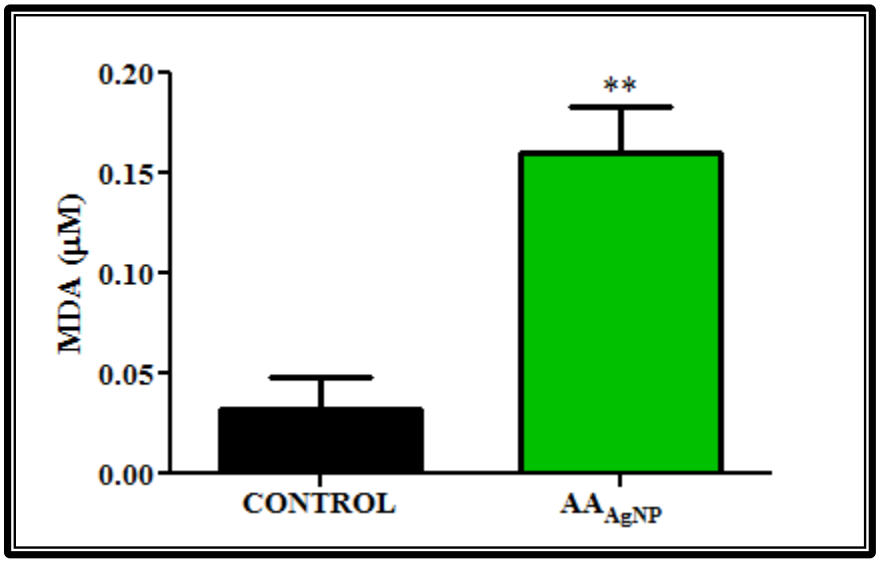

Figure 26: Malondialdehyde (lipid peroxidation) levels in AA_{AgNP} treated cells (p=0.0098).

3.3 Analysis of apoptotic parameters

3.3.1 Analysis of caspases

Caspase-Glo® assays were used to determine caspase activity. AA_{AgNP} significantly increased the activities of caspase-3/-7 (1.7-fold, 95% Cl=-1 000 000 to -260 000; p=0.0180) and -9 (1.4-fold, 95% Cl=-610 000 to -220 000; p=0.0117) compared to the control. The activity of caspase-8 however was significantly decreased by AA_{AgNP} compared to untreated cells (2.5-fold, 95% Cl=550 000 to 840 000; p=0.0024) (Table 1). Bar graphs are shown in Appendix C (1-3).

Table 1: Caspase activity in AA_{AgNP} treated cells. RLU: relative light units.

	CONTROL	**AA_{AgNP}**	
	Mean RLU ± sem	**Mean RLU ± sem**	***p* value**
CASPASE-3/-7	920 000±4 000	1 600 000±86 000	0.0180*
CASPASE-8	1 200 000±26 000	460 000±23 000	0.0024**
CASPASE-9	920 000 ± 33 000	1 300 000±31 000	0.0117*

3.3.2 Annexin-V Fluos assay

The annexin-V-Fluos assay was used to determine the mode of cell death. Treatment with AA_{AgNP} significantly increased PS translocation in A549 cells compared to the control (57±0.59% vs. 10±0.84%, 95% Cl= -50 to -43; p<0.0001) (Figure 27/28). Furthermore, the

percentage of necrotic cells were also significantly higher in AA_{AgNP} treated cells (17±0.79% vs. control: 4.6±0.70%, 95% Cl= -16 to -9.2; p<0.0001) (Figure 27/28).

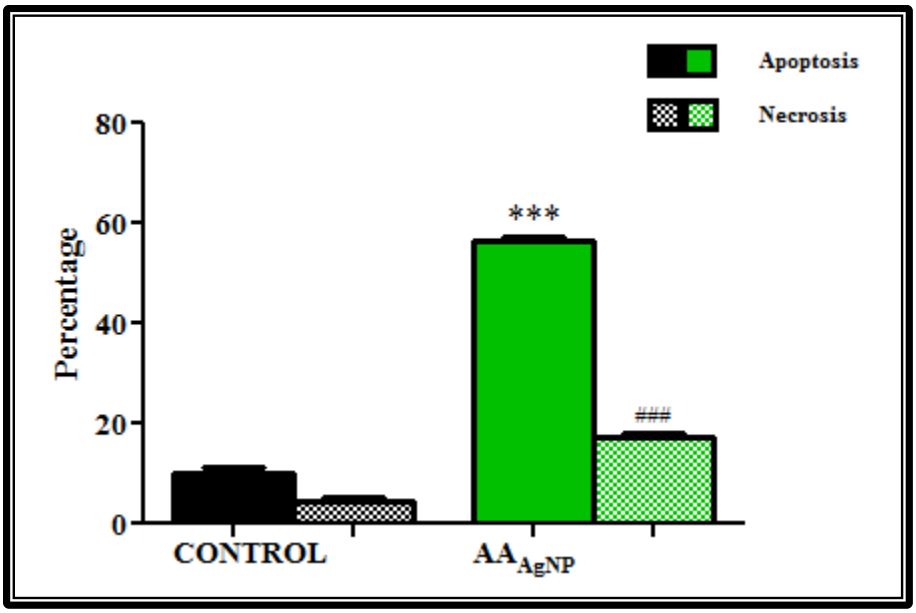

Figure 27: Percentages of apoptotic and necrotic A549 cells (p<0.0001).

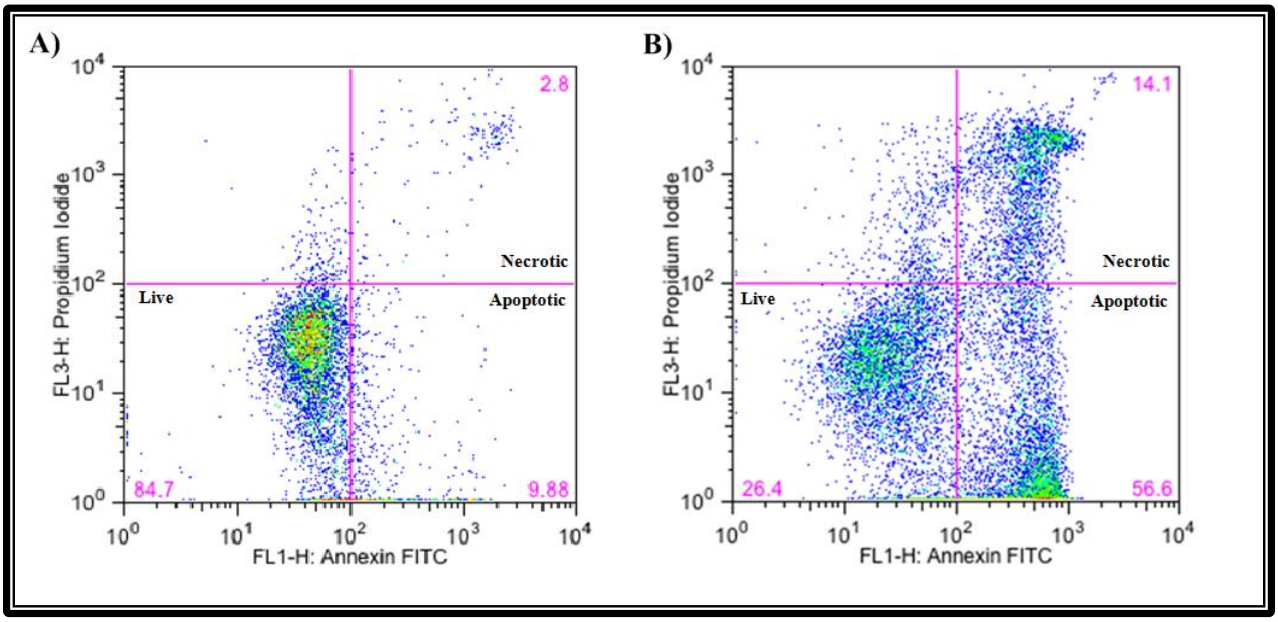

Figure 28: Dot plots showing spectral shifts for flow cytometric analysis of annexin-V and propidium iodide staining in **A**) control cells and **B**) cells treated with AA_{AgNP}.

3.3.3 JC-1 Mitoscreen assay

The apoptosis inducing potential of AA_{AgNP} was further verified in disrupting mt ΔΨ using the BD™ MitoScreen kit. The treated cells had significantly higher mt depolarisation compared to untreated cells (77±0.88% vs. 23±1.8%, 95% Cl= 44 to 57; p<0.0001) (Figure 29/30).

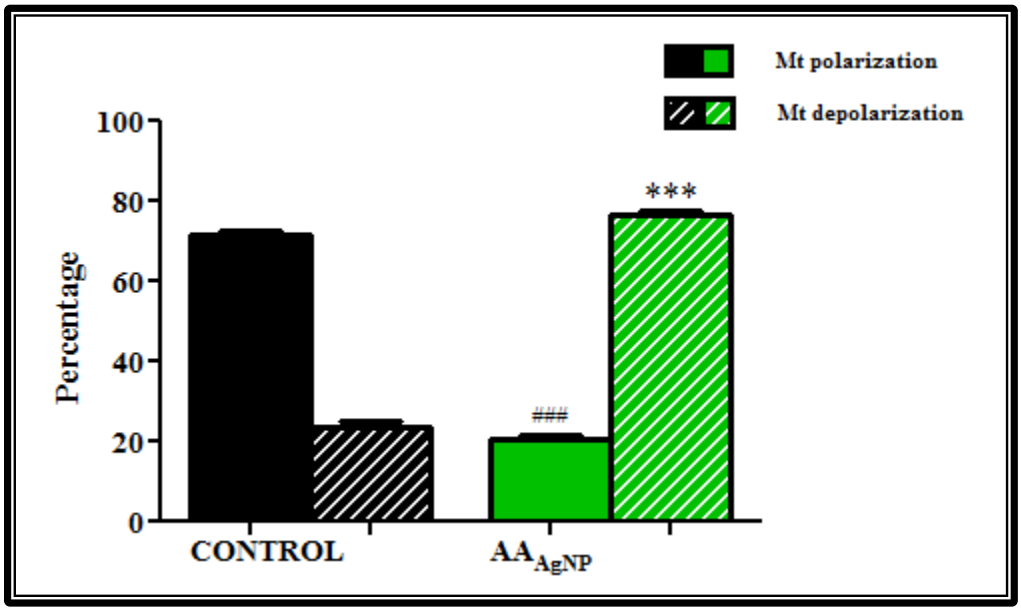

Figure 29: Mitochondrial membrane depolarisation after treatment with AA_{AgNP} (p<0.0001).

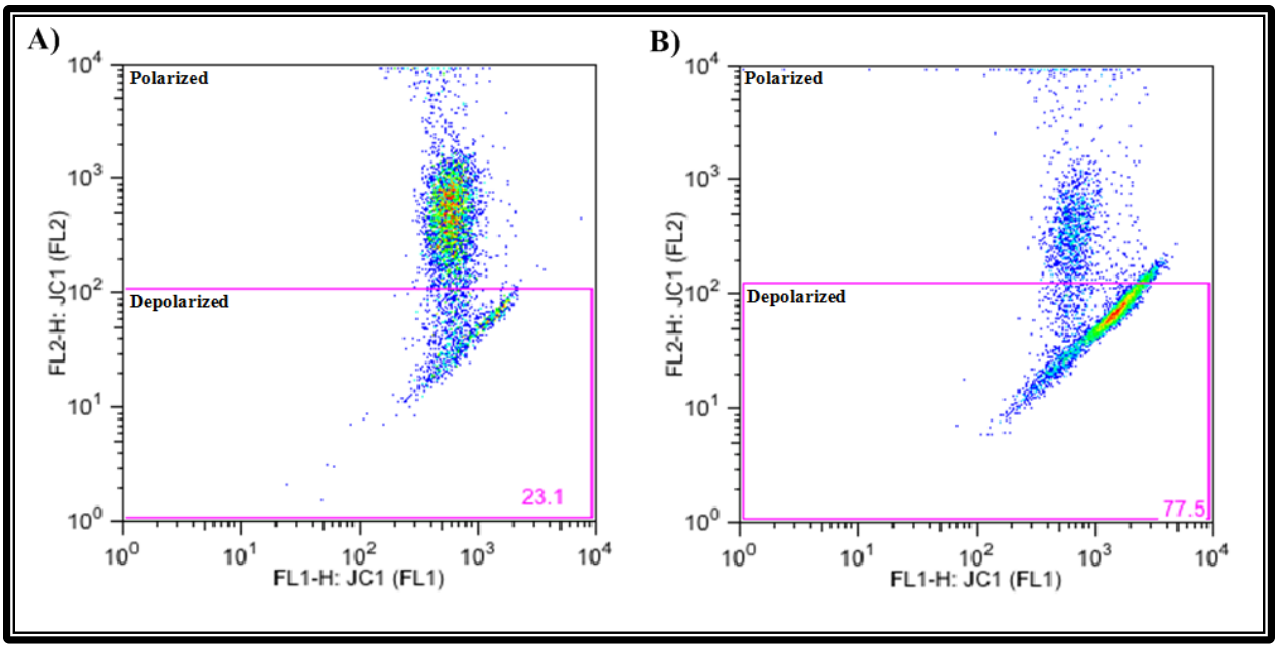

Figure 30: Spectral shift in JC-1 dye for the analysis of mitochondrial membrane integrity. Dots plats obtained from flow cytometric analysis of **A**) control and **B**) treated cells.

3.3.4 Comet assay

The genotoxic effect of AA_{AgNP} was assessed with the comet assay. Comet tail lengths were measured as an indication of DNA fragmentation. Silver nanoparticles of AA were significantly genotoxic to A549 cells as noted by the increased DNA fragmentation (Figure 31). Comet tail lengths were significantly longer in treated (90±1.3µm) compared to untreated cells (20±0.71µm, 95% Cl= -73 to -67; p<0.0001) (Figure 31).

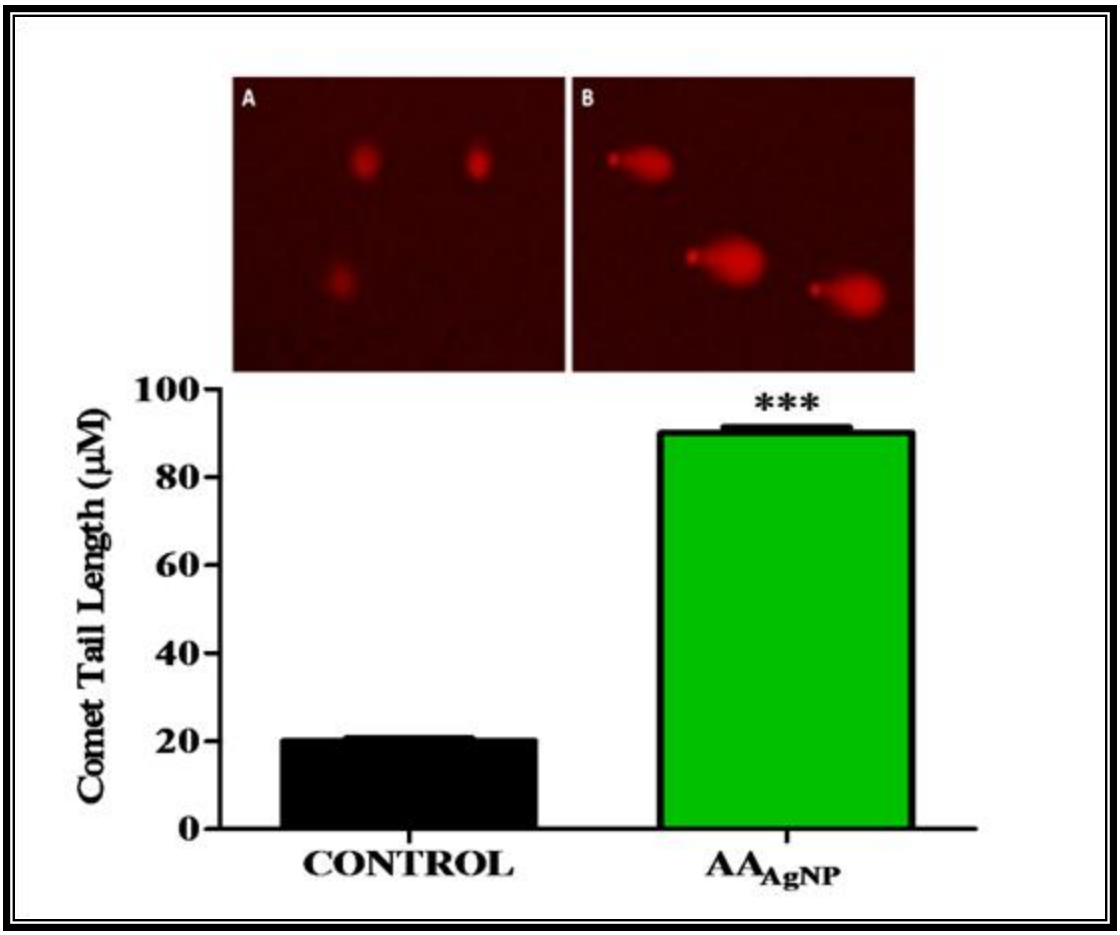

Figure 31: DNA fragmentation was markedly higher in cells exposed to AA_{AgNP} (**B**) than untreated control cells (**A**) (p<0.0001) (100x).

3.3.5 CD95

The expression of CD95 death receptor, assessed by extracellular staining using flow cytometry, was significantly down regulated (2-fold; 2.8±0.58% vs. control: 5±0.44%, 95% Cl=0.13 to 4.2; p=0.0416) (Table 2).

3.3.6 Smac/DIABLO intracellular staining

In contrast, flow cytometric intracellular staining revealed that AA_{AgNP} significantly increased the expression of the pro-apoptotic smac/DIABLO (29±0.32%) compared to the control (18±0.66%, 95% Cl=-13 to -8.5; p<0.0001) (Table 2).

Table 2: Surface expression of CD95 and intracellular smac/DIABLO in A549 cells treated with AA_{AgNP} as determined flow cytometrically.

	CONTROL	**AA_{AgNP}**	
	Mean % ± sem	**Mean % ± sem**	***p* value**
FITC +ve (CD95)	5±0.44	2.8±0.58	0.0416*
APC +ve (smac/DIABLO)	18±0.66	29±0.32	<0.0001***

3.3.7 Western blot analysis

The expression of selected apoptotic proteins and validation of flow cytometric intracellular stained smac/DIABLO was determined by western blotting. The expression of p53 was observed to be significantly higher post AA_{AgNP} exposure (1.0±0.018RBI vs. control: 0.82±0.045RBI, 95% Cl= -0.42 to -0.00037; p=0.0498). A significant increase in the levels of PARP-1 was noted after AA_{AgNP} treatment (3.5±0.069RBI vs. control: 3.1±0.0043RBI, 95% Cl= -0.65 to -0.058; p=0.0359). Evaluation of bax showed higher levels of the protein in cells that were treated with AA_{AgNP} (3.4±0.11RBI) compared to untreated cells (2.1±0.047RBI, 95% Cl= -1.9 to -0.81;

p=0.0083). Highly significant differences were seen in the expression of smac/DIABLO between experimental and control cells. Cells treated with AA_{AgNP} presented with a 4.1-fold greater band intensity (1.1±0.045RBI vs. control: 0.27±0.010RBI, 95% Cl= -0.99 to -0.59; *p*=0.0033) (Figure 32).

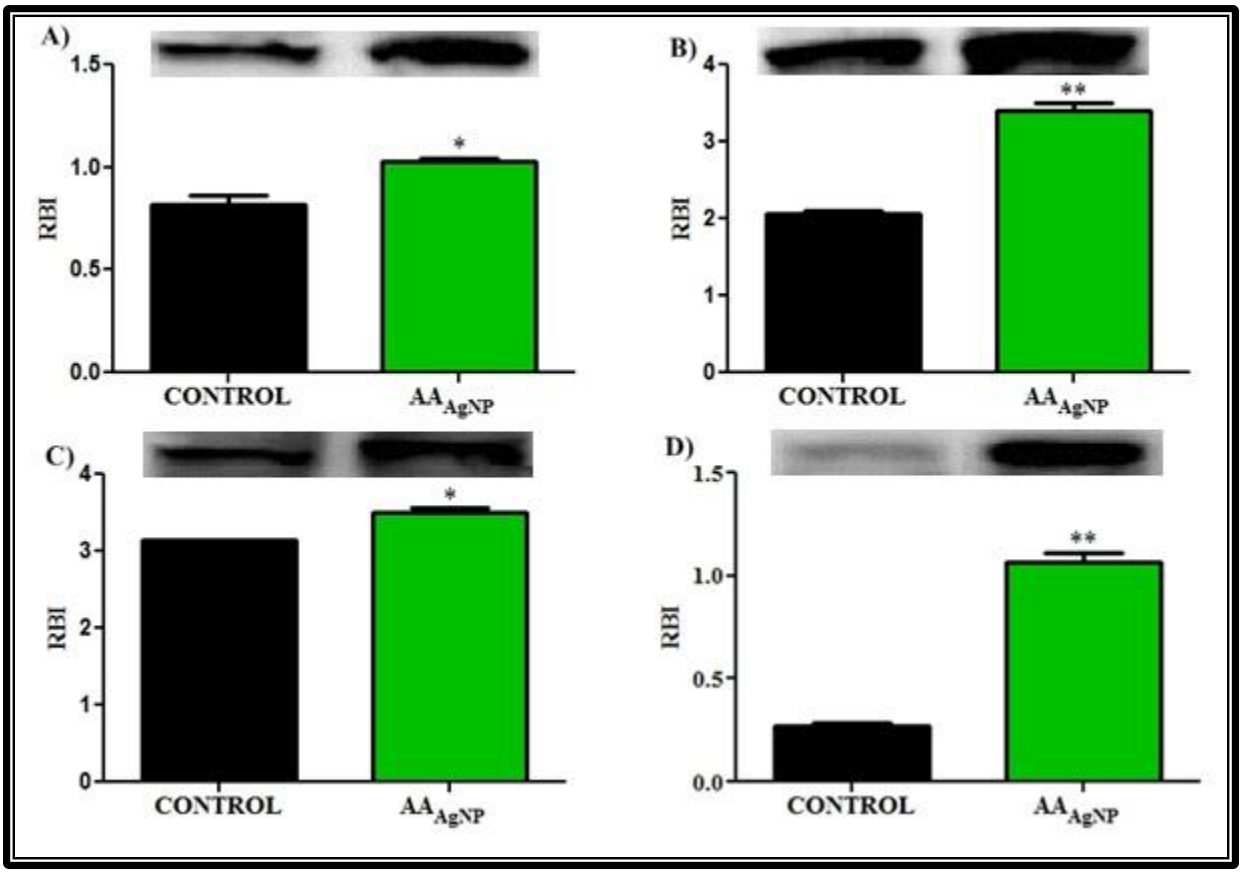

Figure 32: Western blot images and band intensity graphs for the expression of **A**) p53 (*p*=0.0498) **B**) bax (*p*=0.0083) **C**) PARP-1 (*p*=0.0359) and **D**) smac/DIABLO (*p*=0.0033).

3.3.8 Quantitative-polymerase chain reaction

The expression of p53 and bax mRNA was investigated using Q-PCR. Consistent with western blotting data that showed an increase in the expression of p53 and bax proteins, mRNA levels for both proteins were upregulated. A 6-fold (95% CI= -7.267 to -2.733; *p*=0.0036) and 5-fold (95%

CI= -6.267 to -1.733; p=0.0080) increase in mRNA expression were observed for p53 and bax respectively in AA_{AgNP} treated cells (Figure 33).

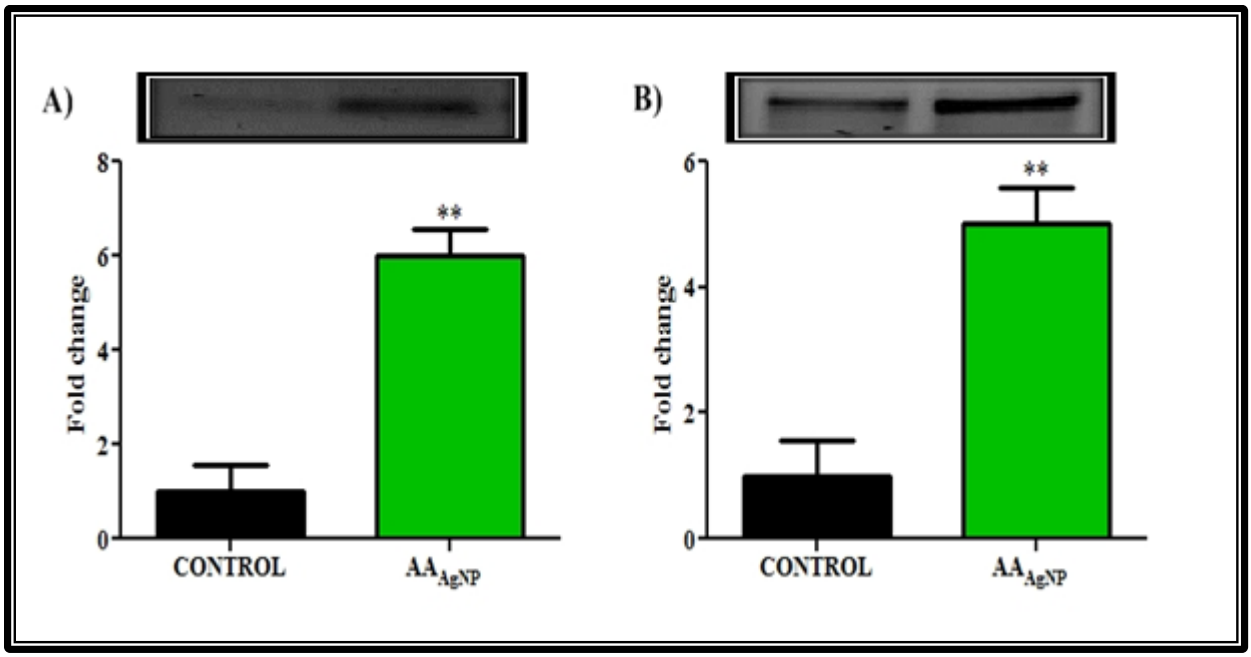

Figure 33: Fold change graphs for the mRNA expression of **A**) p53 (p=0.0036) and **B**) bax (p=0.0080). Gel electrophoresis images with band intensities are also presented above each graph.

CHAPTER FOUR

4 DISCUSSION

Several pathological syndromes such as liver failure, stroke or heart attack are associated with an abrupt death of tissue or organs as a result of apoptotic dysregulation. Conversely, the survival and build up of abnormal cells, in the case of unsuitably low apoptotic rates, may lead to tumourigenesis (Fischer and Schulze-Osthoff, 2005). Apoptosis, a programmed mechanism of cell death, is the outcome of a succession of precisely regulated events, which are commonly altered in cancerous cells (Kasibhatla and Tseng, 2003). In essence, tumour cells have the ability to evade the apoptotic cascade, which represents a notable causative factor for the development and progression of cancer – uncontrolled cell proliferation.

Plant extracts are known to contain weak acids. *Albizia adianthifolia* possesses acids such as ethyl acetate and aurantiamide acetate (Tamokou Jde et al., 2012). Weak acids are known to disrupt mt function by depolarisation of the membrane, disruption of the ETC and decreased ATP production (Komen et al., 2007). The ability of weak acids to penetrate the mt membrane results in metabolic dysfunction; the TCA cycle, which occurs in the mt matrix, is responsible for the production of reducing equivalents required by oxidoreductases. Silver nanoparticles of AA caused a dose-dependent decrease in A549 cell viability as was observed by a decrease in formazan product (dependent on reducing equivalents and the function of oxidoreductases) (Figure 23). This may be due to the weak acids found in the AA extracts. Furthermore, NPs preferentially localise in mt and potentiate structural damage (Derfus et al., 2004; Xia et al., 2006). Various studies have associated AgNP toxicity with mt damage (Carlson et al., 2008; Xia

et al., 2008). This could further contribute to the anti-proliferative properties of AA_{AgNP} as observed in our study.

The signal transduction of apoptosis involves a cascade of initiator and executioner caspases, which form the engine of apoptosis. Caspases are a family of aspartate-specific cysteinyl proteases that are produced as catalytically inactive zymogens in cells (Chai et al., 2000). Executioner caspases-3 and -7 are a subset that cleaves specific substrates leading to alteration changes linked with apoptosis viz. chromatin condensation, DNA fragmentation, blebbing of plasma membrane, cell shrinkage and ultimately cell death (Kasibhatla and Tseng, 2003). Initiator caspses-8 and -9 are responsible for the activation of executioner caspases. AA_{AgNP} significantly up regulated the activities of caspases-3/-7 and -9 (Table 1). Furthermore AA_{AgNP} increased DNA fragmentation (Figure 31)-an end stage characteristic of apoptosis. In response to this DNA damage, the nuclear enzyme PARP-1 catalyzes the transfer of NAD^+ to a specific set of nuclear substrates for the repair of DNA damage (Shall and de Murcia, 2000). During apoptosis, PARP-1 is cleaved, by executioner caspases-3/-7, to a 24kDa DNA binding domain and an 89kDa fragment containing catalytic activity. The silver nanoparticles of AA were responsible for the cleavage of PARP-1 as evidenced by the significant increased expression of 24kDa fragment compared to untreated control cells (Figure 32C).

A biochemical feature associated with apoptosis is the expression of cell surface markers. The externalisation of PS (a transmembrane glycoprotein of the phospholipid bilayer) signals for early phagocytosis of apoptotic cells with minimal compromise to adjacent and surrounding tissue (Bratton et al., 1997). A significant increase in PS externalisation occurred in A549 cells treated with AA_{AgNP} (Figure 27/28).

Mitochondria play an important role in apoptosis, via the intrinsic apoptotic program. An initial crucial step for activation of the intrinsic apoptotic pathway is the depolarisation of the mt membrane. Depolarised mt is as a result of the formation of mt PT pores (Hirsch et al., 1997). Mitochondrial PT has been associated with various metabolic consequences such as halted functioning of the ETC with associated elevation in ROS and decreased production of cellular ATP (Wang, 2001). Bax, a pro-apoptotic protein of the Bcl-2 family, translocates from the cytosol to the outer mt membrane during apoptosis where it interacts with lipids and induces mt PT pores. A significant increase in mt depolarisation was observed after AA_{AgNP} treatment (Figure 29/30), with an accompanying decrease in ATP concentration (Figure 24). As mentioned, weak acids from AA may cause mt dysfunction, as they penetrate the mt membrane. The high levels of bax mRNA (Figure 33B) and its protein expression (Figure 32B), high mt depolarisation and decreased ATP suggests that AA_{AgNP} induced cellular apoptosis in these cancerous lung cells via the intrinsic mt-mediated apoptotic pathway.

Silver has a high affinity for thiol (-SH) groups (Navarro et al., 2008). In this study, the levels of cysteine-rich GSH were decreased (Figure 25) whilst lipid peroxidation was significantly elevated by AA_{AgNP} (Figure 26). This oxidant/anti-oxidant imbalance has previously been documented as an apoptotic mechanism by AgNP-mediated cytotoxicity (Ueda et al., 2002; Foldbjerg et al., 2009). The regulation of GSH/GSSG ensures that cells are not rendered vulnerable to oxidative damage as a result of GSH deficiency. Notably, the imbalance of GSH is strongly associated with pathologies such as HIV, neurodegenerative disorders and cancer (Townsend et al., 2003). Malondialdehyde, a marker for lipid peroxidation due to ROS attack of PUFAs, is known to react with nucleotide bases in DNA and form adducts; an implication for

mutagenesis and possibly cancer (Del Rio et al., 2005). Studies have linked high MDA levels with aetiology of lung cancer (Gonenc et al., 2001).

The extrinsic apoptotic pathway is mediated by death receptors, which include CD95, TNF-R1 and TRAIL-R1/R2. These death receptors contain DDs and upon ligand binding, recruit adapter FADD via the DD. Adapter proteins bind to death effector domain-containing caspases-8 giving rise to the formation DISC. Death inducing signalling complex initiates caspase-8 activation, which can directly cleave and activate effector caspases (Fischer and Schulze-Osthoff, 2005). Our results show that CD95 expression (Table 2) and caspase-8 activity (Table 1) were significantly decreased by AA_{AgNP}. It must be understood that even though initiator caspase-8 activity was reduced, the activities of executioner caspases-3 and -7 were still increased. This is as a result of elevated initiator caspase-9 activity together with increased levels of smac/DIABLO which is responsible for the activation of caspases-3 and -7. The extracts of AA are rich in saponins, which promotes rapid entry of the AA_{AgNP} into the cells resulting in mt-mediated intrinsic apoptosis. A well characterised biological action of saponins is their ability to induce cell membrane permeabilisation (Hostettmann and Martson, 1995). Decreased ATP concentrations and increased MDA as a result ROS may be due to disruptions in the mt respiratory chain.

Several pro-apoptotic molecules are released from the mt during apoptosis. In the presence of ATP, mt released cytochrome c associates with Apaf-1 in the cytosol inducing its oligomerisation. An apoptosome is then formed with the oligomeric Apaf-1 complex and procaspase-9, inducing the activation of caspase-9, which in turn activates effector caspases-3 and -7 (Chai et al., 2000). An interesting finding in this study was that although ATP levels were reduced post AA_{AgNP} treatment, the activity of caspase-9 was still elevated (Table 1).

A class of molecules involved in the regulation of apoptosis is IAP proteins. Inhibitor of apoptosis proteins avert cell death by suppressing the activity of caspases. X-linked mammalian IAP is the most well characterised member of IAPs (Fischer and Schulze-Osthoff, 2005). The ability of IAPs to act as endogenous suppressors of procaspase activation is attributed to the presence of domains referred to as BIR domains. In particular, BIR3 and a region adjacent to BIR2 are responsible for the inhibition of caspases-9, and -3 and -7 respectively. Smac/DIABLO, a mt protein, is able to abolish the inhibitory effects of XIAP (Chai et al., 2000). Both smac/DIABLO and caspases-3,-7 and -9 contain IAP-binding motifs (IMB) that fit into the BIR domains of XIAP. Thus, smac/DIABLO is able to relieve inhibition by replacing and releasing caspases-3, -7 and -9 from the XIAP inhibitory complex (Chai et al., 2000; Fischer and Schulze-Osthoff, 2005). In our study, we postulated that AA_{AgNP} released smac/DIABLO from the mt. The increased intracellular (A549) staining (Table 2) and expression of smac/DIABLO by western blotting (Figure 32D) confirmed that AA_{AgNP} did induce the release of this protein from the mt of the A549 cells.

The p53 (tumour suppressor/transcription) protein mediates a range of anti-proliferative processes in response to different stress stimuli. The p53 protein directly activates apoptosis by promoting the release of bax (Miyashita et al., 1994) and inducing executioner caspase activity (MacLachlan and El-Deiry, 2002) Also, p53 is involved in cell death independent of its transcriptional activity. This is attributed to the BH3-like activity of p53. Upon translocation to the mt, p53 neutralises the anti-apoptotic function of Bcl-2, directly activates bax and interferes with mt integrity and function leading to the release of pro-apoptotic molecules and the generation of ROS (Hwang et al., 2001). Our study clearly shows the increased expression of p53 by AA_{AgNP} in the A549 cells (Figure 32A) and this correlated with an increase in mt

depolarisation and ROS. Furthermore, the levels of mRNA for p53 were upregulated, which validates the increased p53 protein expression (Figure 33A).

A summary of the potential target sites in the apoptotic cascade, by AA_{AgNP} is illustrated in figure 34.

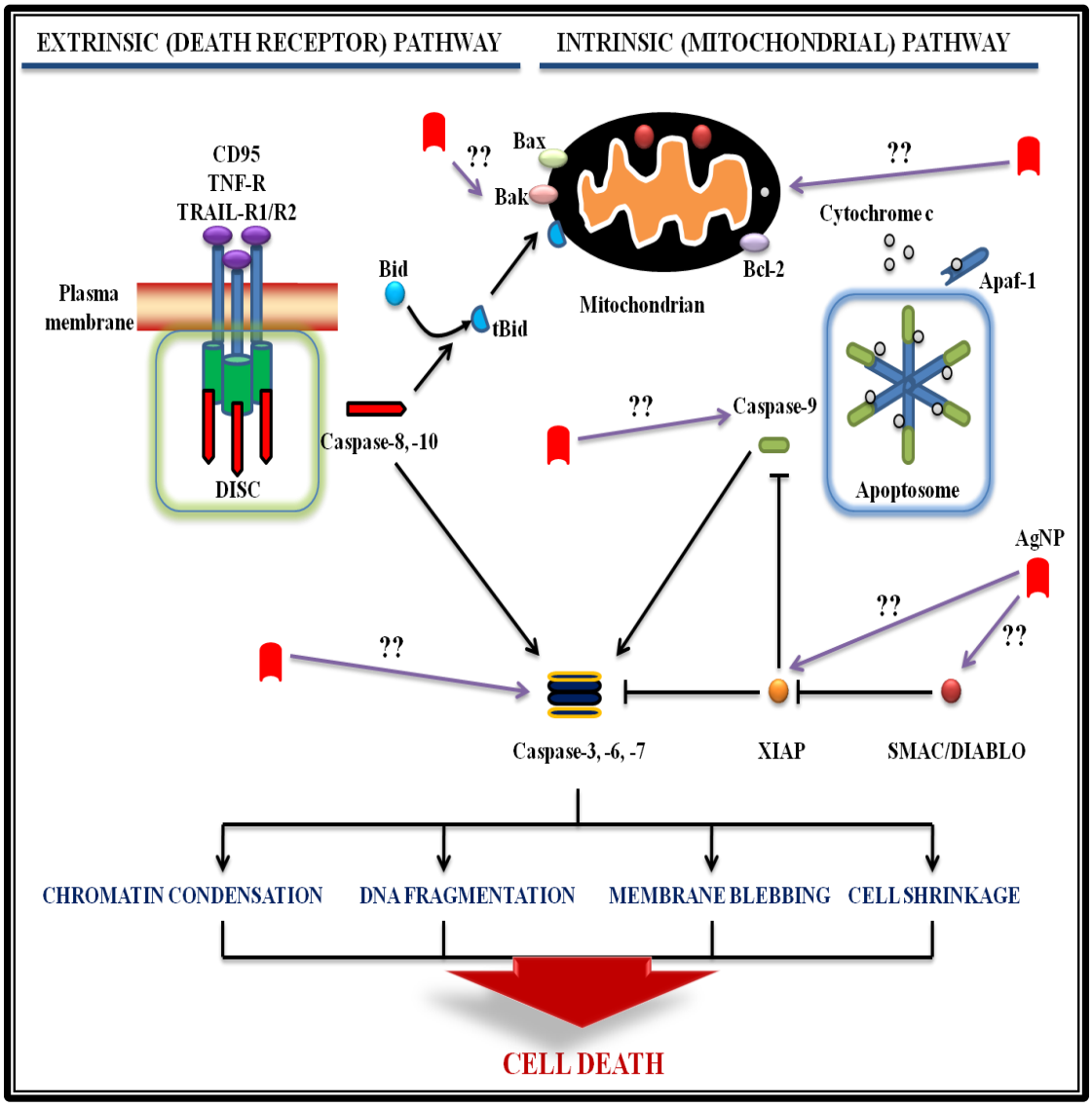

Figure 34: Schematic overview of the apoptotic pathways leading to cell death. Potential sites for AA_{AgNP} -mediated induction of apoptosis in A549 cells are presented.

CHAPTER FIVE

5 CONCLUSION

Mortality and morbidity due to lung cancer is increasing globally. Current cancer therapies are costly, and are associated with a number of adverse effects. Furthermore, individuals receiving treatments for other ailments, such as AIDS (ARV therapy), incur added costs. This emphasises the need for the development of cost-effective and safer therapies. This study was conducted to determine the anti-cancer effects of a novel AgNP synthesised from leaf extracts of AA on the A549 human lung carcinoma cell line.

Silver nanoparticles of AA were found to possess potent pro-apoptotic potential. We have shown, mechanistically, that AA_{AgNP} activates the intrinsic mt-mediated apoptotic pathway in A549 lung carcinoma cells. The effects of AA leaf extract and AgNPs separately on the A549 cells have not been investigated in this study. This creates an avenue for future research.

The findings of this study suggest the potential for AA_{AgNP} in drug development against cancer. None the less, further studies need to be conducted to ascertain if the effects of AA_{AgNP} are consistent in other cancerous cell lines and also specific to cancerous cells, i.e. non-toxic to healthy systems.

REFERENCES

Abdel-Kader, M., Hoch, J., Berger, J.M., Evans, R., Miller, J.S., Wisse, J.H., Mamber, S.W., Dalton, J.M., Kingston, D.G., 2001. Two bioactive saponins from Albizia subdimidiata from the Suriname rainforest. J Nat Prod **64**, 536-539.

Ambrosini, G., Adida, C., Altieri, D.C., 1997. A novel anti-apoptosis gene, survivin, expressed in cancer and lymphoma. Nat Med **3**, 917-921.

Arnt, C.R., Chiorean, M.V., Heldebrant, M.P., Gores, G.J., Kaufmann, S.H., 2002. Synthetic Smac/DIABLO peptides enhance the effects of chemotherapeutic agents by binding XIAP and cIAP1 in situ. J Biol Chem **277**, 44236-44243.

Arora, S., Jain, J., Rajwade, J.M., Paknikar, K.M., 2008. Cellular responses induced by silver nanoparticles: In vitro studies. Toxicol Lett **179**, 93-100.

Ashkenazi, A., Dixit, V.M., 1998. Death receptors: signaling and modulation. Science **281**, 1305-1308.

Ashkenazi, A., Dixit, V.M., 1999. Apoptosis control by death and decoy receptors. Curr Opin Cell Biol **11**, 255-260.

Bachran, C., Bachran, S., Sutherland, M., Bachran, D., Fuchs, H., 2008a. Saponins in tumor therapy. Mini Rev Med Chem **8**, 575-584.

Bachran, C., Heisler, I., Bachran, D., Dassler, K., Ervens, J., Melzig, M.F., Fuchs, H., 2008b. Chimeric toxins inhibit growth of primary oral squamous cell carcinoma cells. Cancer Biol Ther **7**, 237-242.

Baram-Pinto, D., Shukla, S., Perkas, N., Gedanken, A., Sarid, R., 2009. Inhibition of herpes simplex virus type 1 infection by silver nanoparticles capped with mercaptoethane sulfonate. Bioconjug Chem **20**, 1497-1502.

Bello, B., Fadahun, O., Kielkowski, D., Nelson, G., 2011. Trends in lung cancer mortality in South Africa: 1995-2006. BMC Public Health **11**, 209.

Bhattacharya, R., Mukherjee, P., 2008. Biological properties of "naked" metal nanoparticles. Adv Drug Deliv Rev **60**, 1289-1306.

Bratton, D.L., Fadok, V.A., Richter, D.A., Kailey, J.M., Guthrie, L.A., Henson, P.M., 1997. Appearance of phosphatidylserine on apoptotic cells requires calcium-mediated nonspecific flip-flop and is enhanced by loss of the aminophospholipid translocase. J Biol Chem **272**, 26159–26165.

Carlson, C., Hussain, S.M., Schrand, A.M., Braydich-Stolle, L.K., Hess, K.L., Jones, R.L., Schlager, J.J., 2008. Unique cellular interaction of silver nanoparticles: size-dependent generation of reactive oxygen species. J Phys Chem B **112**, 13608-13619.

Chai, J., Du, C., Wu, J.W., Kyin, S., Wang, X., Shi, Y., 2000. Structural and biochemical basis of apoptotic activation by Smac/DIABLO. Nature **406**, 855-862.

Cheung, H.H., Lynn Kelly, N., Liston, P., Korneluk, R.G., 2006. Involvement of caspase-2 and caspase-9 in endoplasmic reticulum stress-induced apoptosis: a role for the IAPs. Exp Cell Res **312**, 2347-2357.

Chicheportiche, Y., Bourdon, P.R., Xu, H., Hsu, Y.M., Scott, H., Hession, C., Garcia, I., Browning, J.L., 1997. TWEAK, a new secreted ligand in the tumor necrosis factor family that weakly induces apoptosis. J Biol Chem **272**, 32401-32410.

Collins, A.R., 2004. The comet assay for DNA damage and repair. Molecular Biotechnology **26**, 249-261.

d'Adda di Fagagna, F., Hande, M.P., Tong, W.M., Lansdorp, P.M., Wang, Z.Q., Jackson, S.P., 1999. Functions of poly(ADP-ribose) polymerase in controlling telomere length and chromosomal stability. Nat Genet **23**, 76-80.

D'Amours, D., Sallmann, F.R., Dixit, V.M., Poirier, G.G., 2001. Gain-of-function of poly(ADP-ribose) polymerase-1 upon cleavage by apoptotic proteases: implications for apoptosis. J Cell Sci **114**, 3771-3778.

de Murcia, J.M., Niedergang, C., Trucco, C., Ricoul, M., Dutrillaux, B., Mark, M., Oliver, F.J., Masson, M., Dierich, A., LeMeur, M., Walztinger, C., Chambon, P., de Murcia, G., 1997. Requirement of poly(ADP-ribose) polymerase in recovery from DNA damage in mice and in cells. Proc Natl Acad Sci U S A **94**, 7303-7307.

Del Rio, D., Stewart, A.J., Pellegrini, N., 2005. A review of recent studies on malondialdehyde as toxic molecule and biological marker of oxidative stress. Nutrition, Metabolism & Cardiovascular Diseases **15**, 316-328.

Derfus, A.M., Chan, W.C.W., Bhatia, S.N., 2004. Intracellular Delivery of Quantum Dots for Live Cell Labeling and Organelle Tracking. Advanced Materials **16**, 961-966.

Driscoll, T., Nelson, D.I., Steenland, K., Leigh, J., Concha-Barrientos, M., Fingerhut, M., Pruss-Ustun, A., 2005. The global burden of disease due to occupational carcinogens. Am J Ind Med **48**, 419-431.

Earnshaw, W.C., Martins, L.M., Kaufmann, S.H., 1999. Mammalian caspases: structure, activation, substrates, and functions during apoptosis. Annu Rev Biochem **68**, 383-424.

el-Deiry, W.S., 1998. Regulation of p53 downstream genes. Semin Cancer Biol **8**, 345-357.

Elmore, S., 2007. Apoptosis: a review of programmed cell death. Toxicol Pathol **35**, 495-516.

Enari, M., Sakahira, H., Yokoyama, H., Okawa, K., Iwamatsu, A., Nagata, S., 1998. A caspase-activated DNase that degrades DNA during apoptosis, and its inhibitor ICAD. Nature **391**, 43-50.

Fan, T.J., Han, L.H., Cong, R.S., Liang, J., 2005. Caspase family proteases and apoptosis. Acta Biochim Biophys Sin (Shanghai) **37**, 719-727.

Fischer, U., Schulze-Osthoff, K., 2005. New approaches and therapeutics targeting apoptosis in disease. Pharmacol Rev **57**, 187-215.

Foldbjerg, R., Dang, D.A., Autrup, H., 2011. Cytotoxicity and genotoxicity of silver nanoparticles in the human lung cancer cell line, A549. Arch Toxicol **85**, 743-750.

Foldbjerg, R., Olesen, P., Hougaard, M., Dang, D.A., Hoffmann, H.J., Autrup, H., 2009. PVP-coated silver nanoparticles and silver ions induce reactive oxygen species, apoptosis and necrosis in THP-1 monocytes. Toxicol Lett **190**, 156-162.

Francis, G., Kerem, Z., Makkar, H.P., Becker, K., 2002. The biological action of saponins in animal systems: a review. Br J Nutr **88**, 587-605.

Fridman, J.S., Lowe, S.W., 2003. Control of apoptosis by p53. Oncogene **22**, 9030-9040.

Friess, S.L., Standaert, F.G., Whitcomb, E.R., Nigrelli, R.F., Chanley, J.D., Sobotka, H., 1960. Some pharmacologic properties of holothurin A, a glycosidic mixture from the sea cucumber. Ann N Y Acad Sci **90**, 893-901.

Fulda, S., Wick, W., Weller, M., Debatin, K.M., 2002. Smac agonists sensitize for Apo2L/TRAIL- or anticancer drug-induced apoptosis and induce regression of malignant glioma in vivo. Nat Med **8**, 808-815.

Gengan, R.M., Anand, K., Phulukdaree, A., Chuturgoon, A.A., 2012. A549 lung cell line activity of biosynthesized silver nanoparticles using *Albiziaadianthifolia* leaf. Colloids and Surfaces B: Biointerfaces (*In Press*).

Gonenc, A., Ozkan, Y., Torun, M., Simsek, B., 2001. Plasma malondialdehyde (MDA) levels in breast and lung cancer patients. J Clin Pharm Ther **26**, 141-144.

Guo, F., Nimmanapalli, R., Paranawithana, S., Wittman, S., Griffin, D., Bali, P., O'Bryan, E., Fumero, C., Wang, H.G., Bhalla, K., 2002. Ectopic overexpression of second mitochondria-derived activator of caspases (Smac/DIABLO) or cotreatment with N-terminus of Smac/DIABLO peptide potentiates epothilone B derivative-(BMS 247550) and Apo-2L/TRAIL-induced apoptosis. Blood **99**, 3419-3426.

Haddad, M., Laurens, V., Lacaille-Dubois, M.A., 2004. Induction of apoptosis in a leukemia cell line by triterpene saponins from Albizia adianthifolia. Bioorg Med Chem **12**, 4725-4734.

Haddad, M., Miyamoto, T., Laurens, V., Lacaille-Dubois, M.A., 2003. Two new biologically active triterpenoidal saponins acylated with salicylic acid from Albizia adianthifolia. J Nat Prod **66**, 372-377.

Hanahan, D., Weinberg, R.A., 2000. The hallmarks of cancer. Cell **100**, 57-70.

Hansen, S.F., Michelson, E.S., Kamper, A., Borling, P., Stuer-Lauridsen, F., Baun, A., 2008. Categorization framework to aid exposure assessment of nanomaterials in consumer products. Ecotoxicology **17**, 438-447.

Harris, C.C., 1996. p53 tumor suppressor gene: from the basic research laboratory to the clinic--an abridged historical perspective. Carcinogenesis **17**, 1187-1198.

Hengartner, M.O., 2000. The biochemistry of apoptosis. Nature **407**, 770-776.

Hirsch, T., Marzo, I., Kroemer, G., 1997. Role of the mitochondrial permeability transition pore in apoptosis. Biosci Rep **17**, 67-76.

Holcik, M., Yeh, C., Korneluk, R.G., Chow, T., 2000. Translational upregulation of X-linked inhibitor of apoptosis (XIAP) increases resistance to radiation induced cell death. Oncogene **19**, 4174-4177.

Hong, S.J., Dawson, T.M., Dawson, V.L., 2004. Nuclear and mitochondrial conversations in cell death: PARP-1 and AIF signaling. Trends Pharmacol Sci **25**, 259-264.

Hostettmann, K., Martson, A., 1995. Saponins. Cambridge University Press.

Hsu, H., Xiong, J., Goeddel, D.V., 1995. The TNF receptor 1-associated protein TRADD signals cell death and NF-kappa B activation. Cell **81**, 495-504.

Hwang, P.M., Bunz, F., Yu, J., Rago, C., Chan, T.A., Murphy, M.P., Kelso, G.F., Smith, R.A., Kinzler, K.W., Vogelstein, B., 2001. Ferredoxin reductase affects p53-dependent, 5-fluorouracil-induced apoptosis in colorectal cancer cells. Nat Med **7**, 1111-1117.

Janero, D.R., 1990. Malondialdehyde and thiobarbituric acid-reactivity as diagnostic indices of lipid peroxidation and peroxidative tissue injury. Free Radic Biol Med **9**, 515-540.

Joza, N., Susin, S.A., Daugas, E., Stanford, W.L., Cho, S.K., Li, C.Y., Sasaki, T., Elia, A.J., Cheng, H.Y., Ravagnan, L., Ferri, K.F., Zamzami, N., Wakeham, A., Hakem, R., Yoshida, H., Kong, Y.Y., Mak, T.W., Zuniga-Pflucker, J.C., Kroemer, G., Penninger, J.M., 2001. Essential role of the mitochondrial apoptosis-inducing factor in programmed cell death. Nature **410**, 549-554.

Kalishwaralal, K., Banumathi, E., Ram Kumar Pandian, S., Deepak, V., Muniyandi, J., Eom, S.H., Gurunathan, S., 2009. Silver nanoparticles inhibit VEGF induced cell proliferation and migration in bovine retinal endothelial cells. Colloids Surf B Biointerfaces **73**, 51-57.

Kalishwaralal, K., Barathmanikanth, S., Pandian, S.R., Deepak, V., Gurunathan, S., 2010. Silver nano - a trove for retinal therapies. J Control Release **145**, 76-90.

Kasibhatla, S., Tseng, B., 2003. Why target apoptosis in cancer treatment? Mol Cancer Ther **2**, 573-580.

Kensil, C.R., 1996. Saponins as vaccine adjuvants. Crit Rev Ther Drug Carrier Syst **13**, 1-55.

Kischkel, F.C., Hellbardt, S., Behrmann, I., Germer, M., Pawlita, M., Krammer, P.H., Peter, M.E., 1995. Cytotoxicity-dependent APO-1 (Fas/CD95)-associated proteins form a death-inducing signaling complex (DISC) with the receptor. EMBO J **14**, 5579-5588.

Komen, J.C., Distelmaier, F., Koopman, W.J., Wanders, R.J., Smeitink, J., Willems, P.H., 2007. Phytanic acid impairs mitochondrial respiration through protonophoric action. Cell Mol Life Sci **64**, 3271-3281.

Krajewska, M., Krajewski, S., Banares, S., Huang, X., Turner, B., Bubendorf, L., Kallioniemi, O.P., Shabaik, A., Vitiello, A., Peehl, D., Gao, G.J., Reed, J.C., 2003. Elevated expression of inhibitor of apoptosis proteins in prostate cancer. Clin Cancer Res **9**, 4914-4925.

Lacaille-Dubois, M.A., Wagner, H., 2000. Bioactive saponins from plants: An update. In Atta ur, R., (Ed.), Studies in Natural Products Chemistry. Elsevier, pp. 633-687.

Lalier, L., Cartron, P.F., Juin, P., Nedelkina, S., Manon, S., Bechinger, B., Vallette, F.M., 2007. Bax activation and mitochondrial insertion during apoptosis. Apoptosis **12**, 887-896.

Lara, H.H., Ayala-Nunez, N.V., Ixtepan-Turrent, L., Rodriguez-Padilla, C., 2010. Mode of antiviral action of silver nanoparticles against HIV-1. J Nanobiotechnology **8**, 1.

Li, L., Thomas, R.M., Suzuki, H., De Brabander, J.K., Wang, X., Harran, P.G., 2004. A small molecule Smac mimic potentiates TRAIL- and TNFalpha-mediated cell death. Science **305**, 1471-1474.

Li, L.Y., Luo, X., Wang, X., 2001. Endonuclease G is an apoptotic DNase when released from mitochondria. Nature **412**, 95-99.

Livak, K.J., Schmittgen, T.D., 2001. Analysis of relative gene expression data using real-time quantitative PCR and the 2(-Delta Delta C(T)) method. Methods **25**.

Long, J.L., Engels, E.A., Moore, R.D., Gebo, K.A., 2008. Incidence and outcomes of malignancy in the HAART era in an urban cohort of HIV-infected individuals. AIDS **22**, 489-496.

Lu, L., Sun, R.W., Chen, R., Hui, C.K., Ho, C.M., Luk, J.M., Lau, G.K., Che, C.M., 2008. Silver nanoparticles inhibit hepatitis B virus replication. Antivir Ther **13**, 253-262.

MacCorkle, R.A., Freeman, K.W., Spencer, D.M., 1998. Synthetic activation of caspases: artificial death switches. Proc Natl Acad Sci U S A **95**, 3655-3660.

MacLachlan, T.K., El-Deiry, W.S., 2002. Apoptotic threshold is lowered by p53 transactivation of caspase-6. Proc Natl Acad Sci U S A **99**, 9492-9497.

Madhumathi, K., Sudheesh Kumar, P.T., Abhilash, S., Sreeja, V., Tamura, H., Manzoor, K., Nair, S.V., Jayakumar, R., 2010. Development of novel chitin/nanosilver composite scaffolds for wound dressing applications. J Mater Sci Mater Med **21**, 807-813.

Man, S., Gao, W., Zhang, Y., Huang, L., Liu, C., 2010. Chemical study and medical application of saponins as anti-cancer agents. Fitoterapia **81**, 703-714.

Marnett, L.J., 1999. Lipid peroxidation-DNA damage by malondialdehyde. Mutat Res **424**, 83-95.

Marsters, S.A., Pitti, R.A., Sheridan, J.P., Ashkenazi, A., 1999. Control of apoptosis signaling by Apo2 ligand. Recent Prog Horm Res **54**, 225-234.

Mayank, T., Matthias, F.M., Hendrick, F., Alexander, W., 2011. Chemistry and pharmacology of saponins: special focus on cytotoxic properties. Botanics: Targets and Therapy **1**, 19-29.

Miyashita, T., Krajewski, S., Krajewska, M., Wang, H.G., Lin, H.K., Liebermann, D.A., Hoffman, B., Reed, J.C., 1994. Tumor suppressor p53 is a regulator of bcl-2 and bax gene expression in vitro and in vivo. Oncogene **9**, 1799-1805.

Miyashita, T., Reed, J.C., 1995. Tumor suppressor p53 is a direct transcriptional activator of the human bax gene. Cell **80**, 293-299.

Moaddab, S., Ahari, H., Shahbazzadeh, D., Motallebi, A.A., Anvar, A.A., Rahman-Nya, J., Shokrgozar, M.R., 2011. Toxicity Study of Nanosilver (Nanocid®) on Osteoblast Cancer Cell Line. Int. Nano Lett **1**, 6.

Mujoo, K., Haridas, V., Hoffmann, J.J., Wachter, G.A., Hutter, L.K., Lu, Y., Blake, M.E., Jayatilake, G.S., Bailey, D., Mills, G.B., Gutterman, J.U., 2001. Triterpenoid saponins from Acacia victoriae (Bentham) decrease tumor cell proliferation and induce apoptosis. Cancer Res **61**, 5486-5490.

Navarro, E., Piccapietra, F., Wagner, B., Marconi, F., Kaegi, R., Odzak, N., Sigg, L., Behra, R., 2008. Toxicity of silver nanoparticles to Chlamydomonas reinhardtii. Environ Sci Technol **42**, 8959-8964.

Owen-Schaub, L., Chan, H., Cusack, J.C., Roth, J., Hill, L.L., 2000. Fas and Fas ligand interactions in malignant disease. Int J Oncol **17**, 5-12.

Peter, M.E., Krammer, P.H., 1998. Mechanisms of CD95 (APO-1/Fas)-mediated apoptosis. Curr Opin Immunol **10**, 545-551.

Pitti, R.M., Marsters, S.A., Lawrence, D.A., Roy, M., Kischkel, F.C., Dowd, P., Huang, A., Donahue, C.J., Sherwood, S.W., Baldwin, D.T., Godowski, P.J., Wood, W.I., Gurney, A.L., Hillan, K.J., Cohen, R.L., Goddard, A.D., Botstein, D., Ashkenazi, A., 1998. Genomic amplification of a decoy receptor for Fas ligand in lung and colon cancer. Nature **396**, 699-703.

Polyak, K., Xia, Y., Zweier, J.L., Kinzler, K.W., Vogelstein, B., 1997. A model for p53-induced apoptosis. Nature **389**, 300-305.

Reed, J.C., 1999. Dysregulation of apoptosis in cancer. J Clin Oncol **17**, 2941-2953.

Reed, J.C., Bischoff, J.R., 2000. BIRinging chromosomes through cell division--and survivin' the experience. Cell **102**, 545-548.

Rogers, J.V., Parkinson, C.V., Choi, Y.W., Speshock, J.L., Hussain, S.M., 2008. A pre-liminary assessment of silver nanoparticle inhibition of monkeypox virus plaque formation. Nanoscale Research Letters **3**, 129-133.

Rubio-Moscardo, F., Blesa, D., Mestre, C., Siebert, R., Balasas, T., Benito, A., Rosenwald, A., Climent, J., Martinez, J.I., Schilhabel, M., Karran, E.L., Gesk, S., Esteller, M., deLeeuw, R., Staudt, L.M., Fernandez-Luna, J.L., Pinkel, D., Dyer, M.J., Martinez-Climent, J.A., 2005. Characterization of 8p21.3 chromosomal deletions in B-cell lymphoma: TRAIL-R1 and TRAIL-R2 as candidate dosage-dependent tumor suppressor genes. Blood **106**, 3214-3222.

Rutberg, F.G., Dubina, M.V., Kolikov, V.A., Moiseenko, F.V., Ignat'eva, E.V., Volkov, N.M., Snetov, V.N., Stogov, A.Y., 2008. Effect of silver oxide nanoparticles on tumor growth in vivo. Dokl Biochem Biophys **421**, 191-193.

Saelens, X., Festjens, N., Vande Walle, L., van Gurp, M., van Loo, G., Vandenabeele, P., 2004. Toxic proteins released from mitochondria in cell death. Oncogene **23**, 2861-2874.

Sahu, S.C., Casciano, D.A. (Eds.), 2009. *Nanotoxicity, from In vivo and In vitro Models to Health Risks*. John Wiley and Sons, Ltd, USA.

Sakahira, H., Enari, M., Nagata, S., 1998. Cleavage of CAD inhibitor in CAD activation and DNA degradation during apoptosis. Nature **391**, 96-99.

Salvesen, G.S., Duckett, C.S., 2002. IAP proteins: blocking the road to death's door. Nat Rev Mol Cell Biol **3**, 401-410.

Sasaki, H., Sheng, Y., Kotsuji, F., Tsang, B.K., 2000. Down-regulation of X-linked inhibitor of apoptosis protein induces apoptosis in chemoresistant human ovarian cancer cells. Cancer Res **60**, 5659-5666.

Sax, J.K., El-Deiry, W.S., 2003. p53 downstream targets and chemosensitivity. Cell Death Differ **10**, 413-417.

Scaffidi, C., Schmitz, I., Krammer, P.H., Peter, M.E., 1999. The role of c-FLIP in modulation of CD95-induced apoptosis. J Biol Chem **274**, 1541-1548.

Schimmer, A.D., 2004. Inhibitor of apoptosis proteins: translating basic knowledge into clinical practice. Cancer Res **64**, 7183-7190.

Shall, S., de Murcia, G., 2000. Poly(ADP-ribose) polymerase-1: what have we learned from the deficient mouse model? Mutat Res **460**, 1-15.

Shariat, S.F., Desai, S., Song, W., Khan, T., Zhao, J., Nguyen, C., Foster, B.A., Greenberg, N., Spencer, D.M., Slawin, K.M., 2001. Adenovirus-mediated transfer of inducible caspases: a novel "death switch" gene therapeutic approach to prostate cancer. Cancer Res **61**, 2562-2571.

Siemiatycki, J., Richardson, L., Straif, K., Latreille, B., Lakhani, R., Campbell, S., Rousseau, M.C., Boffetta, P., 2004. Listing occupational carcinogens. Environ Health Perspect **112**, 1447-1459.

Srinivasula, S.M., Hegde, R., Saleh, A., Datta, P., Shiozaki, E., Chai, J., Lee, R.A., Robbins, P.D., Fernandes-Alnemri, T., Shi, Y., Alnemri, E.S., 2001. A conserved XIAP-interaction motif in caspase-9 and Smac/DIABLO regulates caspase activity and apoptosis. Nature **410**, 112-116.

Sriram, M.I., Kanth, S.B., Kalishwaralal, K., Gurunathan, S., 2010. Antitumor activity of silver nanoparticles in Dalton's lymphoma ascites tumor model. Int J Nanomedicine **5**, 753-762.

Su, J., Zhang, J., Liu, L., Huang, Y., Mason, R.P., 2008. Exploring feasibility of multicolored CdTe quantum dots for in vitro and in vivo fluorescent imaging. J Nanosci Nanotechnol **8**, 1174-1177.

Suliman, A., Lam, A., Datta, R., Srivastava, R.K., 2001. Intracellular mechanisms of TRAIL: apoptosis through mitochondrial-dependent and -independent pathways. Oncogene **20**, 2122-2133.

Sun, H., Nikolovska-Coleska, Z., Yang, C.Y., Xu, L., Tomita, Y., Krajewski, K., Roller, P.P., Wang, S., 2004. Structure-based design, synthesis, and evaluation of conformationally constrained mimetics of the second mitochondria-derived activator of caspase that target the X-linked inhibitor of apoptosis protein/caspase-9 interaction site. J Med Chem **47**, 4147-4150.

Sun, H.X., Xie, Y., Ye, Y.P., 2009. Advances in saponin-based adjuvants. Vaccine **27**, 1787-1796.

Sun, L., Singh, A.K., Vig, K., Pillai, S.R., 2008. Silver nanoparticles inhibit replication of respiratory syncytial virus. J Biomed Biotechnol. **4**, 1497-1502.

Sun, R.W., Chen, R., Chung, N.P., Ho, C.M., Lin, C.L., Che, C.M., 2005. Silver nanoparticles fabricated in Hepes buffer exhibit cytoprotective activities toward HIV-1 infected cells. Chem Commun (Camb), 5059-5061.

Suzuki, Y., Nakabayashi, Y., Takahashi, R., 2001. Ubiquitin-protein ligase activity of X-linked inhibitor of apoptosis protein promotes proteasomal degradation of caspase-3 and enhances its anti-apoptotic effect in Fas-induced cell death. Proc Natl Acad Sci U S A **98**, 8662-8667.

Tamm, I., Trepel, M., Cardo-Vila, M., Sun, Y., Welsh, K., Cabezas, E., Swatterthwait, A., Arap, W., Reed, J.C., Pasqualini, R., 2003. Peptides targeting caspase inhibitors. J Biol Chem **278**, 14401-14405.

Tamokou Jde, D., Simo Mpetga, D.J., Keilah Lunga, P., Tene, M., Tane, P., Kuiate, J.R., 2012. Antioxidant and antimicrobial activities of ethyl acetate extract, fractions and compounds from stem bark of Albizia adianthifolia (Mimosoideae). BMC Complement Altern Med **12**, 99.

Thornberry, N.A., Lazebnik, Y., 1998. Caspases: enemies within. Science **281**, 1312-1316.

Townsend, D.M., Tew, K.D., Tapiero, H., 2003. The importance of glutathione in human disease. Biomedicine & Pharmacotherapy **57**, 145–155.

Trucco, C., Oliver, F.J., de Murcia, G., Menissier-de Murcia, J., 1998. DNA repair defect in poly(ADP-ribose) polymerase-deficient cell lines. Nucleic Acids Res **26**, 2644-2649.

Ueda, S., Masutani, H., Nakamura, H., Tanaka, T., Ueno, M., Yodoi, J., 2002. Redox control of cell death. Antioxid Redox Signal **4**, 405-414.

Uren, A.G., Wong, L., Pakusch, M., Fowler, K.J., Burrows, F.J., Vaux, D.L., Choo, K.H., 2000. Survivin and the inner centromere protein INCENP show similar cell-cycle localization and gene knockout phenotype. Curr Biol **10**, 1319-1328.

Vaidyanathan, R., Kalishwaralal, K., Gopalram, S., Gurunathan, S., 2009. Nanosilver--the burgeoning therapeutic molecule and its green synthesis. Biotechnol Adv **27**, 924-937.

van Loo, G., van Gurp, M., Depuydt, B., Srinivasula, S.M., Rodriguez, I., Alnemri, E.S., Gevaert, K., Vandekerckhove, J., Declercq, W., Vandenabeele, P., 2002. The serine protease Omi/HtrA2 is released from mitochondria during apoptosis. Omi interacts with caspase-inhibitor XIAP and induces enhanced caspase activity. Cell Death Differ **9**, 20-26.

Vaux, D.L., Cory, S., Adams, J.M., 1988. Bcl-2 gene promotes haemopoietic cell survival and cooperates with c-myc to immortalize pre-B cells. Nature **335**, 440-442.

Vodenicharov, M.D., Sallmann, F.R., Satoh, M.S., Poirier, G.G., 2000. Base excision repair is efficient in cells lacking poly(ADP-ribose) polymerase 1. Nucleic Acids Res **28**, 3887-3896.

Wajant, H., 2002. The Fas signaling pathway: more than a paradigm. Science **296**, 1635-1636.

Wang, X., 2001. The expanding role of mitochondria in apoptosis. Genes Dev **15**, 2922-2933.

Wei, Y., Fan, T., Yu, M., 2008. Inhibitor of apoptosis proteins and apoptosis. Acta Biochim Biophys Sin (Shanghai) **40**, 278-288.

Wu, G., Chai, J., Suber, T.L., Wu, J.W., Du, C., Wang, X., Shi, Y., 2000. Structural basis of IAP recognition by Smac/DIABLO. Nature **408**, 1008-1012.

Wu, G., Fang, Y.Z., Yang, S., Lupton, J.R., Turner, N.D., 2004. Glutathione metabolism and its implications for health. J Nutr **134**, 489-492.

Xia, T., Kovochich, M., Brant, J., Hotze, M., Sempf, J., Oberley, T., Sioutas, C., Yeh, J.I., Wiesner, M.R., Nel, A.E., 2006. Comparison of the abilities of ambient and manufactured nanoparticles to induce cellular toxicity according to an oxidative stress paradigm. Nano Lett **6**, 1794-1807.

Xia, T., Kovochich, M., Liong, M., Madler, L., Gilbert, B., Shi, H., Yeh, J.I., Zink, J.I., Nel, A.E., 2008. Comparison of the mechanism of toxicity of zinc oxide and cerium oxide nanoparticles based on dissolution and oxidative stress properties. ACS Nano **2**, 2121-2134.

Xie, X., Zhao, X., Liu, Y., Zhang, J., Matusik, R.J., Slawin, K.M., Spencer, D.M., 2001. Adenovirus-mediated tissue-targeted expression of a caspase-9-based artificial death switch for the treatment of prostate cancer. Cancer Res **61**, 6795-6804.

Yang, L., Mashima, T., Sato, S., Mochizuki, M., Sakamoto, H., Yamori, T., Oh-Hara, T., Tsuruo, T., 2003. Predominant suppression of apoptosome by inhibitor of apoptosis protein in non-small cell lung cancer H460 cells: therapeutic effect of a novel polyarginine-conjugated Smac peptide. Cancer Res **63**, 831-837.

Yang, Y., Fang, S., Jensen, J.P., Weissman, A.M., Ashwell, J.D., 2000. Ubiquitin protein ligase activity of IAPs and their degradation in proteasomes in response to apoptotic stimuli. Science **288**, 874-877.

Yu, J., Zhang, L., Hwang, P.M., Rago, C., Kinzler, K.W., Vogelstein, B., 1999. Identification and classification of p53-regulated genes. Proc Natl Acad Sci U S A **96**, 14517-14522.

APPENDIX A

1)

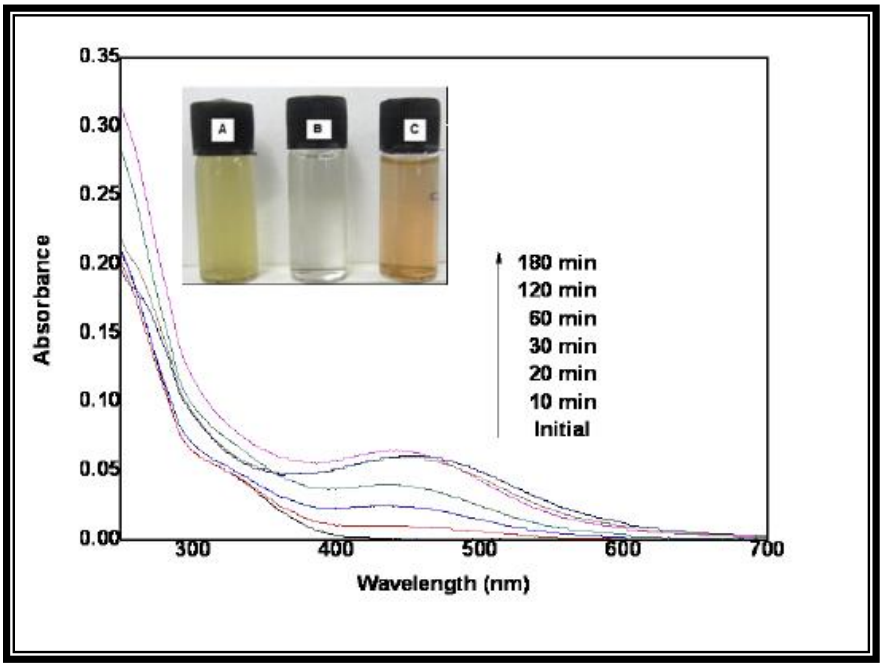

Figure 1: A) Aqueous leaf extracts solution, **B)** silver nitrate solution and **C)** yellowish- brown colloidal solution of AA_{AgNP} and UV-vis spectra of AA_{AgNP} showing the surface Plasmon resonance (448nm) for the reaction at different time intervals.

2)

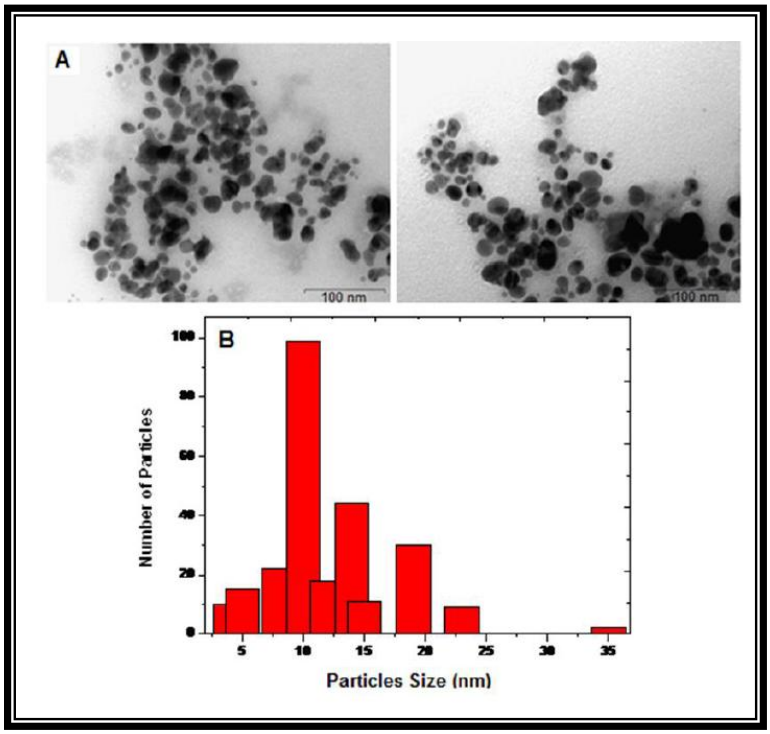

Figure 2: A) Transmission electron microscope micrograph of silver nanoparticles synthesised from aqueous leaf extracts of *Albizia adianthifolia* and **B)** representation of size distribution of $AA_{AgNP}s$.

3)

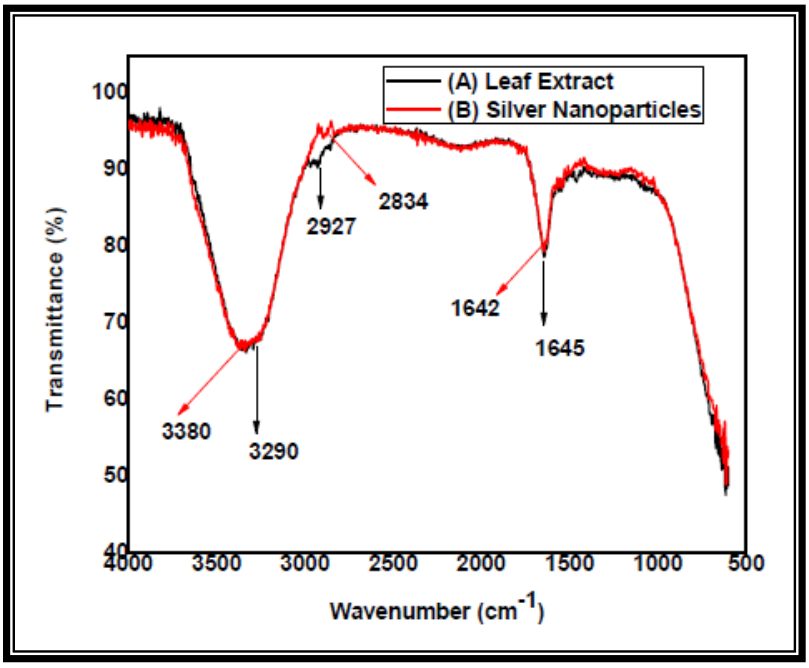

Figure 3: Illustration of Fourier transform infrared spectroscopy spectra of **A**) aqueous leaf extract and **B**) silver nanoparticles synthesised using *Albizia adianthifolia* leaf extract.

APPENDIX B

1)

Table 1: Raw data for the determination of IC_{50} using the cell viability (MTT) assay.

AA_{AgNP} concentration	Average absorbance	%viability	Log [AA_{AgNP}]
0	0.955	100.0	
2	0.938	98.3	0.30103
4	0.872	91.3	0.60206
8	0.819	85.7	0.90309
10	0.738	77.3	1
15	0.803	84.1	1.176091
20	0.680	71.2	1.30103
30	0.564	59.0	1.477121
40	0.377	39.5	1.60206
50	0.247	25.9	1.69897
60	0.212	22.2	1.778151
75	0.123	12.8	1.875061

APPENDIX C

1)

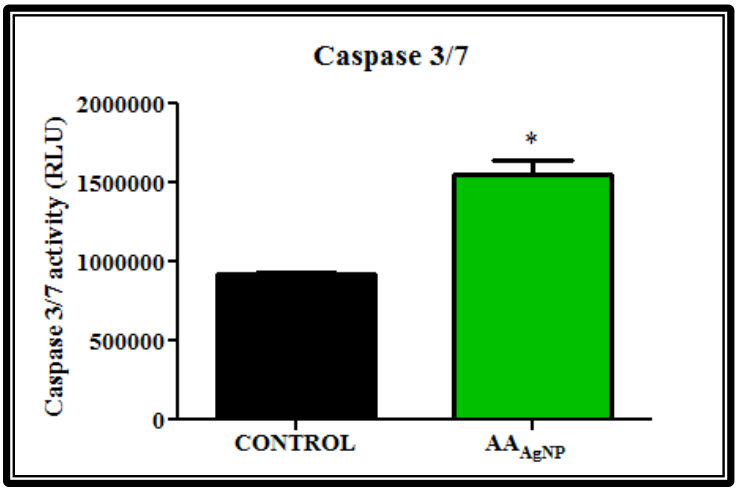

Figure 1: Caspase-3/-7 activity was significantly higher in cells exposed to AA_{AgNP} compared to untreated cells (p=0.0180).

2)

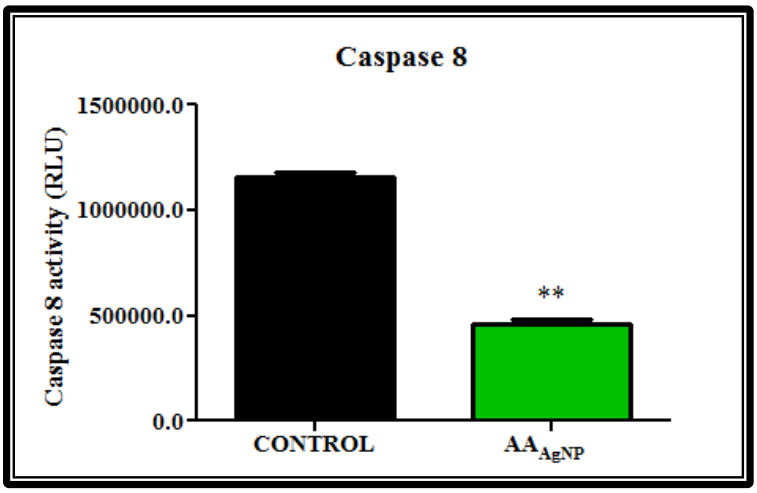

Figure 2: The activity of caspase-8 was significantly reduced in cells exposed to AA_{AgNP} compared to untreated cells (p=0.0024).

3)

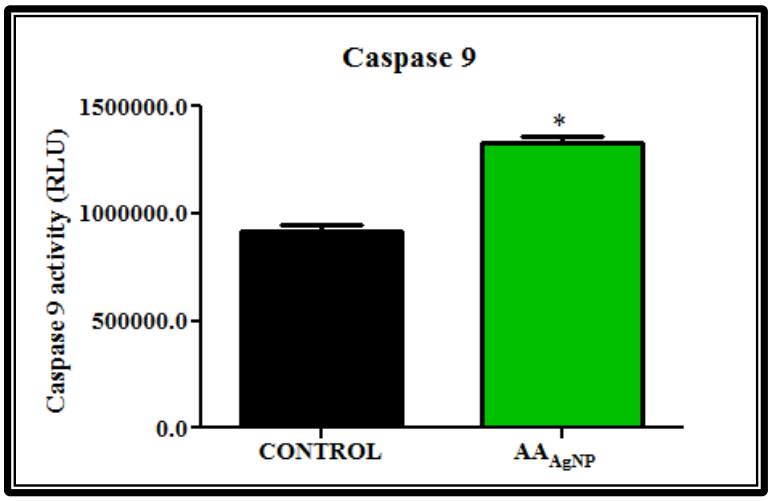

Figure 3: AA_{AgNP} caused a significant increase in the activity of caspase-9 compared to control cells (p=0.0117).

APPENDIX D

1)

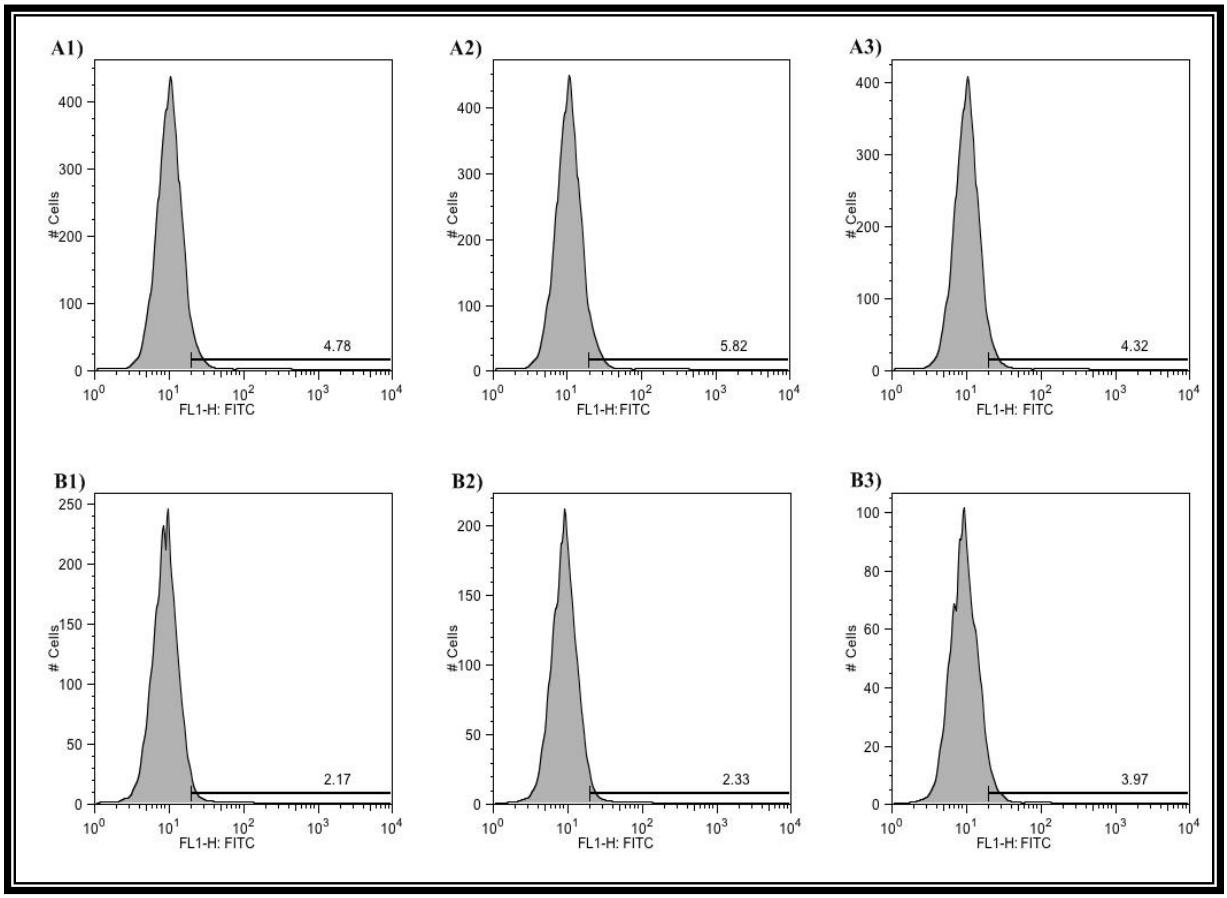

Figure 1: Extracellular staining-flow cytometry was used to evaluate the expression of CD95 (Fas receptor). Three replicates were done for both treated (**B1-B3**) and untreated (**A1-A3**) cells. AA_{AgNP} significantly down regulated the expression of CD95 in A549 cells compared to the control (p=0.0416).

2)

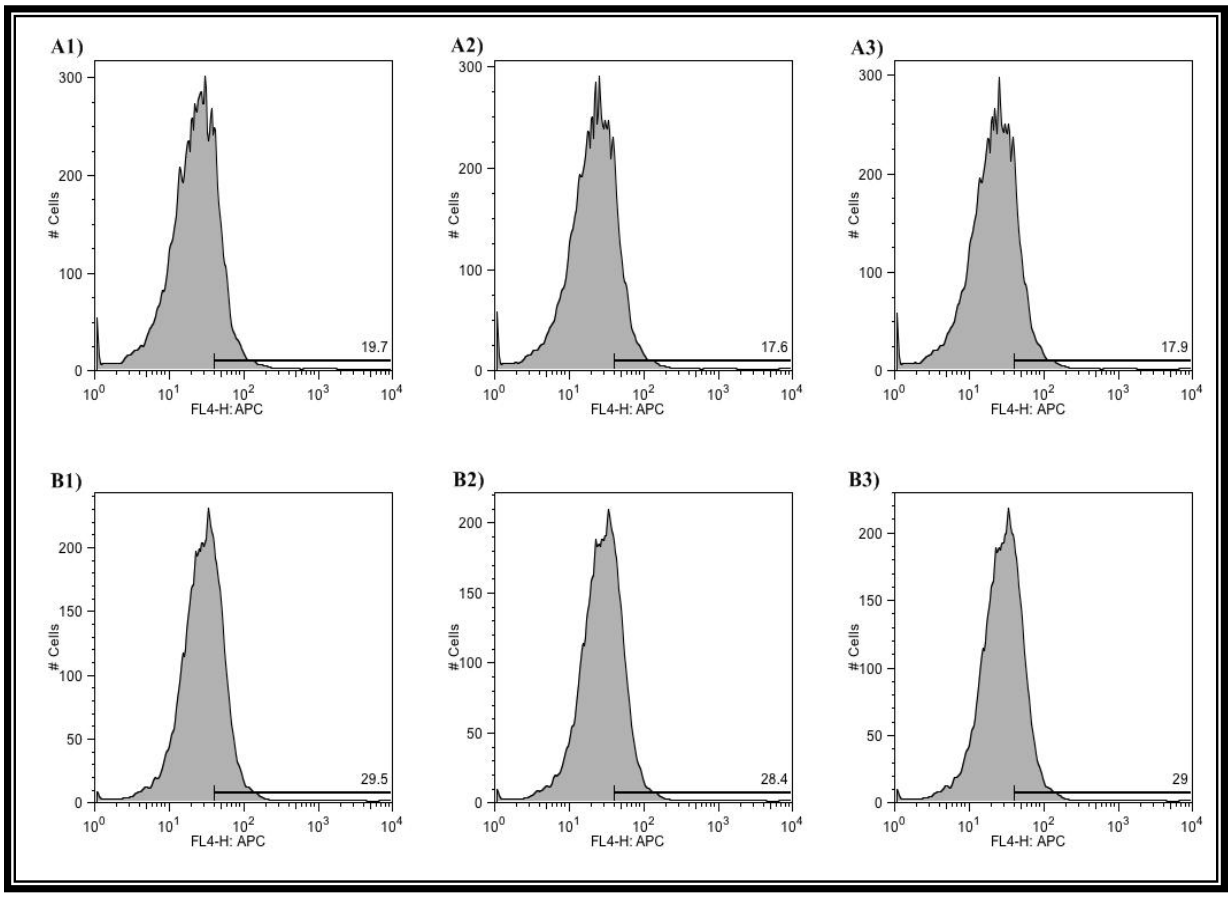

Figure 2: Levels of smac/DIABLO, a pro-apoptotic protein, were determined flow cytometrically using an intracellular staining assay. A significantly higher expression of smac/DIABLO was observed in A549 cells after treatment with AA_{AgNP} (**B1-B3**) compared to untreated cells (**A1-A3**) (p<0.0001).

APPENDIX E

1)

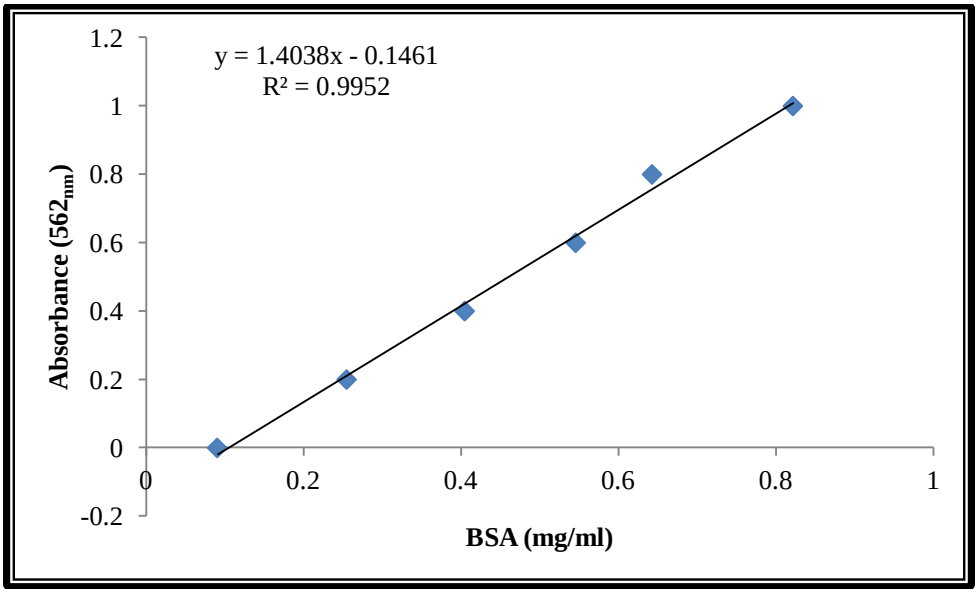

Figure 1: Calibration curve using known concentrations of bovine serum albumin for the determination of protein concentration in samples using the bicinchoninic acid assay.

2)

Table 1: Standardisation of protein using the calibration curve for sodium dodecyl sulphide-polyacrylamide gel electrophoresis.

	Average absorbance	Protein (mg/ml)	C2 (mg/ml)	V2 (µl)	V1 (µl)
Control	1.595	1.240276	1	100	80.62719
Control	1.6425	1.274113	1	100	78.48597
AA_{AgNP}	1.4045	1.104573	1	100	90.5327
AA_{AgNP}	1.338	1.057202	1	100	94.58931